UNIVERSITY OF NAIROBI

University of Nairobi

Analysis and Multivariate Modeling of Heavy Metals and Associated Radiogenic Impact of Gold Mining in the Migori-Transmara Complex of Southwestern Kenya

By

Odumo Benjamin Okang'

I80/83681/2012

A thesis Submitted in the Fulfilment of the Requirements for the Award of the Degree of Doctor of Philosophy in Physics of the University of Nairobi
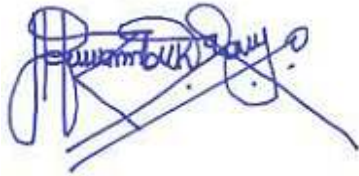
2021

DECLARATION

I declare this thesis is my original work and has not been submitted elsewhere for examination, award of a degree or publication. Where people's work or my own work has been used, this has properly been acknowledged and referenced in accordance with the University of Nairobi's requirements. presented for a degree in any other University

Signature……………………………..   Date 13/09/2021 ………...

Odumo Benjamin Okang'
I80/83681/2012
Department of Physics
Faculty of Science and Technology
University of Nairobi

This thesis has been submitted with the approval of my University Supervisors

13/09/2021

Prof. Angeyo H. Kalambuka
Department of Physics
University of Nairobi
P.O. Box 30197-00100
Nairobi.

Prof. J. P. Patel   …………………………………   15/09/2021
                                    Signature   Date

Department of Technical and Applied Physics
The Technical University of Kenya
P.O. Box 52428- 00200
Nairobi.
Jaypy.patel@gmail.com

ACKNOWLEDGEMENTS

ABSTRACT

Gold mining economically empowers not only the miners but also the entire country. However, it involves massive discharge of wastes like tailings, gangues etc. containing heavy metals and radionuclides that maybe harmful to exposed animals and plants if their concentrations are beyond certain limits. It was necessary analyze and multivariately model heavy metal and associated radiogenic impact of gold mining in The Migori Transamara gold mining complex of Southwestern Kenya in order advice the concerned parties. The aim of this study was to determine elemental concentrations of As, Cd, Cr, Cu, Hg, Ni, Pb and Zn and activity concentrations of ^{40}K, ^{232}Th and ^{238}U in lichens, moss, mine tailings, river sediments and soil. This study also computed absorbed dose, annual effective dose and pollution indices from their concentrations and also identified the sources of the heavy metals. To achieve our objectives lichens, mosses, river sediments, soil and tailings were randomly were collected from various sites and analyzed using AAS and HPGe gamma ray spectrometric techniques. Multivariate and Ordinary Kriging analysis were then used to analyze the heavy metals and radionuclide concentrations, their possible sources and spatial distribution.

Heavy metal concentration in tailings is the highest compared to the rest of the matrices, the concentration of all the heavy metals apart fron Cr in the tailings are at least 9.5 times higher than their background concentration in soil. The median concetration of all the heavy metals apart from Cr and Cd in lichens and mosses respectively were above their background values. The median concentrations of As and Hg are 6 and 5 times higher than the background values in sediments while the median concentration of Cu, As and Hg in soil are 6, 4 and 3 times respectively above the background concentrations in all the sampling locations and the median of mercury is 272 times above the maximum permissible limit by FAO and WHO in soil.

The soils are extremely highly enriched (82 – 3069) by mercury in all the sampling areas, this is supported by mean geo-accumulative index (I_{geo}=6.95). The mean EF, the river sediments are extremely highly (812) and significantly (13) enriched by Hg and As. The median activity concentration (Bq/kg) of ^{238}U, ^{232}Th and ^{40}K in soil were 33.09 ± 10.12, 58.57 ± 18.62 and 417.05 ± 163.95 respectively while the median absorbed dose and annual effective dose were 70.48 nGy/h and 0.09 ± 0.03 mSv/y respectively. Activity concentration of ^{238}U, ^{232}Th and ^{40}K in river

sediments were 28.00 ± 17.83, 42.32 ± 15.32 and 342.00 ±200.03 respectively and its absorbed dose (60.63 ± 19.80 nGy/h) and AEDE (0.07 ± 0.02). Radioactivity in the soil and sediments are within the world's average according to UNSCEAR. As, Cr and Pb and (Cu, Zn, Ni Cd and Ni) originate from gold mining, natural soil formation and a mixture gold mining and anthropogenic processes. Spatial distribution of As, Hg, Cu, Zn and Pb in lichens, mosses and soil show high concentration around the mines implying negative impact of mining. The miners are encouraged to embrace gold recovery methods that do not require mercury besides wearing protective masks and clothing to shield them dust and hence exposure to heavy metals. Direct disposal of tailings to the environment should be discouraged by building tailing dams. Results from this study will help local and national government formulate policies on artisanal gold mining besides acting as a baseline for future studies.

TABLE OF CONTENTS

List of Tables

TABLE OF FIGURES

ACRONYMS

AAS	Atomic Absorbtion Spectrometry
CF	Contamination factor
CV	Coefficient of Variance
ECCBR	European Commission Community Bureau of Reference
GDP	Gross Domestic Product
HBRA	High background radiation areas
IAEA	International Atomic Energy Agency
LOD	Limits of Detection
LOQ	Limit of Quantification
NORM	Naturally occurring radioactive materials
PC	Principal Components
PCA	Principal Component Analysis
PEC	Probable Effect Concentration
PGV	Background Concentration Values
PM	Particulate Matter

TEC   Threshold Effect Concentration

TENORM Technologically enhanced naturally occurring radioactive materials

UNSCEAR United Nations Scientific Committee of Effects of Atomic Radiation

CHAPTER ONE

1.0 Introduction

Discovery and exploitation of natural resources in a country leads to her economic growth and improvement on the livelihood of its citizens. Common natural resources include aluminum, coal, columbite, copper, diamond, gas, gold, oil, silver, titanium and uranium. In the process of accessing and recovering these resources however, other issues like population, structural developments and wastes arise that more often than not have negative impact on the environment if not properly managed. Waste that arises during mining processes is usually dumped near the mines with little attention to their effects on the environment and people living around the mines not to mention the miners themselves. Ninety nine percent of the excavated ore is released in to the environment as wastes (Adler *et al*., 2007). These wastes contain varied concentrations of heavy metals (As, Cd, Co, Cr, Cu, Hg, Pb, U, Th, Y, Zn, etc.), gases (CO, SO_2, CH_4, etc.) and radionuclides (^{238}U, ^{232}Th, ^{40}K, etc.) etc. Repeated dumping and/or discharge of these wastes in the environment may lead to their elevated concentrations in air, soil and water. Depending on the type of waste, medium of transport, and other environmental factors their effect can be realized far and near from the point of discharge thereby affecting the health of the miners and the populace.

Tun *et al*. (2020), found high concentration of As (22.17 ppm), Cd (3.07 ppm), Hg (77.440 ppm) in soils around all gold amalgamation sites in Myanmar, they further observed that miners operated without protective clothing. According to Nurcholis *et al*. (2017) amalgamation around gold mines increases the concentration of mercury and other heavy metals like Mn, Fe, Pb and As in soil. Donkor *et al*. (2005) found high concentration (1752 mg/kg) of As in sediments with decommissioned mines registering the highest concentration of heavy metals, this was attributed to poor management of mine tailings. They also found a significant correlation between total mercury and As (0.864), Cu (0.691) but no correlation between As and Al. High correlation between As and Hg is because of its use in gold recovery process by artisanal gold miners while poor correlation between As and Al was due to their different sources. Significantly high levels of mercury in Plants, soil and sediments with highly significant impact of mercury on the mining environment was registered in Ghana , this suggested artisanal gold mining is responsible for soil and sediment pollution according to Amoakwah *et al*. (2020). Significant correlation was also

observed between Pb/As, Hg/Cu, Hg/Cd, Cu and Cd by Ning *et al*. (2011) in surface waters around Linglong gold mines in China where heavy metal concentration was decreasing with distance from the mines. Assessment of radioactivity in tailings from Rosterdam found in Western Kenya by Wanyama (2020) showed no significant radiological health implications with all the activity concentrations falling below the world's average. They also found external hazard assessment to be below 370 Bq/kg as was also found by Blanchard *et al*. (2017a) and Ademola *et al*. (2010) in Cameroon and Nigeria respectively. As much as Faanu *et al*. (2014) also found activities below the world's average however in Gold mines in the vicinity of Chirano gold mines in Ghana, they found absorbed dose of 230 nGy/h at a topsoil pile at the mining site. In South Africa, Kamunda *et al*. (2016a) found high radioactivity in tailings and soil at to be ^{238}U (785.3 Bq/kg) compared to the background ^{238}U (17.01 Bq/kg), Raeq was also above 370 Bq/kg. High radioactivity was due to the fact that gold was being processed to extract uranium, this presented a possible radiological hazard as high uranium concentrations in human hair was found in residents of gold mining area in Gauteng province in South Africa by Winde *et al*. (2019). Gold mining therefore may contribute to higher radiation exposure depending on the ore accompanying mineral.

Gold miners are exposed inadvertently to heavy metals and ionizing radiations internally through ingestion, inhalation and externally through dermal contact in the course of mining. Most of heavy metals encountered during gold mining operation like zinc and copper are of biological use to human however arsenic, cadmium, lead, mercury etc. have no biological significance to humans (Zhao *et al*., 1997). Even the biologically beneficial heavy metals are harmful when consumed beyond certain limits while others like arsenic are harmful even at low concentrations. Arsenic, Cadmium, Chromium and Nickel expose humans to various kinds cancer (Martinez *et al*., 2011; Cui *et al*., 2021). Apart from being a carcinogen, arsenic inhibits DNA repair and induces chromosol aberrations among others (Abernathy *et al*., 2003). Arsenis pollution of soils and water is an issue that affects over 40 million peoples' health in more than 70 countries due to contamination of food and water causing Keratosis and cancer related diseases (Ng *et al*., 2019). Ngole-Jemme *et al*. (2017) found highest risk factors for As (3.5×10^3) and high quotient factor indicated high exposure to As (53.7) with children being at the highest risk.

Cadmium is highly toxic to animals human beings and even plants causing pulmonary and

gastrointestinal irritation, vomiting and convulsions to humans (Basely and Cravey, 1995). Exposure to lead may lead to premature birth, reduced birth weight and birth to mentally retarded children to women during tryster (Andrews *et al*., 1994). Children are more vulnerable to effect of lead than adults, their expose to lead may lead to low Intelligent Quotient (IQ), retarded growth, hearing problems etc. (Factor-Litvak *et al*., 1998; Needleman, 2004). In plants, lead can interfere with some mitosis, photosynthesis, absorption of water etc. (Bhattacharya *et al.*, 2012). Exposure to copper and zinc causes nausea, vomiting, abdominal pain among other effects. Mercury, the main gold extraction agent, may expose one to diarrhea, kidney failure, Minamata disease, nausea, neurological disorder, ulceration, etc. (Yard *et al*., 2012; Harada, 1978). Humans exposed to ionizing radiation may suffered from cancer, genetic defects, nausea, vomiting that can eventually lead to death((Zeeb *et al*., 2009); Mettler, 2012; Boice, 2012. Effect of radiation however, depends on the absorbed dose, dose rate, quality of radiation, tissue irradiated, age of the recipient etc. It is evident the miners and even the populace maybe exposed to health risks due to gold mining and therefore require information on the levels of heavy metals and ionizing radiations they are exposed to during their mining operations.

Several studies have been carried out to find the concentration of heavy metals and radionuclides in the environment either by directly measuring their concentration in environmental matrices like soil, air and water, others have used organisms as proxies to determine their concentrations. Nyangababo *et al*. (1987) and Nyarko *et al*. (2006) used lichens to determine the levels of heavy metals from industries in Uganda and trace element deposition around an industrial in Ghana respectively. Major and trace and trace elements deposition around the largest power plant in Serbia was evaluated using moss in Serbia (Ćujić *et al*., 2014). Heavy metal concentration was in tailings, soil, river sediments around gold mining areas has been investigated by (Rashed, 2010a);Weissenstein and Sinkala, 2011);   Herman and Kihampa, 2015); Aucamp and van Schalkwyk, 2003) . Radioactivity concentration in tailings and soil around gold mines to ascertain the level of exposure of the miners and the populace in Ghana, South Africa, Sudan Nigeria etc. (Adukpo *et al*., 2014; Faanu *et al*., 2011;Ademola *et al*., 2014; Kamunda *et al*., 2016). However, no study had been carried that analyzes and multivariately model radioecological and heavy metal impact of gold mining in various environmental matrices simultaneously.

We therefore carried out this study to determine the concentration of As, Cd, Cr, Cu, Hg, Pb and Zn in lichens, mosses, river sediments, soils and mine tailings and calculate pollution indices of soil and river sediments. The study also determined the activity concentration of ^{40}K, ^{232}Th and ^{238}U in river sediments and soil using a HPGe based gamma ray spectrometer, from the activity concentrations absorbed and corresponding annual effective doses were calculated. Chemometrics was then used to identify sources and relationship between the heavy metals. Ordinary kriging was then used to model the spectrometer, from radioecological and heavy metal impact of gold mining in the study area. Results from this study will not only provide useful information to the concerned parties for necessary action and policy making but will also act as a baseline for further studies and provide additional information on preceding studies in the region and outside the region.

1.1 Gold mining in Migori - Transmara Region

Gold mining in Migori -Transmara area started in 1920's, during this period mining was only done in large scale. The mines were located at Macalder, Osiri, Mikei, Masara, Kitere and Lolgorien. Large scale mining ended in 1966 when a total of 20,000 tons of copper, 4,248 Kg of gold and 1,210 Kg of silver had been exploited (Ogola, *et al.*, 2002). The end of large scale gold mining ushered artisanal gold mining operations that has continued to date. Large large-scale scale gold mining resumed around Lolgorien in 2011 when new rich gold bearing reefs were discovered. Artisanal gold miners rely exclusively on the use of mercury to extract gold from finely comminuted gold ore using hammers. Use of hummer is however being replaced by fuel/electricity driven mills especially in the newly discovered gold reefs in areas like Kamwango and Nyarombo in Migori County and other Counties like Homa-Bay and Siaya.

1.2 Geology and Mineralization of the Migori-Transmara Gold Mining Complex

The Migori–Transmara gold mining complex also referred to as the Migori segment is a component of the Archean Nyanza greenstone belt containing central, proximal and distal facies, **Figure 1.1**. An intervening basin contains distal tuffs and turbiditic greywacke sediments. The rocks from the Migori Group consist of the Macalder and Lolgorien subgroups. The volcanic rocks constitute a bimodal mafic-felsic suite with the felsic mode dominating. The mafic rocks are tholeiitic and the selfic ones are calc-alkaline and high-potassium dacites. High potassium dacites

are the predominant volcanic rocks in the segment and form a chemical series with majority of the granites. The basalts and calc-alkaline felsic rocks were erupted into a submarine environment and the younger high-K dacites subaerially. The mixed tholeiitic and calc-alkaline association is typical of volcanic arc settings where occurrence of elevated potassium volcanics suggest the presence of continental crust (Gill, 1981).

Figure 1. 1 Geology of Migori segment (Migori-Transmara) Gold mining complex (adopted from Ichang'l and MacLean, 1991)**.**

The Macalder volcanogenic massive sulphide deposit and accompanying sulphide bearing iron formation are in central volcanic facies. Auriferous chert horizons and banded iron formations are in proximal facies while auriferous quartz veins are in late strike-slip fault structures. The mineral potential of the Migori segment is because of the massive sulphide deposits in close proximity to the Macalder and Lolgorien volcanic centers and gold mineralization throughout the belt.

1.3 Problem Statement

Various studies have been carried out on the impact of mining on the environment. However, hardly any study has been carried out that integrates the analysis and multivariate modeling of

heavy metal and radioecological aspects including their geostatistical modeling of the impact in a complex terrain, which is a multivariate problem.

1.4 Objectives

1.4.1 General Objective

The main goal of this study was to determine the concentrations of primordial radionuclides, as well as heavy metals in biomonitors (lichens and moss) growing around the mines, soil and river sediments and geostatistically model their spatial variability the Migori –Transmara gold mining complex of southwestern Kenya for the purpose of assessing and modeling of their radioecological and associated impact and risk, using geostatistical techniques.

1.4.2 Specific Objectives

The specific objectives of this study were to:

i.   Determine the concentration of As, Cd, Cr, Cu, Hg, Ni, Pb and Zn in biomonitors (lichens and moss), river sediments, soil and mine tailings from the Migori-Transmara gold mining complex.

ii.   Determine the activity concentration of ^{40}K, ^{232}Th and ^{238}U in soils and river sediments.

iii.   Compute the absorbed and corresponding annual effective dose at various soil and sediment sampling sites

iv.   Compute the pollution indices of soil and river sediments by the above heavy metals.

v.   Identify possible sources of the heavy metals in soil, river sediments and biota (lichens and moss)

vi.   Explore, using PCA, HCA and Pearson's Correlation, the relationship among the measured data.

vii.   Use Ordinary kriging to model the radioecological and heavy metal impact of gold mining in the Migori-Transmara gold mining area.

1.5 Justification and Significance of the Study

Several studies have been carried out on heavy metals and radionuclides in gold mining areas in Ghana, Nigeria, Brazil etc. Most of these studies have only reported either the concentration of

heavy metals or radioactivity around gold mines in one or more environmental matrix in one study. Others have presented studies on heavy metals and exposure to radioactivity in only in one environmental matrix. But no study has been caried out that determines heavy metal concentration and radioactivity in biomonitors, river sediments, soil and tailings in a gold mining area at the same time. In the process of gold mining, miners and populace are exposed to heavy metals and radionuclides that may cause several diseases including cancer, reduced IQ and Minamata disease, a study was therefore necessary that simultaneously determines heavy metal concentration and radioactivity, their sources and spatial distribution in biomonitors, river sediments, soil and tailings. This study therefore analyzed and multivariately modeled heavy metal and associated radiogenic impact of gold mining in the Migori Transamara gold mining areas of Southwestern Kenya.

Findings from this study will provide useful information and data on the radiogenic and heavy metal impact of gold mining and extract multivariate and spatial relationships between the radiogenic, heavy metals, and radiation exposure levels uniquely associated with gold mining in the Migori-Transmara gold mining complex, which is not available. This study will create awareness and provide information to all stake holders including miners, the populace and the concerned authorities on the impact of (artisanal) gold mining operations in Migori – Transmara gold mining areas of southwestern Kenya. Results from this study will also complement available information on impact of (artisanal) gold mining in other areas in Kenya and even in other countries and hence act as a baseline for further studies.

CHAPTER TWO

2.0 Literature Review

2.1 Radioactive Materials in Gold Mining

Humans are at all times exposed to radiation from natural sources also referred to as the background radiation. This can be from primordial radionuclides, radionuclides that existed before the creation of the earth like ^{238}U and ^{232}Th (and their daughters) and ^{40}K. Humans are also exposed

to cosmogenic radiations as a result of cosmic interactions. Natural radiations contribute over 80% to the external dose to exposed population (IAEA, 1996). Terrestrial radionuclides, also referred to as Naturally Occurring Radioactive Materials (NORM) are present in rocks, soils, water, etc. Concentration of NORM depends on geological composition and geographical locations, the mean annual effective dose is about 2.4 mSv/y (UNSCEAR, 2000). However, in geological formations where radioactive minerals occur, (very) high levels of background radiation exposure could result; these are called High Background Radiation Areas (HBRA). Examples of these areas include Yangjiang in China, Kerala and Tamil in India, Lazio and Campania in Brazil. Mrima Hill (Coast Province) is one of the high background areas in Kenya where the external radiation dose was found to be about 50 times above the natural background dose (Patel, 1991). In addition to the normal background radiation mining, agricultural activities, etc., can lead to enhanced exposure to natural sources of radiation. Humans are also exposed to radiation due to advancement in technology e.g. ^{137}Cs is from fallout from weapon testing, these kind of radiations are called the Technologically Enhanced Naturally Occurring Radioactive Materials (TENORM) (Dowdall *et al.*, 2004). High and low radionuclide concentrations have been linked with igneous rocks (like granite) and sedimentary rocks (rocks of basaltic and ultramafic composition) respectively (Faanu *et al.*, 2014).

According to United Nations Scientific Committee on the Effects of Atomic Radiation, UNSCEAR, (2000), mining has been identified among the potential sources of exposure to NORM. Gold miners are externally exposed to gamma radiation from the ground and mine tailing heaps as well as when submerged in dust rich in radionuclides. Miners are also internally exposed to radiation through inhalation of contaminated dust and/or inadvertent ingestion of contaminated gamma radiation enriched particles during the extraction, leaching, transportation, processing the ore and use of contaminated equipment (UNSCEAR, 2000). Consumption of food crops grown on soils contaminated with radionuclides or living in houses built from soils and/or tailings can also expose humans internally to NORM. Studies show gold mining activities elevate the concentrations of radionuclides in soil, ambient air, plants, sediments and water around the mines. Kamunda *et al.* (2016a) found the average concentration of ^{238}U (578.3 Bq/kg) and ^{232}Th (43.9 Bq/kg) in tailings around Gauteng gold mining area in South Africa to be above their concentration

^{238}U (17.0 Bq/kg) and ^{232}Th (22.2 Bq/kg) in the control area as was also reported by Aguko *et al.* (2013). Even though the concentrations of ^{238}U and ^{232}Th in tailings were higher than their concentrations in the background which was likely to be due to the impact on gold mining, the concentration of ^{40}K (237.4 Bq/kg) in the tailings was lower in the control area (496.8 Bq/kg). High concentration of potassium was associated with the use potassium-based fertilizers in agricultural activities that might have raised its concentration. Ademola *et al.* (2014) found higher calculated absorbed dose (66.3 nGy/h) and effective dose (0.084 mSv/y) around gold mines in a gold mine in Nigeria compared to (20.4 nGy/h) and (0.025 mSv/y) in living areas. Activity concentrations in soil samples from undisturbed soil were also lower compared to soil samples from waste heaps (Ademola and Okpalaonwuka, 2010; Al-Geed and Sam, 2000). According to Esiole *et al.*, (2019), high radioactivity at gold processing sites compared to gold mines is due to repeated disposal of tailings and other wastes. These findings show that miners and the populace are exposed to higher radiation doses during gold mining processes. As much as these studies by Kamunda *et al*. Ademola *et al*., Esiole *et al* and Aguko *et al*., investigated radioactivity in gold mining, they mainly concentrated on radioactivity in tailings and soil. They failed to study radioactivity in the river sediments draining these gold mining areas. Since tailings are the major source of ionizing radiations that finally find their way to nearby rivers due to surface runoffs, wind and even atmospheric deposition, it was prudent to determine their concentrations in the river sediments.

Gold miners are even exposed to higher radiation doses when mining under the surface, this is majorly due gamma exposure from radon (^{222}Ra), an inert gas that diffuses from underground into the atmosphere (Banzi, *et al.*, 2002). According to UNSCEAR, (2013), underground mine workers in poorly ventilated mines are likely to suffer from lung cancer due to inhalation of radon decay products. However, the rate at which radon diffuses in the atmosphere depends on meteorological conditions, soil, type of rock, and water content (Schubert and Schulz, 2002). Shahbazi-Gahrouei *et al.* (2013) reported that 50% of natural exposure to radiation arise from radon gas, radon enters the body through drinking water and breathing. Darko *et al*. (2005) found effective dose in underground mines (1.83 mSv/y) to be higher than effective dose (0.26 mSv/y) in the surface mines. Banzi *et al*. (2016) reported higher activity concentration in ground water of ^{232}U (20.61-

47.21mBq/L), ^{234}U (21.70 – 49.11 mBq/L), ^{226}Ra (16.80 – 43.45), ^{232}Th (0.12 – 2.80 mBq/L) and ^{228}Ra (0.10-2.43 mBq/L) compared to surface water ^{232}U (17.33-27.24 mBq/L), ^{234}U (21.06 – 34.43 mBq/L), ^{226}Ra (15.00 – 25.61), ^{232}Th (0.16 – 2.10 mBq/L) and ^{228}Ra (0.11-1.99 mBq/L). Darko *et al.*, however failed to map out the concentration of the radionuclides in soil to show their spatial distribution.

Adukpo *et al.* (2014) found high radioactivity in soil followed by sediments and water respectively along the lower basin of river Pra. High radioactivity along river banks was due illegal mines in the basin. Miners erect processing plants along rivers banks because of placer gold and also because gold processing requires substantial amount of water. In the course of ore washing processes, mine tailings are directly emptied in the rivers which end up polluting river waters and sediments with the radionuclides. Sediment plays a pivotal role in radioecology because it acts as a medium of migration of radionuclides to the biological system through food chain, therefore presence of NORM in sediments may lead to radiological effects to humans. According to Caridi *et al.* (2015), radionuclide content of river sediments mainly depends on the chemistry of the rivers as well as the mineralogical features of the catchment area. The study by Adukpo et al. determined radioactivity in soil, sediments and water, however they failed to geostatistically map out the spatial distribution of the measured radionuclides in soil. This was essential since it would help identify areas that require remediation.

2.2 Heavy Metals in Gold Mining

Although heavy metals occur naturally in the earth's crust, environmental contamination and human exposure to them mainly arise from human activities like sewage effluents discharge and emissions from fossil fuel combustion, mining, petrol production, agricultural applications, pharmaceuticals, metal production, coal burning, nuclear power stations and microelectronics. Heavy metal concentration in a locality depends on the catchment area, mining waste, agrochemicals, parent rock, geological settings etc. Heavy metals pollute the environment because of their toxicity and persistence in the environment which translates to long half-life hence becoming a constant danger to the environment in which they are found (Adriano *et al.*, 2004;) Asaduzzaman *et al.,* 2015). They become contaminants when their rate of generation from anthropogenic activities is faster than their rate of generation from natural sources (D'Amore *et*

al., 2005). Bioavailability of heavy metals is dependent on physical (e.g., temperature, phase association, adsorption and sequestration) and biological (e.g., species characteristics and trophic interactions) factors. Chemical factors that influence speciation, complex kinetics, lipid solubility, octano/water partition coefficients and thermodynamic equilibrium also influence their bioavailability (Hamelink, 1994).

Gold mining operations like excavation of the ore, grinding, sloshing, disposal of wastes (tailings, gangues, overburden, wastewater, etc.), emission of dust and mercury in the air, etc., are obvious sources of heavy metals depending on the local geological composition. Wind blowing away mine wastes (especially heaps of tailings) abet the dispersal of the associated heavy metals to the atmosphere, soil and water bodies. Chemical leaching and transportation of metals occur when water from rainfall and surface runoffs come into contact with the mining wastes leading to absorption, adsorption and dissolution of metals in the wastes. Once in water, heavy metals find their way into, aquifers, boreholes, lakes, rivers, soils, streams, wells and other water bodies thereby contaminating them. Sulphide oxidation resulting from biological and chemical processes from wastes from gold mining lower the pH of ground water, this increases dissolution of heavy metals in ground water system resulting into their contamination (Bhattacharya *et al.,* 2012).

Rashed, (2010) found high concentration of Cd, Cu, Hg, Ni and Pb around tailings with Hg and As having especially high concentrations around tailings damp. This was supported by contamination factor (CF) (CF>6) and CF (0-3) for As and Hg respectively near and away from the mines. A study by Herman and Kihampa (2015) found high concentration of Cu, Hg and Pb in soil, the concentration of Hg was higher than allowed limits in Tanzania (TZS, 2007). High mean EF of As (70.58), Hg (256.93), Pb (22.32) and Cd (10.52) were also found in soils near a gold mining site by Rafiei *et al.*(2010). According to Basavarajappa and Manjunatha (2015), gold mine tailings are the main sources of xenobiotic contamination from weathering of heaps of waste materials. However, with proper management, active tailing dams can have low metal contamination around them compared to decommissioned ones as was reported by Antwi-Agyei *et al.*,(2009). Olobatoke and Mathuthu (2016) found very high contamination index for As (7.39) and medium pollution by Cr (2.16) in soil at the vicinity of mine tailings in South Africa with

higher concentrations of the heavy metals found in the top 15 cm of soil compared to concentration in deep strata. A study by Weissenstein and Sankala (2011) however, found the concentration of heavy metals to be increasing with increase in distance from a mine. This observation can be explained by the fact that surface run offs and/or wind erosion can carry away the metals from the tailings. Tailings as a source of heavy metal contamination was confirmed by Bowell *et al.,* (1995) who found higher metal concentration in water from tailings compared to adits. Bowell *et al.* (1995) however, did not observe presence of uranium at elevated concentrations as was found in the gold mining areas of the Witwatersrand (F. Winde and Sandham, 2004) and those located in eastern Johannesburg (Aucamp and van Schalkwyk, 2003). High concentration of uranium around gold mines in South Africa is because gold and uranium metals accompany each other in gold ores in the region. Association of these two metals has enabled processing of uranium as an offshoot from gold mines in South Africa since 1952 (Frank Winde and Sandham, 2004).

Streams and rivers draining artisanal gold mining areas also show the effects of pollution by heavy metals. Arhin *et al.*(2015) found extreme contamination of river sediments by Cd, Hg and Se and strong to extreme contamination by As and Cr when studying the impact of gold mining in stream sediments in Ghana. High heavy metal concentrations were attributed to the artisanal miners directly disposing tailings into the nearby rivers as was also reported by Nwanosike *et al.* (2018), Bempah *et al.* (2013) and Lim *et al.* (2009). Nwanosike *et al.* (2018) found high pollution index of Hg, Cd and Pb and moderate pollution with As. This they attributed to processing of gold along the river channel, they recommended washing of gold ore along the rivers should be stopped and encouraged miners to embrace modern methods of gold processing that are environment friendly. High heavy metal concentration in sediments is a reflection on pollution of water in rivers since sediments act as a sink for heavy metals and heavy metals in them can reach several orders above the overlying water. Since sediments receive heavy metals discharged into aquatic environments from different sources including atmospheric fallout, eroded soils and tailings and sewage discharge, it can act as an important source of assessment of anthropogenic contamination of rivers (Amadi *et al.,* 2017). Low pH in water due to acid mine drainage increases sorption and mobility rate of heavy metals thereby increasing availability of heavy metals in the sediments.

Artisanal gold mining is one of the leading contributors of heavy metals to surface and ground water because of indiscriminate use of mercury and other chemicals during gold recovery that may be harmful to humans (Donkor *et al.,* 2009). Artisanal gold miners, in a rush to recover gold from gold bearing ore do not care about the heavy metals that are associated with gold mining. Miners more often are not aware of the negative effects of heavy metals like arsenic, copper, lead, mercury, zinc etc. that are often associated with gold ore to themselves and the environment and therefore inadvertently or otherwise end up polluting the environment. Apart from the heavy metals related with the local geology hosting gold ore, the main heavy metal associated with AGM is metallic mercury (Hg). In the course of using mercury to recover gold from gold bearing ore, substantial is lost to the surrounding through spillage, tailings and during heating. This makes mercury one of the leading heavy metal pollutants in the AGM process.

Human exposure pathways to heavy metals are through direct ingestion (inadvertent ingestion, pica and geophagia (geophagy)), inhalation, direct/dermal contact, drinking water or through food chain. Exposure to heavy metals may lead to their accumulation in the kidney, liver, etc. leading to cardiovascular, nervous, kidney and bone diseases. For instance, exposure to even low level of cadmium than previously thought can lead to cancer, hypertension, liver and kidney disfunction (Mushtakova *et al.*, 2005). Neurological disorder has been reported in fetus and children exposed to lead while developmental disability has been reported in those exposed to mercury (Laws, 2000). Serious mercury pollution in Minamata (Japan) caused birth to infants with severe developmental disorders. Consumption of heavy metal contaminated food can seriously deplete some essential nutrients in the body reducing immunological defenses, intrauterine growth retardation, impaired psycho-social behavior, disabilities associated with malnutrition and a high prevalence of upper intestinal cancer (Arora *et al*., 2008). All these studies concentrated on the heavy metal and pollution indices but failed to map out their spatial distribution in order to identify hot spots on the measured matrices. They also failed to study the radiological impact of gold mining at the same time.

2.3 Biomonitors in monitoring heavy metal concentration in the environment.

Use of lichens, mosses, fern etc. have been in use since 1860's to monitor heavy metal pollution in air pollution (Rühling, 1994). These plants are used as biomonitors and/or bioindicators, bioindicators measure the quality of the environmental changes while biomonitors provide the quantitative information on the quality of the environment (Markert *et al.*, 1997). It therefore follows that all the biomonitors are bioindicators but this does not necessarily apply for bioindicators. Lichens and mosses are preferred as biomonitors because they lack real roots, they cannot take nutrients directly from soil but instead really on obtaining nutrients for wet and dry deposition. Intracellular spaces in their thallus accumulate and retain heavy metals by trapping insoluble particles and they can retain heavy metals to very high concentrations among other factors. The advantage of using lichens and mosses as biomonitors over conventional monitors is because they are cheap, have a good nutrient uptake, widely distributed etc. According to Brunialti *et al*. (2002), the concentration of heavy metals in lichen thalli are directly correlated with their atmospheric concentrations or depositions, thereby making them good biomonitors.

Using biomonitors to monitor major and minor trace element deposition around a power plant in Serbia, Cujic *et al*. (2014) found elevated concentrations of As, Cd, Co , Hg, Ni and V in the vicinity of the largest power plant to be higher. A study by Nyangababo *et al.* (1987) and Nyarko *et al*. (2006) found the concentration of respectively found heavy metals to have been enriched by heavy metals from industries and motor vehicles. Source apportionment of heavy metals around Tarakwa mines found anthropogenic and natural soil formation processes as the main source of heavy metals (Boamponsem *et al*., 2010). MN, Co, Hg and As were found to be coming from gold mining and Cd to originating from fertilizers since it has low crustal abundance (Bargagli, 1995).

These studies are only on heavy metal and / or radiological impact of gold mining on the environment; however, they do not simultaneously analyze and multivariately model the radiological and associated heavy metal impact of gold mining using various environmental matrices. This study therefore used Ordinary kriging to model the radiological impact and associated heavy metal impact of gold mining using various environmental matrices simultaneously. They determined the concentration of As, Cd, Cr, Cu, Hg, Pb and Zn in lichens, mosses, river sediments, soils and mine tailings and from the concentration of the heavy metals using AAS teccnhique. Pollution indices of soil and river sediments were then calculated from the

results of the heavy metal concentrations. The study also determined the activity concentration of ^{40}K, ^{232}Th and ^{238}U in river sediments and soil using a HPGe based gamma ray spectrometer, from the activity concentrations absorbed and corresponding annual effective doses were calculated. Chemometrics was used to identify sources and relationship between the heavy metals. Ordinary kriging was then used to model the radioecological and heavy metal impact of gold mining in the Migori-Transmara gold mining area. Results from this study will not only provide useful information to the concerned parties for the necessary action but will also act as a basis for further studies and provide additional information on preceding studies in the region.

.

CHAPTER THREE

Theoretical Framework

3.0 Basic Theory of Gamma Ray Spectrometry and Multivariate Chemometrics

3.1 Analytical Techniques

Gamma rays from spontaneous nucleus decay are emitted with a rate and energy spectrum that is unique to the nuclear species that is decaying, this uniqueness provides the basis for gamma ray spectrometry. Gamma rays must interact with the sample through photoelectric effect, Compton scattering or pair production processes to be detected.

3.1.1 Atomic Absorption Spectroscopy (AAS)

Atomic absorption spectroscopy is a quantitative method used to detect metals and a few nonmetals in a solution. The atoms absorb specific wavelengths of electromagnetic radiation when the sample to be analyzed is atomized to free the atoms from bonds with other elements, **Figure 3.1**.

AAS can be used to measure the presence of a very small quantity of an element even when other elements are present in the same sample in high concentrations and therefore doesn't need metal separation. It is cheap, fast, simple and exhibits minimum spectral interference. Elements like Al, Ti, W, Mo, V and Si cannot be detected by AAS since they give rise to oxides of the atoms in the flame. If aqueous solutions are used the prominent anion can affect the signal to a noticeable degree.

The sample to be analyzed is made in aqueous solution mostly through digestion and pre-concentration. Nitric acid (HNO_3) is preferred in digestion because of its chemical compatibility, oxidizing ability, availability, purity and low cost.
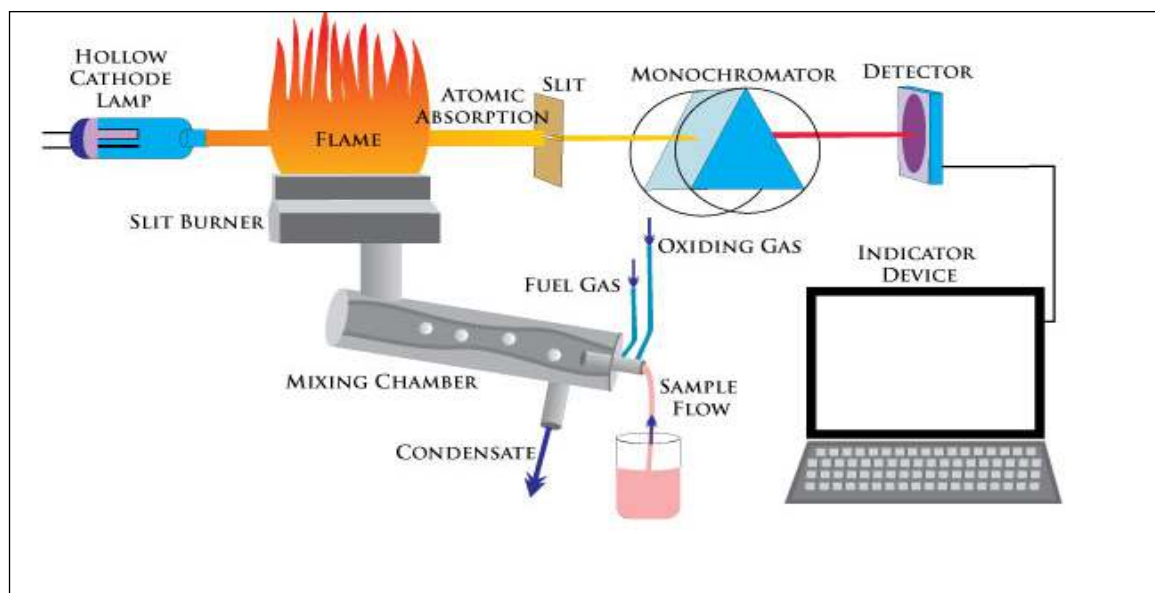
Figure 3. 1: Schematic Diagram of Flame Atomic Absorption Spectrometer.

Absorption ability of a dissolved substance is directly proportional to the product of the length of light through the solution and concentration of the solution. The concentration of the solution is given by **Eq 3.1**.

$$C = \frac{log(I|I_\circ)}{\varepsilon l} = \frac{A}{\varepsilon l} \qquad\qquad (3.1)$$

Where

A is the absorptivity of the substance, A= log (I/I$_o$)

I is the intensity of incident gamma radiation

I$_o$ intensity of immerging radiation

ε is the molar extinction coefficient (molar absorptivity) (M.cm)$^{-1}$

ℓ is the length of the path of light in the solution (cm)

C is the concentration of the liquid (M/L)

3.1.2 Gamma-ray Spectroscopy using HPGe Detector

Primordial radionuclides,^{238}U and ^{232}Th, are detected through gamma emission from their daughters once they reach secular equilibrium while ^{40}K is directly detected. Secular equilibrium is achieved by packing the samples in an air tight container for at least seven-fold half-lives of the targeted radionuclide before analysis.

The most important properties of the gamma ray detection are the energy resolution and the detector efficiency, **Figure 3.2**. For the purposes of decay counting, these kinds of detectors have a more efficient and uniform cross section of the detector active volume to samples that are counted at a short distance from the detector. For low activity concentration, the counting system must be properly shielded from background radiations.
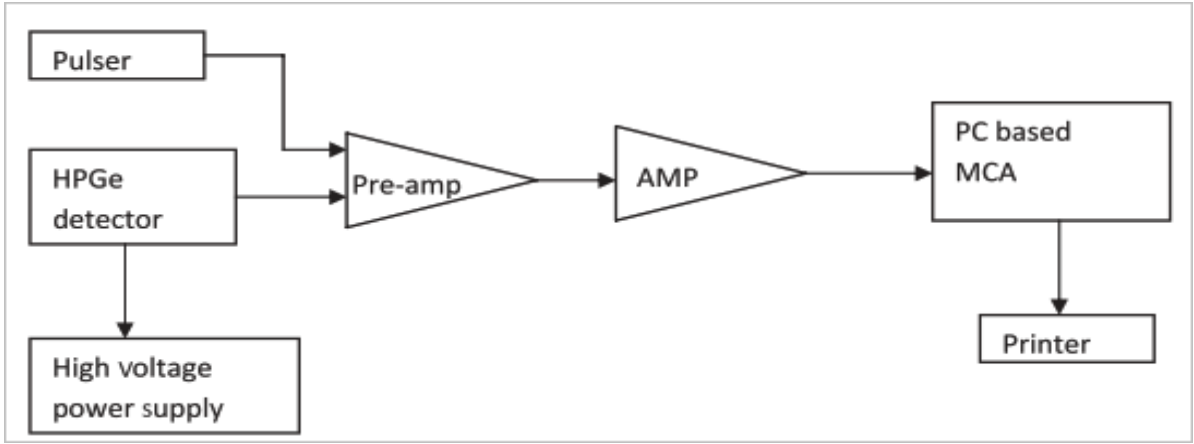
Figure 3. 2: Experimental Circuit Diagram of HPGe Detector System.

Calculation of the location of the peak centroid positions allow automatic analysis of unknown spectra. A list of the nuclides to be examined are normally known in advance, nuclide search is done by optimizing the window, a suitable window will cover the drift and at the same time eliminate false nuclide identification. Regular calibration of the spectrometer is normally carried out to take care of drift.

Once the location and the number peaks have been identified and their peak areas are calculated, activity can then be calculated (Asaduzzaman *et al.,* 2015), **Eq. 3.2**.

$$A = \frac{1000x(N|T)}{Mx\varepsilon xP_\gamma} \tag{3.2}$$

Where

N is net counts

T is the live time of the measurements

M is the mass of the sample in grams

ε is the detection efficiency of the specific gamma ray energy

P_γ is the gamma transition probability of the corresponding gamma ray energy through the specific energy.

The dead time is corrected by, **Eq. 3.3.**

$$N = \frac{n}{(1 - Ct)} \qquad (1.3)$$

Where

n is the observed count rate per second

C is the count rate over all channels

t is the equipment's dead time per pulse

3.1.2.1 Calculation of Doses

3.1.2.1.1 Calculation of the Absorbed Dose (D)

Absorbed dose is the average energy deposited by ionizing radiation on a medium per unit mass (J/kg), its SI unit is Gray (Gy). The absorbed dose in air was calculated using **Eq 3.4**.

$$D = 0.427C_U + 0.662C_{Th} + 0.042C_k \qquad (3.2)$$

Where D is the dose rate in $nGy.h^{-1}$, C_U, C_{Th} and C_K are the activity concentrations of ^{238}U, ^{234}Th and ^{40}K respectively (in Bq/kg). while 0.427, 0.662 and 0.042 are the dose conversion factors of C_U, C_{Th} and C_K respectively in nGyh^{-1}/Bq.kg^{-1} (UNSCEAR, 2000).

3.1.2.1.2 Calculation of Annual Effective Dose (AED)

Annual effective dose relates to the long-term effect of radiation to the persons of interest to a procedure, it is used to calculate annual radiation limits to workers and even the populace in a given work environment in Sievert (Sv). Annual effective dose rate was calculated using **Eq. 3.5.**

$$E = Dx8766x0.2x0.7x10^{-3} \qquad (3.3)$$

Where E is the annual effective dose in ($\mu Sv.yr^{-1}$), D is the absorbed dose rate in air, 8766 is the number of hours per year, 0.2 is the outdoor occupancy factor (the miners take an average of 4.8 hours in the mines per day in a year) and 0.7 is the conversion coefficient.

3.2 Geostatistical Modelling

Geostatistical methods describe and show the pattern of spatial data and give an estimate and quantitative map of variability of the variable in question with minimum variance (Komnitsas and Modis, 2007). The technique was first published by Krige (1951), but G. Matheron derived the formulas and basically established the whole field of linear geostatistics (Cressie 1990; Webster and Oliver 2007; Zhou *et al.*, 2007).

Geostatistical interpolation starts with the recognition that the spatial variation of any continuous attribute is often too irregular to be modeled by a simple mathematical function and instead the variation can be described by a stochastic surface otherwise known as the regionalized variable. Regionalized variable theory assumes that the spatial variation of a variable can be expressed as the sum of a structural component which has a constant mean or trend, a random but spatially correlated component and a random residual error or spatially uncorrelated random noise. This can be expressed as, **Eq. 3.6.**

$$Z(x) = m(x) + \varepsilon'(x) + \varepsilon''(x) \tag{3.4}$$

Where Z is the random function, x is the position in 1, 2, or 3 dimensions, $m(x)$ is the deterministic function describing the structural component of Z at x, $\varepsilon'(x)$ denotes the regionalized variable and $\varepsilon''(x)$ is the residual, spatially independent Gaussian noise having a zero mean and variance (σ^2).

Primary tools used for spatial structure analysis are the semivariogram and the variogram. The variogram is a mathematical description of the relationship between the variance of the pairs of observations $z(x)$ and the distance (lag distance) h separating these observations. Semivariance is expressed as (Luo *et al.,* 2010), **Eq. 3.7.**

$$\gamma(h) = \frac{1}{2N(h)} \sum_{i=1}^{N(h)} \left[z(x_i) - z(x_{(i+h)}) \right]^2 \qquad (3.5)$$

Where z is the measured attribute, $N(h)$ is the number of sample pairs at each lag distance h, $z(x_{i+h})$ and $z(x_i)$ are the variable at location x_{i+h} and x_i (Einax and Soldt, 1998).

3.2.1 Characteristics of the Semivariogram

Graphical presentation of the semivariance $\gamma(h)$ as a function h is called the semivariogram, usually referred to simply as variogram, is the first step towards quantitative description of the regionalized variable, **Figure 3.3**.
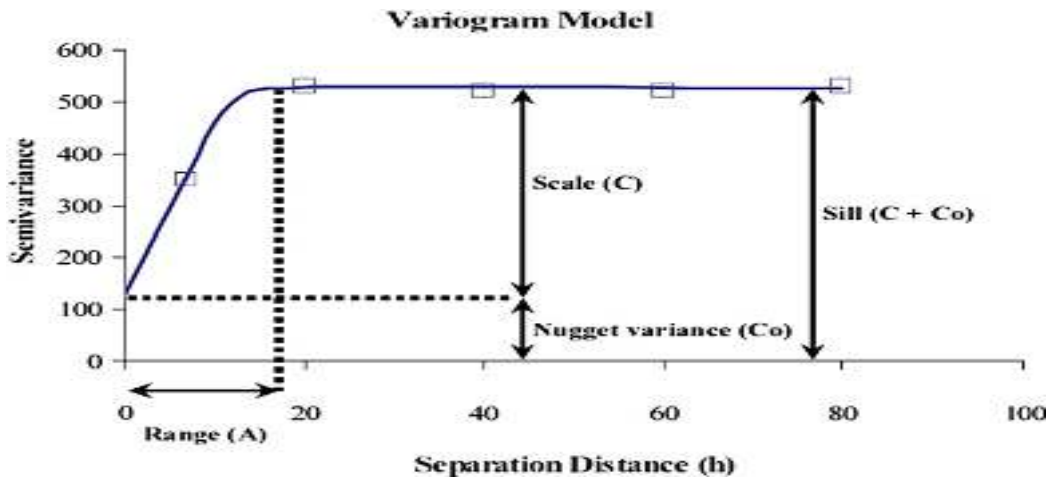
Figure 3. 3: Viriogram model

21

Semivariograms are used to establish the degree of spatial continuity and the range of spatial dependence (Yang *et al.,* 2009).Variograms are defined through the nugget variance (C_o), scale (C), sill ($C+C_o$) and range (A). Range is the distance where the model first flattens out, the distance beyond which the data are no longer autocorrelated. Sites that are closer to each other are likely to show similar characteristics. Sill is the concentration that the semivariogram model attains the range on the y- axis, it corresponds to the model asymptote (scale and data variance) and should be equal to the variance of the data. It is the $lim_{h\rightarrow\infty}\gamma(h)$ representing the variance of the random field. Nugget variance is estimated from the environmental variogram as the concentration of $\gamma(h)$ for $h = 0$. It is a non-zero concentration produced by various sources of unexplained error like measurement error, sampling error, inter-sample error and unexplained and inherent variability for $\gamma(h)$ for $h = 0$. Total sill (often just referred to as sill) is the sum of nugget and partial sill, partial sill represents spatial variation.

An experimental semivariogram can be modified by fitting a simple function of the data points using exponential, Gaussian, linear and spherical models. Spherical model is preferred when the nugget variance is important but not too large and there is a clear range and sill (Goovaerts, 1999), **Eq. 3.8.**

$$\gamma(h) = C + C_o \left\{ \frac{3h}{3A} - \frac{1}{2}\left(\frac{h}{A}\right)^3 \right\} for\ 0 < h < A$$

$$C + C_o \quad for\ h \leq A$$

$$\gamma(0) = 0$$

(3.8)

Where A is the range. If there is clear nugget and sill but only a gradual approach to the range then exponential model is applicable (Trauth, 2015), **Eq. 3.9**.

$$\gamma(h) = C + C_o \left\{ 1 - exp\left(\frac{h}{A}\right) \right\} \qquad (3.6)$$

Very smooth variation and very small nugget variance ε'' compared to spatially dependent random variable ε' then Gaussian model in most appropriate (Trauth, 2015), **Eq. 3.10.**

$$\gamma(h) = C + C_\circ \left\{ 1 - exp\left(\frac{h}{A}\right)^2 \right\} \qquad (3.7)$$

A linear model, typifies attributes which vary at all scales, **Eq. 3.11**

$$\gamma(h) = C_\circ + bh \qquad (3.8)$$

b is the slope of the line.

The scale to sill ratio (C / (C+C$_\circ$)) or nugget to sill ratio n= (C$_\circ$ / (C+C$_\circ$)) can be used to determine the degree of spatial autocorrelation. If n <0.25, 0.25 ≥ n < 0.75 and n ≥ 0.75, then the spatial correlation will be considered as strong, moderate and weak respectively (Cambardella *et al.,* 1994).

3.2.2 Intrinsic Hypothesis

A random function $Z(x)$ accomplishes intrinsic hypothesis if the expectation concentration of the difference between $Z(x + h)$ and $Z(x)$ equals to zero (Bardossy, 1997), **Eq. 3.12**.

$$E = [Z(x + h) - Z(x)] = 0 \qquad (3.9)$$

It also accomplishes intrinsic hypothesis if the variance of the differences between the realizations of the random variable depends only on h, **Eq. 3.13**

$$Var[\{Z(x+h) - Z(x)\}^2] = 2\text{y}(h) \tag{3.10}$$

3.2.3 Estimation of New Points in the Sampling Area- Kriging

Kriging is the best linear unbiased estimator (BLUE) of the concentration of a variable at a given point, a process of a theoretical weighted moving average (McGrath *et al.*, 2004a), **Eq. 3.14.**

$$Z(x_\circ) = \sum_{i=1}^{n} \lambda_i \cdot z(x_i) \tag{3.11}$$

$Z(x_o)$ is the concentration to be estimated at the location of x_o, $z(x_i)$ is concentration at the sampling site x_i and λ_i is the weighting function. The λ_i are such chosen so that the estimate $Z(x_o)$ is unbiased and the estimation variance (Kriging variance) σ_e^2 is less for any other linear combination of observed concentrations. To ensure the estimate is unbiased, the sum of the weight must be equal to one (McGrath *et al.*, 2004b), **Eq. 3.15.**

$$\sum_{i=1}^{n} \lambda_i = 1 \tag{3.12}$$

and the estimation errors (kriging variance) need to be minimized. The expected (average) error for the estimation must be zero, **Eq. 3.16**.

$$E[Z(x_o) - z(x_o)] = 0 \tag{3.13}$$

Where E is the estimation or kriging variance.

3.3 Multivariate Chemometrics Techniques

3.3.1 Principal Component Analysis (PCA)

Principal Component Analysis (PCA) is a multivariate statistical variable reduction method favorable for a large environmental dataset on observed variables. Artificial variables called principal components (PCs) are generated in PCA, PCs account for most variance in the observed variables thereby reducing redundancy in the variables since some variables are intercorrelated (Anazawa and Ohmori, 2005). The first PC is the linear combination of the original variables which explain maximum variability in the original data, the second PC explains the variability not explained by the first PC and is correlated with some of the observed variables that didn't display strong correlation with the first component and so on. Each of the PCs show some degree of correlation with the observed variables, however, PCs are not correlated at all with each other. The number of PCs to retain is determined by the eigen concentrations, the ones that are greater than one is usually retained. For ease of interpretation PC is transformed through VARIMAX rotation, once rotated the PCs are referred to as factors or varifactors, VARIMAX rotation maximizes correlation between variables and factors (Schaug $et\ al.$, 1990; Qu $et\ al.$, 2013; Hani $et\ al.$, 2010). In the PCA, data is presented inform of a matrix D, a $m \times n$ matrix where m is the number of samples and n is the number of elements. D is arranged such that each row gives the analysis of one sample and each column give analysis of one element. D can be normalized to D', such that its ij^{th} element is given by **Eq** 3.17

$$d'_{ij} = \frac{d_{ij} - \mu_{ij}}{\sigma_j}$$
(3.17)

where,

d_{ij} -concentration of j in the ith sample

μ_j - average concentration of element j over all samples

σ_j - standard deviation of element j over all samples

The principal component decomposition of D is $D' = RC$, Where R is $m \times f$ matrix which is the column of PC scores, C is $f \times n$ matrix of the rows of PC loadings and f is the number of factors retained in the analysis. Rows of C tells us which elements are important in defining the PC while the columns of R tells us how strong each PC is in each sample.

The general formula that is used to compute scores on the first two principal components extracted (created) in a principal component analysis is

$$C_1 = a_{11}(x_1) + a_{12}(x_2) + ... + a_{1n}(x_n)$$

(3.18)

$$C_2 = a_{21}(x_1) + a_{22}(x_2) + ... + a_{2n}(x_n)$$

Where C_1 and C_2 = the subject's score on principal component 1 and 2 respectively a_{1n} and a_{2n} are the regression coefficient (or weight) for observed variable n, as used in creating principal component 1 and 2 respectively

x_n = the subject's score on observed variable n.

The weights are optimal and unique because no other set of weight can produce a set that is more successful in accounting for variance in the observed variables. The weights are created so as to satisfy the principle of least squares (PLS). The variance for C_1 (Var C_1), C_2 (Var C_2), C_3 (Var C_3) ... Cn (Var C_n) are referred to as eigenvalues and Var C_1> Var C_2>Var C_3…Var C_n. The principal components are a linear combination of the original variables and they are normally arranged in the order of decreasing variance.

Principal components are represented by a single figure called biplots, biplots help to visualize the relationship between the variables and the observations. The longer the length of the principal component in the biplot the higher is the variance. Variables that form a cluster have the least angle between them and therefore correlation between them is said to be strong.

26

3.3.2 Hierarchical Cluster Analysis

Cluster analysis groups objects based only on the information found in the data that describes the objects and their relationships. It assigns observations to groups (clusters) so that the observations within each group are similar to one another with respect to variables of interest and the groups themselves stand apart from one another thereby dividing the observations into homogenous and distinct groups. Clustering is done by measuring distances between utilities so that distances between similar utilities are a short distance apart. A popular distance measured based on variables that take continuous concentrations is to standardize the concentrations by dividing by the standard deviation and then compute the distance between objects using the Euclidean distance.

The Euclidean distance d_{ij} between two cases, i and j with variable concentrations $(x_{i1}, x_{i2}, \ldots, x_{ip})$ and $(x_{j1}, x_{j2}, \ldots, x_{jp})$ is defined by **Eq. 3.19,** (Trauth, 2015)

$$d_{ij} = \left\{ (x_{i1} - x_{j1})^2 + (x_{i2} - x_{j2})^2 + \cdots + (x_{ip} - x_{jp})^2 \right\}^{1/2} \tag{3.19}$$

Often weighted Euclidean distance is preferred by multiplying the Euclidean distances by the weights, **Eq. 3.20,**

$$d_{ij} = \left\{ w_1(x_{i1} - x_{j1})^2 + w_2(x_{i2} - x_{j2})^2 + \cdots + w_p(x_{ip} - x_{jp})^2 \right\}^{1/2} \tag{3.20}$$

where $w_1, w_2, \ldots, w_p$ are the weights of the variables $1,2, \ldots, p$ so that $w_i \geq 0$, the sum of the weights must be equal to 1, **Eq. 3.21.**

$$\sum_{i=0}^{p} w_i = 1 \tag{3.21}$$

3.3.3 Linear Regression (Correlation) Analysis

Correlation assesses the relationship between two quantitative random variables by making use of the linear product moment correlation coefficient (Pearson's correlation coefficient) to express the strength of their relationship. Pearson's correlation r is given by **Eq. 3.22.**

$$r = \frac{n\Sigma xy - \Sigma x \Sigma y}{\sqrt{\{n\Sigma x^2 - (\Sigma x)^2\}\{n\Sigma y^2 - (\Sigma y)^2\}}}$$

(3.22)

Correlation r lies between -1 and +1, ($-1 \leq r \leq +1$), there exist perfect positive, perfect negative and zero correlation when r is +1, -1 and 0 respectively.

3.4 Pollution Indices

The level and extent of heavy metal pollution in soil and river sediments around the Migori Transmara gold mining area were estimated by calculating the contamination factor, enrichment factor and geo-accumulation index. This was done in order to assess the quality of ecological and geochemistry environments and therefore help understand heavy metal pollution in the area.

3.4.1 Geo-accumulation Index (I_{geo})

Geo-accumulation index (I_{geo}) assesses the contamination by comparing current and pre-industrial concentration of heavy metals. The mean metal concentration of heavy metals in shale was used as a reference concentration implicating the pre-industrial environment (Turekian and Wedepohl, 1961). Geo-accumulation is given by, **Eq. 3.23.**

$$I_{geo} = log_2 \left(\frac{C_n}{1.5B_n}\right)$$

(3.23)

Where C_n is the concentration of the element in the soil, B_n is the geochemical background concentration (the concentration in the earth's crust), natural fluctuations in the content of the

given environment and very small anthropogenic influences are allowed using a factor 1.5 (Loska *et al.*, 2004). Nilin *et al.* (2013) , grouped I_{geo} in seven distinguished classes, **Table 3.1**.

Table 3. 1: Classes of Geo-accumulation Index

Class	Concentration	Soil quality
0	$I_{geo}{\leq}0$	Practically uncontaminated
1	$0{<}I_{geo}{\leq}1$	Uncontaminated to moderately contaminated
2	$1{<}I_{geo}{<}2$	Moderately contaminated
3	$2{<}I_{geo}{<}3$	Moderately contaminated to heavily contaminated
4	$3{<}I_{geo}{<}4$	Heavily contaminated
5	$4{<}I_{geo}{<}5$	Heavily contaminated to very heavily (extremely) contaminated
6	$5{<}I_{geo}$	Very heavily (extremely) contaminated

Class 6 is open and includes all concentrations of geo-accumulation index that are above than class 5.

3.4.2 Enrichment Factor (EF)

Enrichment factor (EF) is based on the standardization of a tested element against a reference element. A reference element has low occurrence and mobility in nature e.g. Al, Fe, Zn, Sc, Mn and Ti in soil and sediments (Younis, 2018; Pacyna and Winchester, 1990; Quevauviller *et al.*, 1989; Reimann *et al.,* 2012). Average concentration of elements in the earth's crust was adopted to enable comparison between I_{geo} and EF. The formula modified by Loska *et al.* (2004) was used to calculate EF, **Eq. 3.24**

$$EF = \frac{\frac{C_n \, sample}{C_{ref} \, sample}}{\frac{B_n \, (Background)}{B_{ref}(Backround)}}$$

(3.24)

Where C_{ref} (sample) is the concentration of the reference element examined in the environment, B_{ref} is the concentration of the reference element in the earth's crust. C_{ref} of the studied elements were (As 1.6; Cd 0.1; Cr 69; Cu 39; Hg 0.08; Ni 55; Pb 17; Zn 67 mg/kg), adopted from reference concentrations for soil by Taylor and McLennan (1995). Zinc was used as reference element (B_{ref}) because it shows no or very low vertical mobility or degradation phenomenon in soil (Barbieri, 2016; Younis, 2018a). Enrichment factors are categorized in 5 classes (Sutherland, 2000), **Table 3.2**.

Table 3. 2: Classes of Enrichment Factors

Class	Description
EF<2	Deficiency to minimal enrichment
EF=2-5	Moderate enrichment
EF=5-20	Significant enrichment
EF=20-440	Very high enrichment
EF>40	Extremely high enrichment

3.4.3 Contamination Factor (CF)

This is ratio of contamination of the elements in the sample to the baseline concentrations of the same element, **Eq. 3.25.**

$$CF = \frac{C_n}{B_n}$$

(3.25)

where B_n is the geochemical background concentration of the examined heavy metal in soil which was calculated by summing geometric mean and twice the geometric standard deviation. For the sediments, the median of the concentrations was used as the geochemical background because it

is a representative of the local data and is rarely affected by outliers (Ohta *et al*., 2005). Contamination factor was classified in four classes by Hakanson (1980), **Table 3.3**.

Table 3. 3: Classes of Contamination Factors

Class	Description
CF<1	Low contamination factor indicating low contamination
1≤CF<3	Moderate contamination factor
3≤CF<6	Considerable contamination factor
6≤CF	Very high contamination

3.4.4 Degree of Contamination (C_{deg})

Degree of contamination is the sum of contamination factors of all the elements studied in the environment, **Eq. 3.25**.

$$C_{deg} = \sum_{i=1}^{n} CF_i$$

(3.26)

Where i= 1, 2,…, n

Hakanson (1980) categorized degree of contamination into four classes, **Table 3.4**.

Table 3. 4: Classes of Degree of Contamination Factors

Class	Description
$C_{deg} < 8$	Low degree of contamination
$8 \leq C_{deg} < 16$	Moderate degree of contamination
$16 \leq C_{deg} < 32$	Considerable degree of contamination
$32 \leq C_{deg}$	Very high degree of contamination

CF and C_{deg} are open scale that is equal or greater than 6 and 32 respectively.

CHAPTER FOUR

Materials and Methods

4.1 Study Area and Mining Sites

The Migori-Transmara gold mining complex covers parts of Migori and Narok counties in southwestern Kenya, it covers an area of about 5724 km^2. The main gold mining areas in Transmara are Farah, Lolgorien and Red Ray while Akala, Kabobo, Kitere, Macalder, Masara, Mikey, Namba and Osiri are in Migori County, **Figure 4.1**. Most of the mines in Transmara are located around Lolgorien (1º13′51.64″S and 34º48′36.47E″; Elevation 5377 ft) while most mines in Migori around are located around Macalder (0º58′16.93″S and 34º15′27.03E″; Elevation 3906 ft). The main rivers draining this region include Ibwa, Kuja, Kwach, Lolgorien, Migori, Mikei, Munyu, Pasaris and Regete.
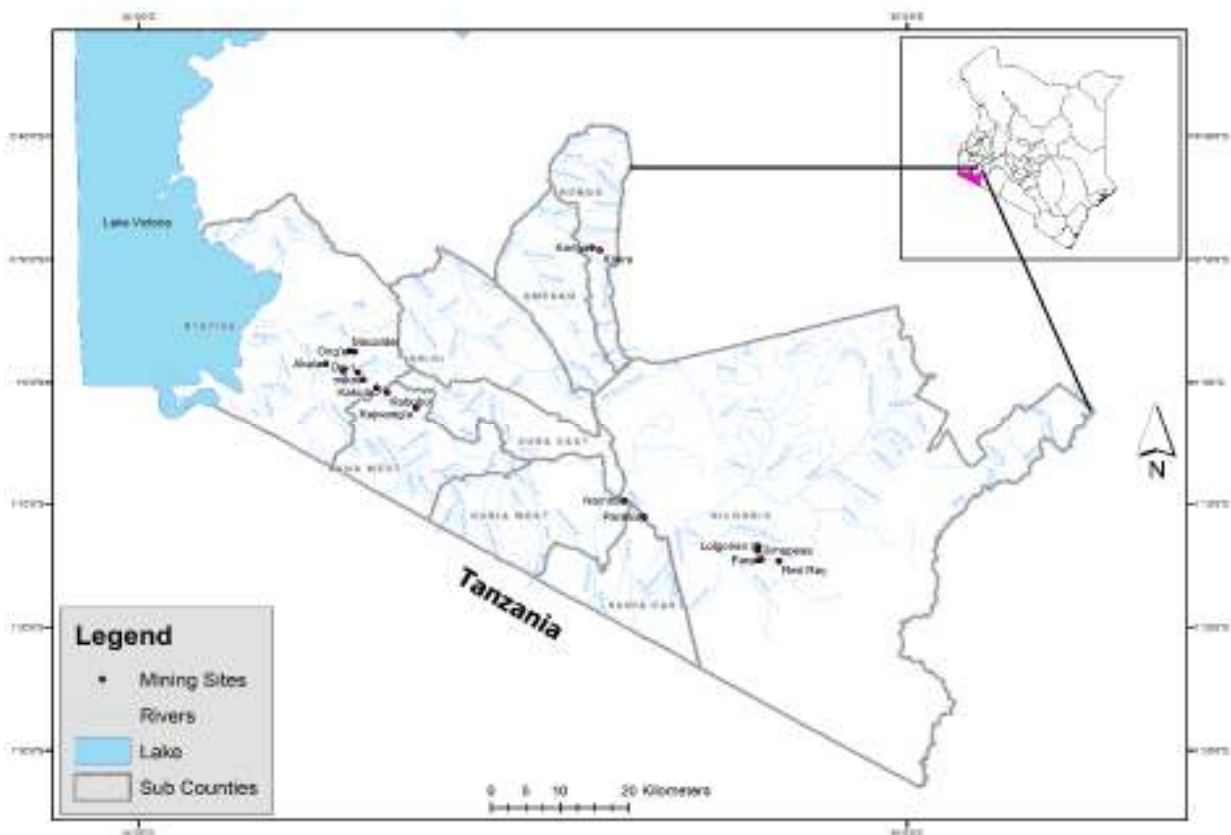
Figure 4. 1**:** Migori Transamara Gold Mining Sites**.**

4.2 Sample Collection

Fifty-six, forty-four, twenty-eight, eighteen and fourteen soil, river sediment, moss, lichen and tailing samples respectively were collected using a mixture of random and judgmental sampling methods. Judgmental sampling was preferred in areas of interest like mines and flood prone areas like Kabuto while random sampling was mostly carried out away from the from the mines. Accessibility of the sampling location and availability of the sample, especially for the biomonitorswas also considered during sampling. To determine the background values of the various heavy metals and radionuclides, control samples were collected away at a location 25 kilometers away from the nearest mine, the location had no mining history and had no sign of human interference.

4.2.1 Collection of Soil Samples

About one kilogram of soil was collected at a depth of about 15 cm from undisturbed locations using a hand trowel within and away from the mining areas, **Figure 4.2**. To avoid any contamination by dust blown from the nearby weather roads, the samples were collected at least 300 meters away from roads. Plant roots, stones and other debris were removed before packing in self-zipping bags labeled with the geographical location, reference number of the location and date of collection. Before collecting the next sample, the hand trowel was thoroughly cleaned with distilled water and wiped dry to avoid contamination. In the laboratory the samples were air dried in the open for seven days at room temperature of about 25˚C.
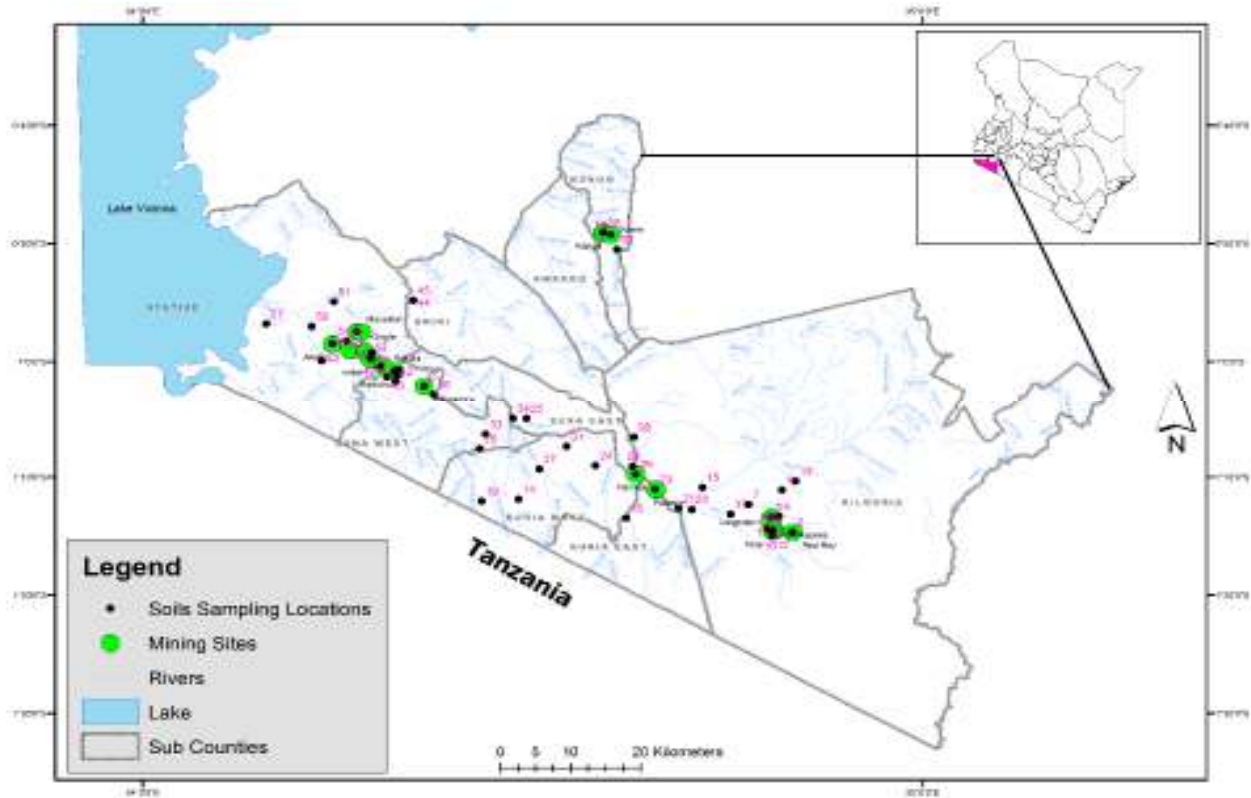
Figure 4. 2: Soil Sampling Locations

4.2.2 Collection of River Sediment Samples

River sediment samples, each weighing about one kilogram, were collected from the river beds rivers beds (**Figure 4.3**) using stainless trowels at the middle of the flowing rivers. Pieces of stones, leaves, other debris removed and excess water was poured out before packing the samples in self-zipping bags marked accordingly. Before collecting at the next sample, the hand trowel was cleaned accordingly. In the laboratory the samples were initially air dried in the open for seven days at room temperature of about 25˚C.
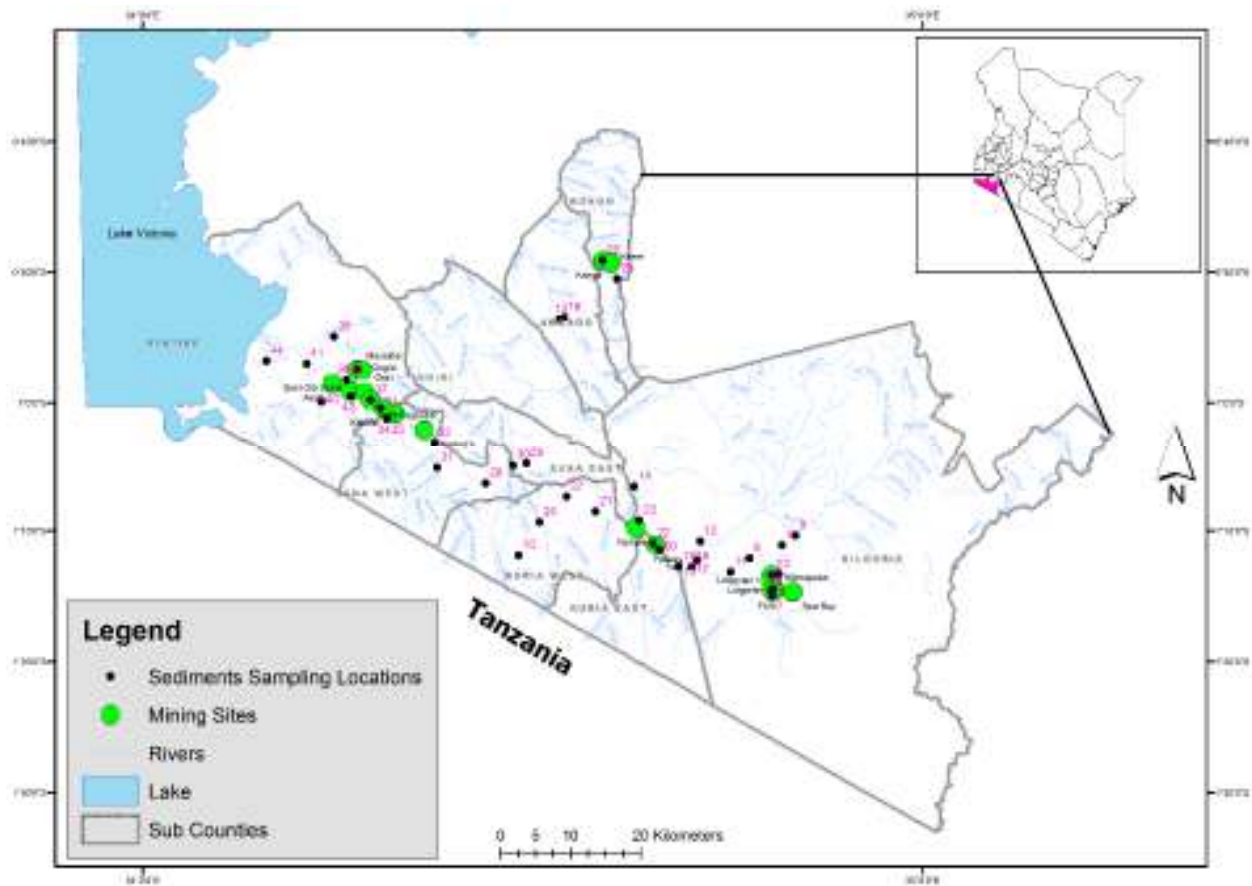
Figure 4. 3: River Sediment Sampling Locations.

4.2.3 Collection of Mine Tailing Samples

Wet and dry tailings each weighing about one kilogram were collected from the bottom of panning ponds and tailing heaps around panning ponds respectively (**Figure 4.4**). Excess water and debris were discarded before packing and labelling accordingly. Before collecting the next sample, the hand trowel was cleaned accordingly. In the laboratory the samples were initially air dried in the open for seven days at room temperature of about 25˚C.
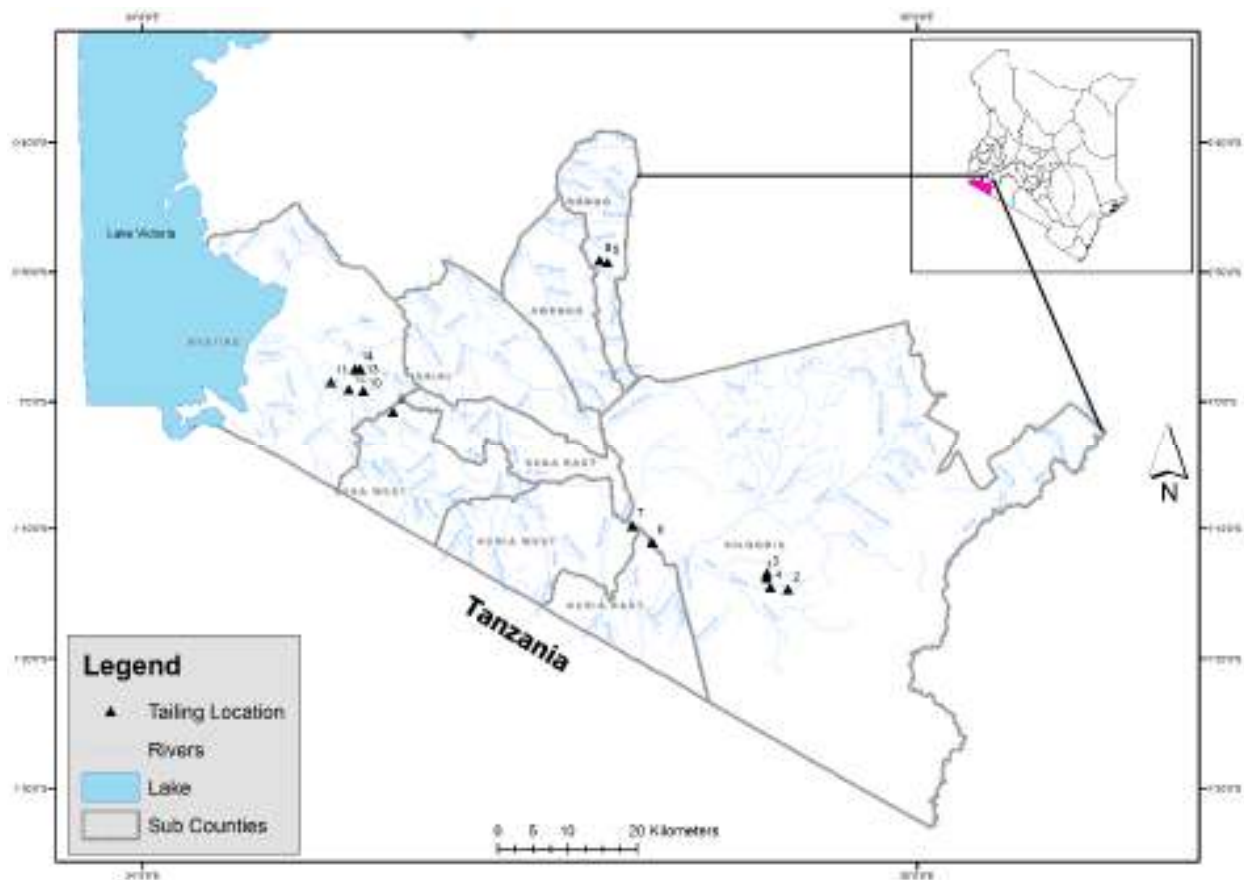
Figure 4. 4: Tailing Sampling Locations

4.2.4 Collection of Lichen and Moss Samples

Thallus of lichens and moss samples were carefully removed from the back of trees and rocks using stainless steel knives (**Figure 4.5** and **4.6**). Soil and other visible foreign materials were then removed before packing in self-zipping polythene bags and labeled accordingly. The samples were collected at least 2.5 meters above the ground away from busy roads to avoid contamination by soil and dust. Before collecting the next sample, the stainless-steel knives were thoroughly cleaned with distilled water and wiped dry to avoid contamination. In the laboratory the samples were initially air dried in the open for seven days at room temperature of about 25˚C.
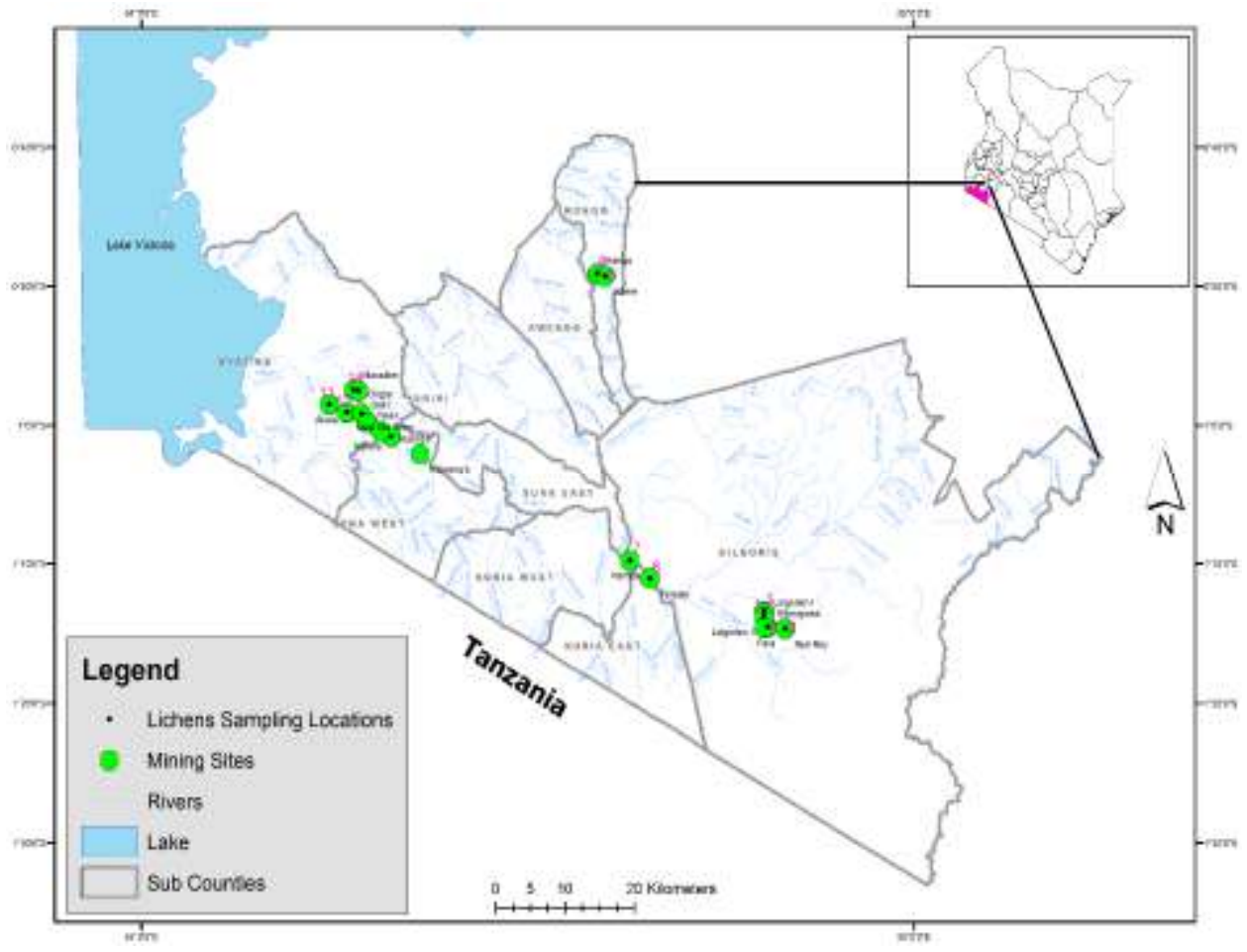
Figure 4. 5: Lichens Sampling Locations
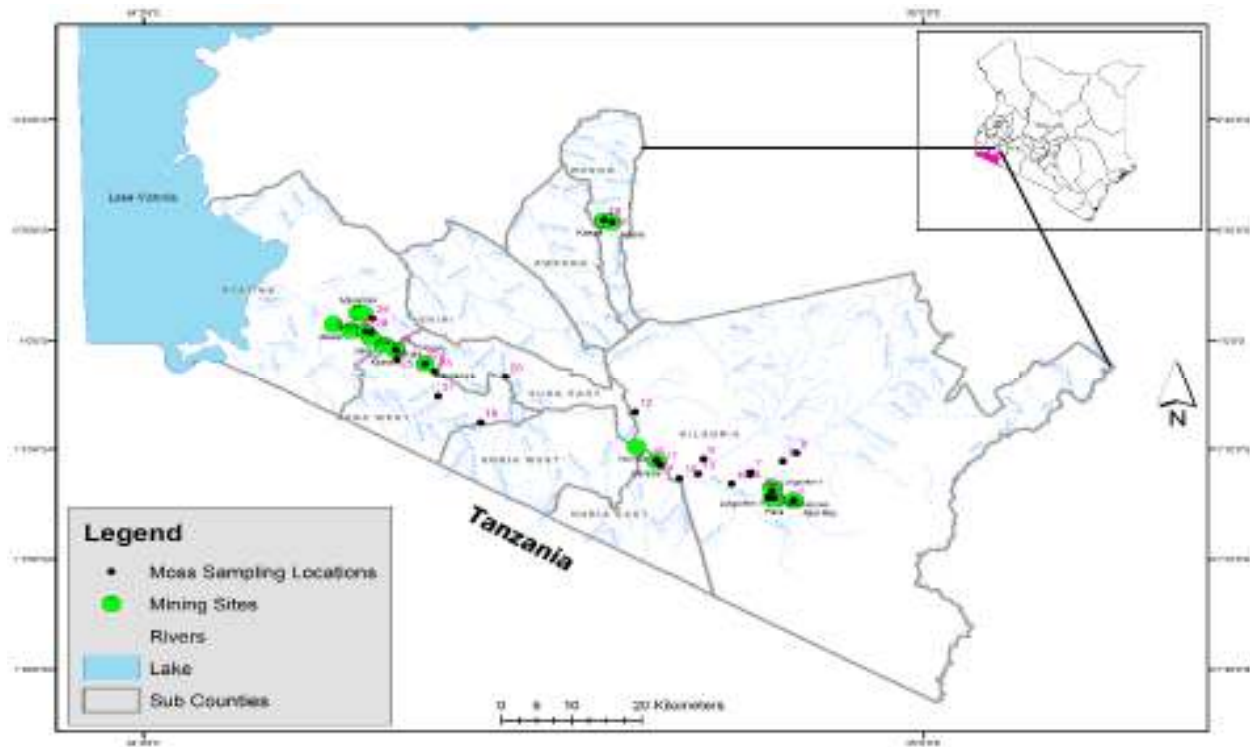
Figure 4. 6: Moss Sampling Locations.

4.3 Preparation of Samples for Analysis

4.3.1 General Sample Preparation

Before analysis all the samples were prepared as described below:

i.   About 500 grams of dry soil, river sediment and tailing samples was first pulverized using the agate motor.

ii.   The pulverized sample was then sieved through a (90-100) micrometer nylon sieve.

iii. The samples were then dried in the oven at $105°C$ for 12 hours

iv.   Moisture content of the samples was then determined by weighing an empty sample holder W_h

v.   About 50 grams of the sample was placed on the sample holder and re-weighed W_w before drying in the oven for 12 hours at $105°C$.

vi.   The weight of the dried sample plus the sample holder was again taken W_d

vii. Moisture content of the samples was then calculated

$$Moisture\ Content = \frac{W_w - W_d}{W_d - W_h}$$

(4.1)

4.3.1.1 Preparation of Samples for Analysis of As, Co, Cr, Cu, Ni, Pb and Zn by AAS

0.5 grams of each of the sieved lichen, river sediment, soil and tailing samples were digested in a mixture of concentrated nitric acid (HNO_3) of 70% purity and perchloric acid ($HCIO_4$) of 70% purity in the ratio {3:1; [15 ml (HNO_3): 5 ml ($HCIO_4$)]} using Teflon beakers on a hot plate. The beakers were loosely covered to avoid contamination. Heating of the digestes went on until white fumes of $HCIO_4$ were seen, indicating all the HNO_3 had evaporated. The digestes were diluted with 20 ml of deionized distilled water and filtered through a Whatman filter paper number 42 into a volumetric flask. Each filtrate in the volumetric flask was then topped up to 100 ml with deionized distilled water. A series of blank samples were prepared using the same digestion method and the filtrates were analyzed for the concentration of the heavy metals.

4.3.1.2 Preparation of Samples for Gamma Ray Spectrometric Analysis

Before packaging each of the pulverized soil and river sediment sample in standard 250 ml plastic containers for gamma counting, a standard 250 ml empty plastic container was first weighed then filled with the sample and weighed again in order to get the net weight of the sample. Four-stage sealing was done for each package to prevent radon from escaping from the containers, first the inner ream of each ream lid was smeared with Vaseline, in cases where there were gaps between the sample and the lid, candle wax was used to fill the gap before replacing the cap tightly, aluminum foil was then put above the sample. Masking tape was finally used to seal the edge of the lid all round. The samples were then left for at least thirty days to allow ^{238}U and ^{232}Th and their short-lived daughters to reach secular equilibrium before gamma spectrometric analysis.

4.4 Elemental and Activity Analysis

4.4.1 Elemental Analysis

4.4.1.1 Mercury Analysis in Plants, Soil, Sediments and Tailings

The total Hg in lichen, moss, river sediment, soil and tailings, samples was determined using a Direct Mercury Analyzer (DMA80), atomic absorption spectrophotometer, Milestone, Wesleyan University, Middletown, CT, USA), **Figure 4.7**. This method was preferred over liquid digested method because it is less labor intensive hence minimizing mercury losses, there is minimal contamination compared to digestion, it is automated therefore less time consuming and it doesn't generate liquid chemical waste among others (Melendez-Perez *et al., 2*014).

A weighed sample (150-200 mg) was deposited into a sample boat and then introduced into the DMA where oxygen began to flow over the sample. Decomposition oven temperature was increased; first for drying the sample, then for decomposing it.

Figure 4. 7: DMA80 Atomic Absorption Spectrophotometer**.**

A continuous flow of oxygen was carried out on the decomposition products through a catalyst bed, where interferants were trapped. All the mercury species were reduced to elemental Hg before

transferring to a gold amalgamator where mercury was selectively trapped. The system was purged and the amalgamator was subsequently heated to release all the mercury vapors to the single-beam, fixed wavelength atomic absorption spectrophotometer. The absorbance measured at 253.7 nm was proportional to the mercury content in the sample. To determine method precision, three replicates of each sample were considered.

DMA80 provides two working ranges for Hg detection: 0-40 and 40-600 ng. Each range is calibrated independently to optimize the response over the entire dynamic range. Calibration samples containing 0, 10, 20, 30, and 40 µl of 1 or 10 ppm Hg were processed to calibrate the instrument for 0-40 and 40-400 ng, respectively, **Appendix F3**. The limit of detection (LOD) and limit of quantification (LOQ) were 0.5 and 1.25 µg kg^{-1} respectively. Analytical procedure validation of the soil and sediment samples was performed with a calcareous loam soil (BCR-141 R) obtained from the European Commission Community Bureau of Reference (ECCBR). There was a good agreement between the obtained and the certified / recommended (0.24 ± 0.03 µg kg^{-1}, of total Hg, for soil) concentrations in mercury, showing an average recovery of 98.7%.

4.4.1.2 Analysis of As, Cd, Cu, Cr, Ni, Pb, and Zn

The concentration of As and other metals (Cd, Cu, Cr, Ni, Pb, and Zn) in soil, sediment (mine tailing and river), as well as in lichen and moss samples were established by Atomic Absorption Spectrometry (PerkinElmer, Shelton, CT, USA 06484-4794) applying Flame Atomic Absorption Spectrometry equipment for the As and Zn analyses, whereas Graphite Furnace Atomic Absorption Spectrophotometry was used for the analysis of Cu, Cr, Cd, Pb, and Ni (Carbonell *et al.,* 2011), **Figure 4.8**. The analytical procedures were validated using reference samples (river sediment, BCR-320; olive leaves, BCR-62; and calcareous loam soil, BCR-141R) obtained from ECCBR. Percentage recoveries of metals in the reference soil were as follows: 105% for Cr, 97% for Ni, 99% for Cd, 98% for Pb, 95% for Cu, and 101% for Zn. The recoveries regarding the olive leave reference material were 99% for Cu, 97% for Pb, 101% for Cd, and 108% for Zn.

Figure 4. 8: Perkin Elmer Atomic Absorption Spectrometer.

4.4.1.3 Calculation of the limits of detection

The limits of detection (LOD) and limit of quantification (LOQ) were calculated using the **Eqs** 4.2 and 4.3 respectively (Şengül, 2016)

$$LOD = 3\left(\frac{\sigma}{S}\right) \qquad (4.2)$$

$$LOQ = 10\left(\frac{\sigma}{S}\right) \qquad (4.3)$$

Where σ is the standard deviation of the response curve and S is the slope of the callibration curve.

4.4.2 Activity Analysis

Every day before analysis energy and efficiency calibration and resolution was performed on the detector inorder to identify and quantify the radionuclides of interest.

4.4.2.1 Energy and Efficiency Calibration and energy resolution of the HPGe detector

RGMix was run in the same set up where the samples would be run and energies (keV) of the identified radionuclides was plotted against peak efficiency **Appendix F1, Table 4.1**. The activity concentration of ^{238}U, ^{232}Th and ^{40}K in RGMix is 4940 Bq/kg, 3250 Bq/kg and 14,000 Bq/kg respectively.

Table 4. 1: Energy, Peak Efficiency and Radionuclide of RGMix

ENERGY	Peak Efficiency	Radionuclide
77.11	0.009801	Pt-190
87.3	0.015952	Eu-155
186.1	0.027222	Ra-226
351.92	0.009124	Pb-214
609.31	0.004897	Bi-214
911.21	0.00384	Ac-228
1460.81	0.002132	K-40

To acquire a spectrum of a multinuclide standard, SRM-1, was run for 10 minutes. Maestro software was then used to perform energy calibration based on the acquired spectrum, respective energies were then assigned against the channel numbers and plotted, **Table 4.2, Appendix F2**.

Table 4. 2: Chanel, Energy and Radionuclide of SRM-1

Channel	Energy (KeV)	Radionuclide
246	60	Am-241
2773	662	Cs-137
4917	1173	Cs-137
5587	1333	Co-60

The energy resolution of the of the detector was determined by running 137Cs in the detector for 600 seconds and the spectrum obtained at energy peak of 662 keV was determined to be 2.21±0.24.

Figure 4. 9: High Purity Germanium (HPGe) gamma ray detector

4.7.1.3 Activity Counting and Activity Calculation

Before running the samples in the detector, background intensity was done on the detector by counting distilled water in similar containers used to pack the samples and run for the same period under the same geometry. The background intensity was then subtracted from the gross intensity of the samples to get the net intensity of the samples.

Each of the samples was put in shielded high purity germanium (HPGe) detector and activity counted for 12 hours live time. Following the spectrum, count rates for each of the detected photopeak and activity per mass unit (specific activity or radiological concentration) was then calculated using(Mustapha et al., 1999) **Eq. 4.3**

$$A_s = \frac{M_{st} x A_{st} x I_s}{M_s x I_{st}}$$
(4.3)

Where A_s is the activity of the sample, M_{st} is the mass of the standard, A_{st} is the activity of RGU-1, RGTh-1RGK-1 which were 4940 Bq/kg, 3250 Bq/kg and 14,000 Bq/kg respectively, I_s is the intensity of the sample, M_s is the mass of the sample and I_{st} is the intensity of the standard. Based on the measured gamma-ray photopeaks emitted by the specific radionuclides in the ^{238}U and ^{232}Th decay series and in ^{40}K, their radiological concentrations in the samples were determined. Calculations relied on the establishment of secular equilibrium in the samples, due to much smaller half-life of daughter radionuclides in the decay series of ^{238}U and ^{232}Th. Specific activity of ^{238}U was determined from the average concentrations of ^{214}Pb and ^{214}Bi at energies of 352 keV and 609 keV respectively while that of ^{232}Th was calculated from the averages of concentrations of ^{212}Pb, ^{208}Tl and ^{228}Ac at energies of 238.63 keV, 583 keV and 911.21 keV respectively. In the process of considering particular energy peaks for calculating the activities of ^{238}U and ^{232}Th, when more than one energy peak of a particular decay series was present, average activity concentration was considered. Otherwise for one energy peak, the energy peak was taken to be the activity concentration of that particular radionuclide. The activity concentration of ^{40}K was directly determined from the peak areas of gamma- ray transition energy of 1460 keV.

CHAPTER FIVE

5. 0 Results and Discussions

The results of analysis, multivariate chemometric and geostatistical modeling of the radioecological and associated heavy metal impact of gold mining in the Migori-Transmara complex of Southwestern Kenya are hereby presented and discussed. The results consist of heavy metal and activity concentrations, spatial variability and source apportionment of biomonitors (lichens and moss), river sediments, soil and mine tailings. Activity concentration of soil and river sediments and their spatial variability is also presented together with their pollution indices. The LOD of the heavy metals were As-0.2, Cd-0.008, Cr-0.03, Cu-0.1, Hg-0.5, Ni-0.3, Pb-0.05, Zn-0.1 (x10^{-3}mg/kg) and LOD of activity concentration were 5 Bq/kg for ^{238}U Bq/kg and ^{232}Th Bq/kg and 30 Bq/kg for ^{40}K.

Geostatistical inetrpolation was done using Ordinary kiriging and maps were drawn using ArcGis 10 and Surfer 13. During interpolation, simples collected at Kanga and Kitere since they were far from rest and their interpolation would not give realistic results.

For ease of interpretation of geostatistical maps, activity and heavy metal concentration and radiation doses were groups as shown, **Table 5.1.**

Table 5. 1: Classes of activity and elemental concentration and radiation doses

Class	Description
1	Blue ≤ Background
2	Background< Green ≤ 2*Background
3	2*Background < Yellow< ≤5* Background
4	5*Background < Orange ≤ 10*Background
5	10*Background <Red

5.1 Heavy Metal concentration in mosses and lichens

4.1.1 Heavy Metal Concentration in Lichens

The concentration of mercury was highest at all the sampling locations apart from Kabobo where the concentration of arsenic (0.798 mg/kg) was the highest; however, the concentration of cadmium was the lowest at all the sampled locations, **Appendix A, Table 5.2**. High mercury concentrations were found at Lolgorien Center (1.646 mg/kg), Kajwang'a (1.037 mg/kg), Kitere (0.745 mg/kg) and Kanga (0.593 mg/kg). The concentrations of mercury at Kanga and Kitere are nearly the same, this is due to proximity to each other which may imply the same miners are involved. The concentration of mercury is however comparable to that of arsenic and zinc at Kabobo and Mikeyi even though the other metals have lower concentrations at the same site. Mercury concentrations (0.10 – 3.10 mg/kg) in lichens in Mugusu and Mweru Tanzania where artisanal gold mining staretd in 1990's were higher than in this study (Ikingura and Akagi, 2002), this difference is due to the high number (over 7000) of miners that were at the mines at the time.

The mean and median of the heavy metal concentrations in lichen decrease in the order Hg>Zn>As>Cu>Pb>Cr>Ni>Cd and Hg>Zn>Cu>Ni>Cr>Pb>As>Cd respectively (**Table 5.2**). All the mean and median concentrations are higher than the backround concentrations, this shows gold mining has impact on the concentration of heavy meyals in the atmosphere in the Migori Transmara gold mining area. The minimum and maximum concentration of mercury in this study is lower and higher respectively than the minimum and maximum concentration of mercury in lichens growing around gold mines in Imweru and Mugusu in Tanzania (Ikingura and Akagi, 2002). The range of mean concentration of As (0.10 – 8.00 mg/kg), Cd (0.26 – 1.41 mg/kg), Cu (0.26 – 370.00 mg/kg) and Hg (0.16 – 1.24 mg/kg) in lichens at Tarakwa gold mines in Ghana are however higher than all the maximum concentrations of the heavy metals in this study apart from Hg whose maximum concentration at Lolgorien, is higher than the maximum mean range (Boamponsem *et al.,* 2010).

The coefficient of variation (CV) increases in the order Zn< Ni<Cu<Cr<Cd<Hg<Pb<As that is 47.27, 55.61, 59.14, 69.48, 103.23, 105.72, 117.79 and 263.54 respectively, an indication that the levels of Zn and As in the ambient atmosphere are the least and most impacted by the gold mining

respectively. High CV of Cd, Hg, Pb and As shows their concentartion are heavyly influenced by gold mining e.g. Kajwang'a, Kabobo and and Macalder where all the mentioned heavy metals are at high concentrations (Sun et al., 2021) . All these hot spots were around active gold mines confirming the impact of gold mining in the ambient atmosphere in gold mines.

Table 5. 2: Summary of Concentration of Heavy Metals in Lichens (x 10^{-3} mg/kg)

Description		As	Cd	Cr	Cu	Ni	Pb	Zn	Hg
Mean		75.80	0.31	20.35	25.67	19.26	21.30	82.23	390.64
Std. Deviation		199.76	0.32	14.14	15.18	10.71	25.09	38.87	412.98
Median		4.05	0.22	14.81	19.55	16.23	12.11	72.29	204.67
MAD		2.83	0.08	2.95	4.76	4.11	7.24	18.32	66.67
CV (%)		263.54	103.23	69.48	59.14	55.61	117.79	47.27	105.72
Skewness		3.29	3.15	2.08	1.46	1.63	2.39	0.98	2.05
Minimum		0.70	0.01	7.34	11.19	6.24	3.53	38.00	57.33
Maximum		797.73	1.49	63.69	66.47	49.83	102.63	164.77	1645.99
BGV		1.54	0.18	11.85	12.18	14.44	5.77	43.84	97.68
Percentiles	25	2.23	0.14	12.40	15.42	12.15	5.67	54.27	158.16
	50	4.05	0.22	14.81	19.55	16.23	12.11	72.29	204.67
	75	28.11	0.33	22.86	38.11	23.09	26.46	111.80	621.73

5.1.2 Heavy Metal Concentration in Moss

The concentration of mercury and cadmium are highest and lowest respectively in all the sampling locations as was observed in lichens. The highest concentration of mercury was found at Kajwang'a (2.017 mg/kg), followed by 1.004 mg/kg and 0.086 mg/kg at Lolgorien and Farah respectively, **Appendix A**. High concentration of mercury and arsenic at Kajwang'a suggests the position of this location at the edge of a valley played a role in accumulating them in the atmosphere apart from high number of miners that were present during sample collection.

The mean and median concentrations (mg/kg) of the heavy metals found in moss are decreasing in the order Hg>Zn>Cr>Cu>As>Ni>Pb>Cd and Hg>Zn>Cu>Cr>Ni>Pb>As>Cd respectively, **Table 5.3**. Almost the same order of median is seen in lichens with only Cr and Ni swarping positions. The median concetration of Hg, Cu, and Cr are almost the same in both biomonitors and those of Pb, As and Cd in lichens are twice that of moss, this confirms lichens as good bioaccumulators of Pb and Cd as was also found by Kłos *et al*. (2018). The high BGV of Cr compared to the mean concentration shows Cr is likely not to be emanating from gold mining in Transmara. Hg and Zn have the highest mean as was also observed in lichens; this confirms impact of gold mining on the availability of mercury in the atmosphere. The concentration of mercury found in this study is at least six times higher than the concentration of the other metals investigated confirming mercury is the highest air polluter in this region. The mean concentration of (Cr and Cu) and (Ni and Pb) are within the same range.

The CV (%) in moss increases in the order Zn<Cu<Ni<Cd<Pb<Hg<Cr<As with values 35.27, 62.53, 67.76, 78.57, 82.03, 118. 71, 119.6 and 313.59 respectively, As is the most anthropogenically influenced while Zn is the least. Even though the magnitude of impact of mining differ in lichens and moss, Zn and As are the least and the most influenced by anthropogenic activities respectively as was in lichens. Difference in lichens and moss have different bioaccumulation abilities of the studied heavy metals (Bargagli *et al*., 2002; Loppi and Bonini, 2000).

Table 5. 3: Summary of the Concentration of Heavy Metals in Moss (x 10^{-3}mg/kg)

Description		As	Cd	Cr	Cu	Ni	Pb	Zn	Hg
Mean		14.35	0.14	25.26	20.79	13.06	9.74	53.87	336.96
Standard Deviation		44.93	0.00	30.61	13.00	8.80	7.96	18.98	400.03
Median		2.56	0.11	11.71	16.36	10.34	5.90	51.36	198.91
MAD		1.30	0.06	3.54	5.70	3.01	2.16	10.30	76.64
CV (%)		313.59	78.57	119.6	62.53	67.76	82.03	35.27	118.71
Skewness		4.72	1.65	1.86	1.23	2.17	1.62	1.43	3.19
Kurtosis		23.19	3.27	1.95	0.78	4.42	1.86	2.65	11.61
Minimum		0.54	0.01	5.07	7.27	6.30	3.13	31.00	98.23
Maximum		234.41	0.47	102.40	57.00	41.90	33.09	113.15	2016.91
BGV		1.00	0.03	102.40	37.00	8.60	3.70	41.00	181.22
Percentiles	25	1.51	0.06	8.60	11.63	7.59	4.16	41.03	135.11
	50	2.56	0.11	11.71	16.36	10.34	5.90	51.36	198.91
	75	8.15	0.18	17.38	27.27	13.55	12.42	62.31	314.84

5.1.3 Spatial Variability of the Heavy Metals in Moss

Spatial variability of heavy metals in mosses in discussed below: -

The spatial distribution of the investigated heavy metals in moss shows different patterns however there is evidence of influence from gold mining, this is seen in the spatial distribution of Hg, Pb, and As (**Fig 5.1 (a-d) and Fig 5.2 (a-d)**). Since these heavy metals are volatile, they readily evaporate into the atmosphere where their residential period is rather long thereby settling on the biomonitors. According to Veiga (2011) artisanal gold mining is one of the main point sources of elemental mercury in the atmosphere. Once elemental mercury is released into the environment, it is easily transformed to methyl mercury that is very volatile and once released into the environment it can be transported to nearby environments. Highest concentration (above ten times the background) of As is seen Mikei, Kajwanga and Kakula, this decreases towards Suna West to background concentration where there are no mining activities. Arsenic concentration around Namba and Parasis again increases 2*background -5*Background after which it decreases. Spatial distribution pattern of Cd, Ni and Zn appear not to be entirely influenced by mining, Cd and Zn could also be originating from fertilizers and combustion of fuels while Ni could be coming from

the natural sources like windblown dust (Ćujić *et al.*, 2014). The origin of Cd from other sources is supported by the fact that it is not abundant in crust and therefore it is likely not to be coming from soil (Boamponsem *et al.*, 2010). Cr and Cu show no influence from gold mining, Cr is majorly forming the windblown dust while Cu could be coming from fungicidal sprays (Wuana and Okieimen, 2011).
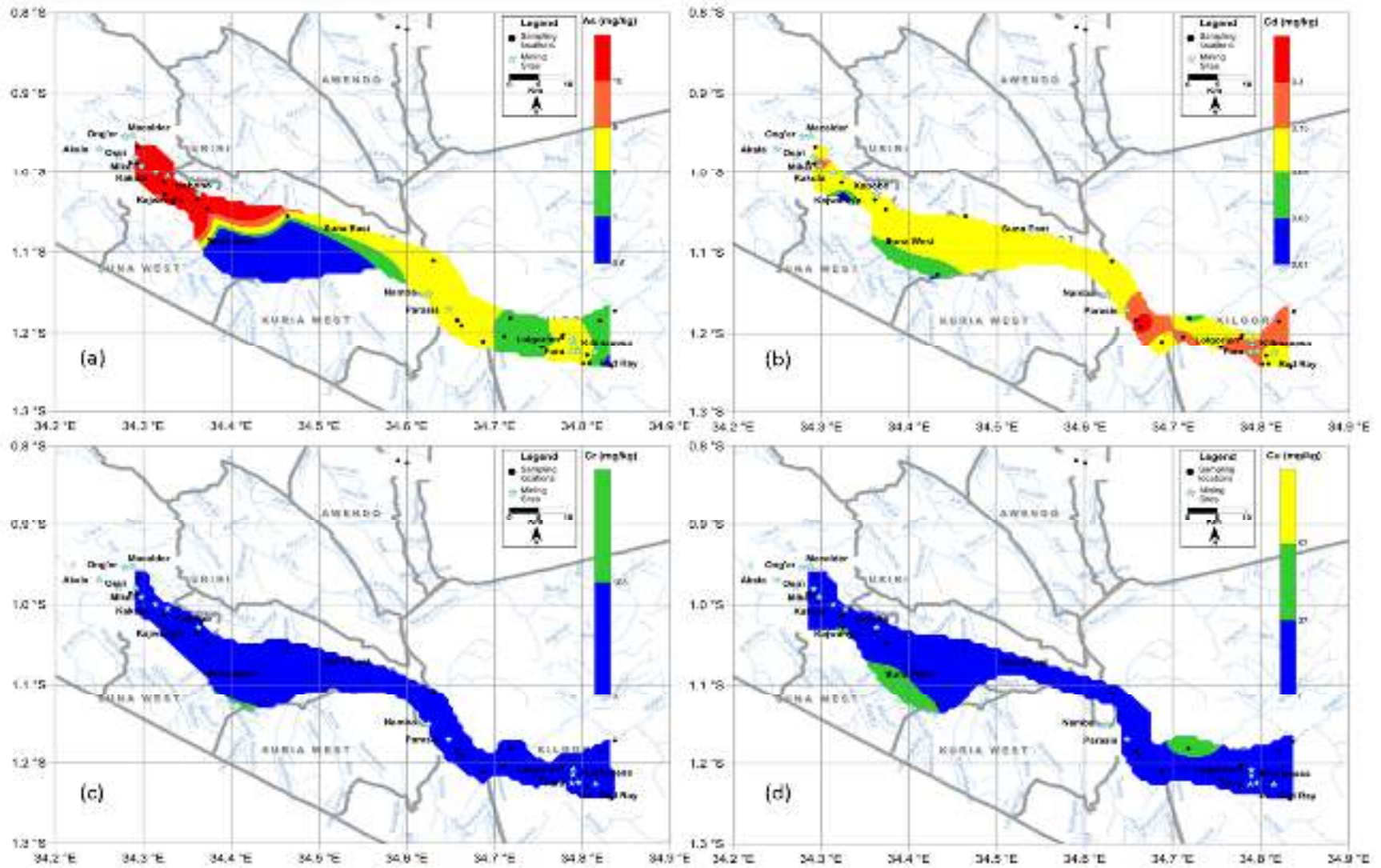
Figure 5. 1: Spatial distribution of a) As b) Cd c) Cr d) Cu in moss
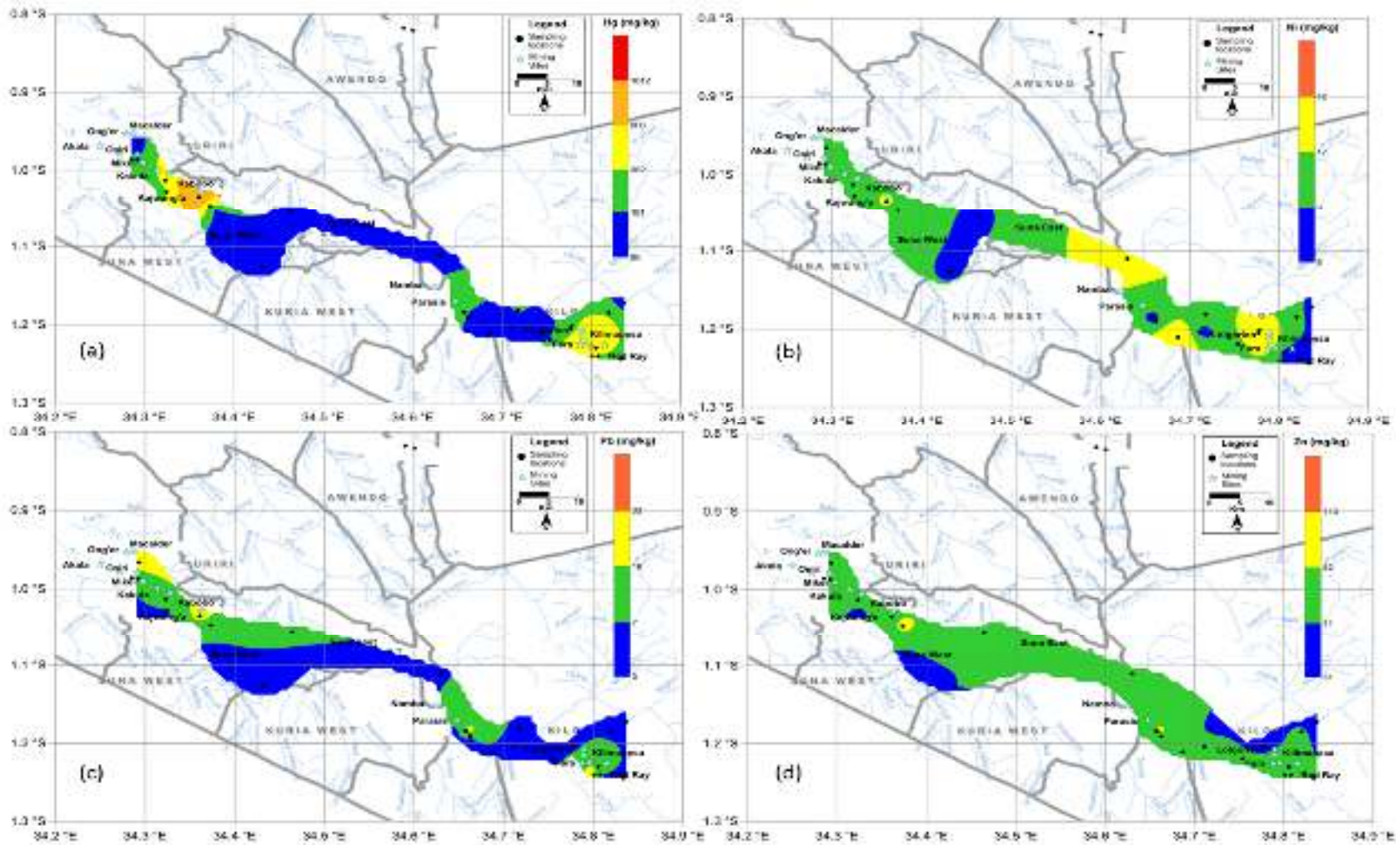
Figure 5. 2: Spatial distribution maps of a) Hg b) Ni, c) Pb d)Zn in moss

5.1.4 Spatial distribution of heavy metals in lichens

There is agreement between moss and lichens on the spatial distribution pattern of As, Hg and Pb, since both biomonitors have high concentration of the said heavy metals around the mines, this therefore confirms artisanal gold mining as their source, **Fig 5.3: (a - d)** and Fig **5.4: (a - d)**. Lichens and mosses also agree Cd, Ni and Zn are not entirely influenced by gold mining due to their mixed spatial distribution patterns away and near the mines. However, spatial distribution pattern of Cr and Cu in lichens suggest their distribution is not influenced entirely by artisanal gold mining contrary to moss that suggest mining does not influence their distribution pattern.

According to Brunialti *et al*. (2013), there is a positive correlation between the concentration of heavy metals in the atmosphere and their concentration in lichens. This therefore shows miners and the populace are likely to be exposed to diseases related to inhalation of Hg, As and Pb like lung irritation, infertility, Minamata disease, vomiting etc. since inhalation is one of the exposure pathways to them (Tchounwou *et al*., 2012).
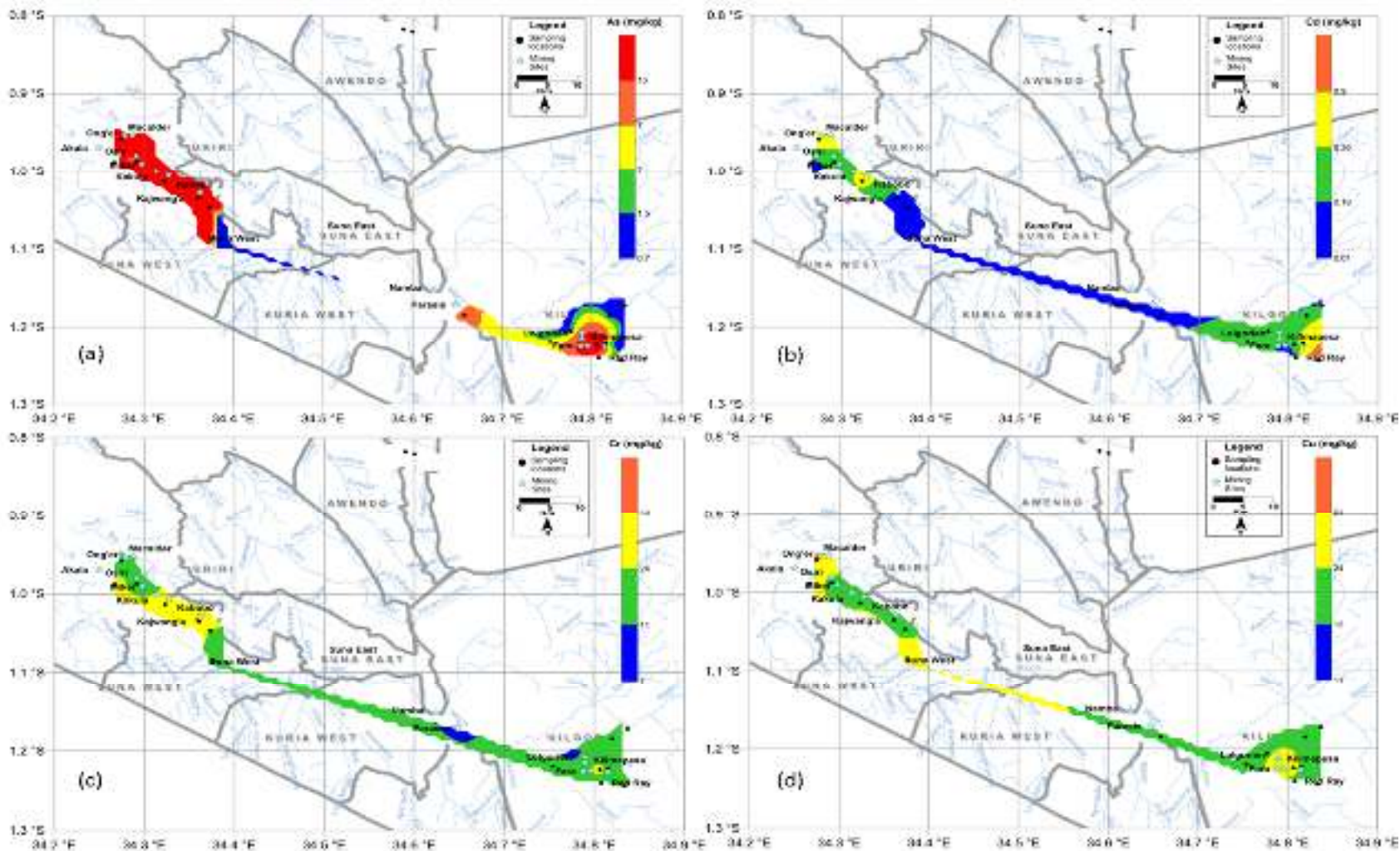
Figure 5. 3: Spatial distribution of a) As b) Cd c) Cr d) Cu in lichens
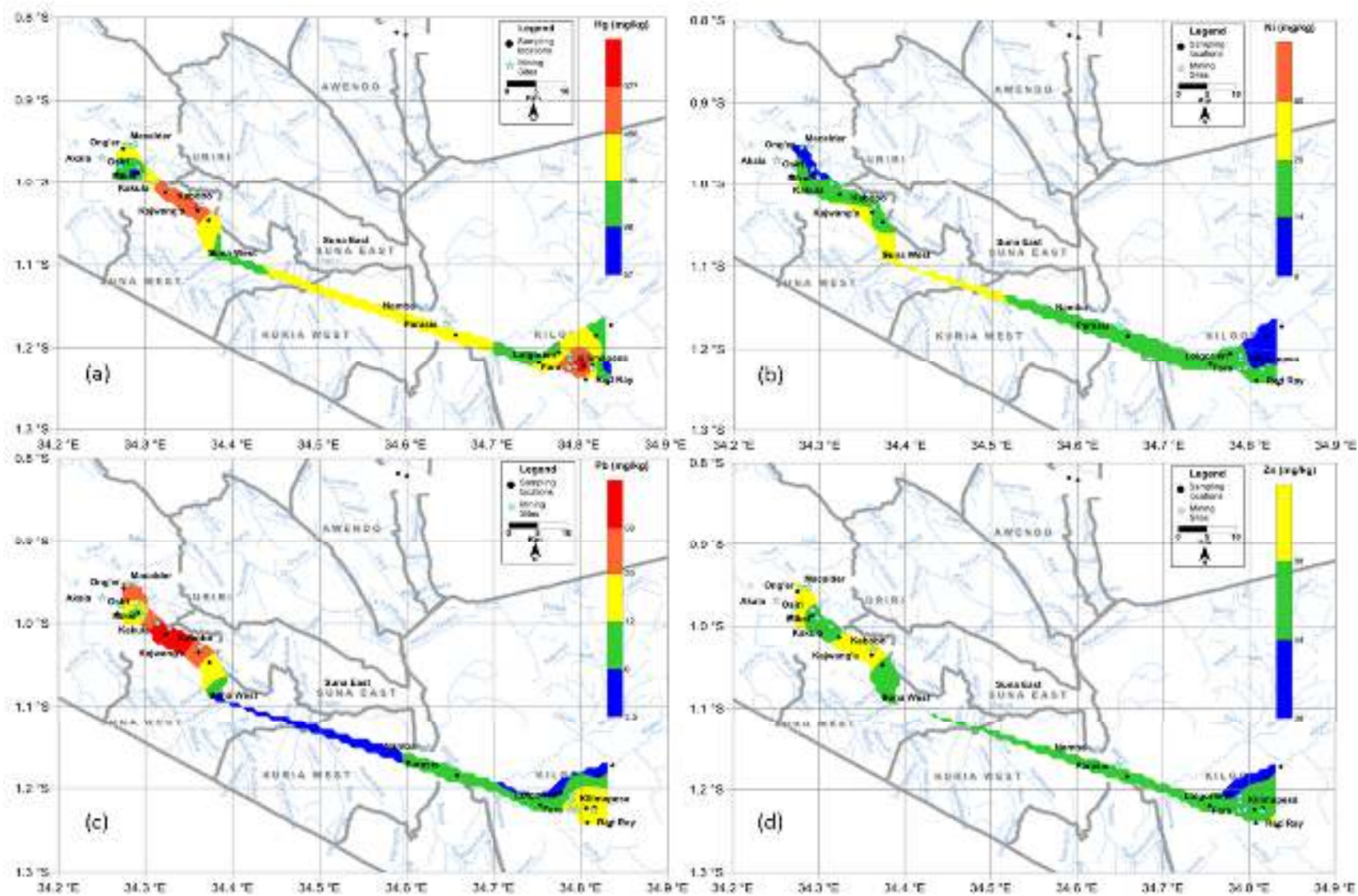
Figure 5. 4: Spatial distribution maps of a) Hg b) Ni, c) Pb d) Zn in moss

5.2 Source apportionment of heavy metals in lichens and mosses

Principal Component Analysis, Pearson's correlation and Hierarchical Cluster Analysis of heavy metals in lichens and moss is presented and discussed by comparing them.

5.2.1 Principal Component analysis of heavy metals in lichens and moss

The first four principal components in lichen and moss account for 89.704% and 87.944% of the total variance respectively, **Table 5.4 – 5.7**. PC-1, PC-2, PC-3 and PC-4 in lichens consists of (As and Pb), (Cr, Zn and Ni), Cu and Cd respectively while PC-1, PC-2, PC-3 and PC-4 in moss consists of (Cd, Pb, and Zn), (Cr and Cu), As and Ni. The PCs in both biomonitors account for almost the same variance even though the same variance, this is an indication of the same even of accumulation of the heavy metals. However, different groupings is due to difference in bioaccumulation of mosses and lichens as was found by Bargagli *et al*. (2002b). High loading of As and Ni (**Table 5.4**) and Cu and Cd (**Table 5.5**) show they originate from mainly from point sources.

Table 5. 4: Varimax rotated principal component loadings for four principal components for heavy metals in moss

	Component			
	1	2	3	4
As	0.130	-0.038	**0.939**	0.057
Cd	**0.673**	-0.317	-0.374	-0.134
Cr	-0.247	**0.934**	0.052	-0.145
Cu	-0.183	**0.879**	-0.106	0.388
Ni	-0.112	0.073	0.070	**0.983**
Pb	**0.835**	-0.060	0.378	-0.076
Zn	0.844	-0.240	0.085	-0.055

Table 5. 5: Varimax rotated principal component loadings for four principal components for heavy metals in lichens

	Component			
	1	**2**	**3**	**4**
As	**0.939**	0.278	-0.089	-0.016
Cd	0.048	-0.110	0.013	**0.930**
Cr	0.444	**0.820**	0.040	-0.009
Cu	0.065	0.134	**0.979**	-0.045
Ni	-0.005	**0.713**	0.190	-0.406
Pb	**0.948**	0.075	0.255	0.118
Zn	0.211	0.620	0.543	0.405

Table 5. 6: Eigen Concentrations and Percentages of Total Variance by Different Principal Components for Heavy Metals in moss

Component	Initial Eigenvalues			Rotation Sums of Squared Loadings		
	Total	% of Variance	Cumulative %	Total	% of Variance	Cumulative %
1	2.920	41.709	41.709	1.987	28.380	28.380
2	1.341	19.152	60.861	1.813	25.903	54.283
3	1.012	14.453	75.313	1.190	17.000	71.283
4	0.884	12.631	87.944	1.166	16.661	87.944
5	0.495	7.069	95.013			
6	0.278	3.965	98.978			
7	0.072	1.022	100.000			

Table 5. 7: Eigen Concentrations and Percentages of Total Variance by Different Principal Components for Heavy Metals in lichens

Component	Initial Eigenvalues			Rotation Sums of Squared Loadings		
	Total	% of Variance	Cumulative %	Total	% of Variance	Cumulative %
1	2.991	42.725	42.725	2.029	28.985	28.985
2	1.398	19.97	62.695	1.679	23.982	52.968
3	1.228	17.55	80.245	1.362	19.464	72.431
4	0.662	9.459	89.704	1.209	17.273	89.704
5	0.563	8.038	97.742			
6	0.125	1.782	99.524			
7	0.033	0.476	100			

5.2.2 Pearson's correlation analysis of heavy metals in lichens and moss

Pearsons correlation in moss shows large and significant correlation ($p<0.01$) between As and Cr ($r=0.595$), Cr and Zn ($r=0.642$), As and Pb ($r=0.879$), and large and significant correlation ($p<0.05$) between Cr and Pb ($r=0.475$), Zn and Cu ($r=0.573$), **Table 5.8**. Pearson's correlation analysis between heavy metals in lichens found there is a large, positive and significant correlation ($p<0.01$) between Cu and Cr ($r=0.775$) and Zn and Pb ($r=0.666$) and large positive and significant correlation ($p<0.05$) between Zn and Cd ($r=0.460$), Ni and Cu ($r=0.440$), Pb and Cd ($r=0.375$), and Pb and As ($r=0.381$). There is also a moderate and significant ($p<0.05$) but negative correlation between Cu and Cd ($r=-0.415$), Zn and Cu ($r=-0.396$) and Zn and Cr ($p=-0.425$), **Table 5.9**.

Table 5. 8: Pearson's Correlation for Heavy Metals in moss

	As	Cd	Cr	Cu	Ni	Pb	Zn
As	1.000						
Cd	0.034	1.000					
Cr	0.595**	-0.153	1.000				
Cu	0.016	-0.017	0.193	1.000			
Ni	0.245	-0.276	0.433	0.313	1.000		
Pb	0.879**	0.167	0.475*	0.310	0.084	1.000	
Zn	0.299	0.222	0.642**	0.573*	0.255	0.421	1.000

NB. * and ** denote statistically significant correlation at 0.05 and 0.01 probability level respectively.

Table 5. 9: Pearson's Correlation for Heavy Metals in lichens

	As	Cd	Cr	Cu	Ni	Pb	Zn
As	1.000						
Cd	-0.104	1.000					
Cr	0.004	-0.405	1.000				
Cu	-0.127	-0.415*	0.775**	1.000			
Ni	0.112	-0.231	-0.022	0.440*	1.000		
Pb	0.381*	0.375*	-0.269	-0.279	-0.148	1.000	
Zn	0.149	0.460*	-0.425*	-0.396*	-0.174	0.666**	1.000

NB. * and ** denote statistically significant correlation at 0.05 and 0.01 probability level respectively.

5.2.3 Hierarchical Cluster Analysis of heavy metals in lichens and mosses

Hierarchical Cluster analysis results in lichens and moss agree on broad classification of the investigated heavy metals in three groups; As, Zn and (Cr, Ni, Cu, Pb, Cd), **Fig 5.5 (a) and (b)**. However, HCA in mosses has further classified (Cd and Pb) and (Ni and Cu).
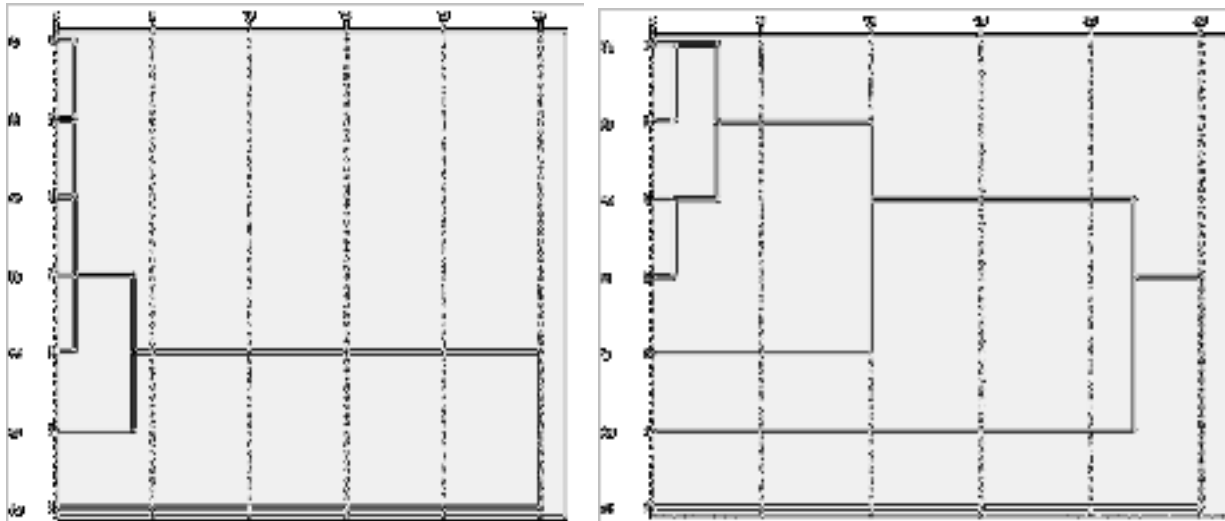
a) Dendrogram in Lichens   b) Dendrogram for moss

Figure 5. 5: Dendrogram of the Hierarchical cluster analysis of heavy metals in lichens and moss

From the HCA, As is coming for gold mining processes, this is supported by its high PC loading in both biomonitors. Association of Cr , Cu and Ni in HCA is supported by findings by Betsou *et al*. (2021) in when they were performing source apportionment analysis on particulate matter using moss in goldmines in Greece. According to Stamenkovic *et al*. (2013) atmospheric deposition of Ni, Cr and Pb results from mining and particles from vehicular exhaust emissions. However, HCA in mosses has further classified (Cd and Pb) and (Ni and Cu) to be originating from a common source as is also supported by their significant and positive correlation groping of Cd and Pb in moss and lichens by PCA. Cd and Pb is likely to be originating from vehicles exhaust with Ni and Cu coming from natural soil formation processes. Nickel also originate from dust blown from soils, forest fires and volcanic emissions, according to Nieminen *et al.* (2007). According to Aslan *et al*. (2011) Ni and Cr are mainly from the crust, they are associated with deposition of air born dust blown from roads that finally settle on the biomonitors, association of Ni and Cr is supported by their clustering in by PCA in moss and lichens and grouping by Moss in by high loading PCA. Both biomonitors show positive and significant correlation between As and Pb suggesting they originate from a common source. As and Pb accompany gold bearing rock as arsenopyrite (FeAsS) and galena (PbS) respectively and are normally in stable states but once exposed to water and oxygen are transformed to their respective oxides (Ogola *et al.,* 2002). During the process of commination and transportation of the comminuted ore to the panning ponds, these elements are blown by wind and eventually find their way to the biomonitors. Arsenic is also naturally released into the environment by naturally decomposing arsenopyrite in the gold bearing veins which is exuberated by gold mining, *(Craw et al*., 2000).

5.2.4 Correlation of the Concentration of Heavy Metals in Lichens and Moss Collected at the same Location.

The concentration of heavy metals in lichens and moss collected at same location were compared to determine correlation them, **Appendix A, Table A3.** Positive correlation existed in all the cases but decreased in the order Pb>Hg>Cr>Zn>As> Ni>Cu>Cd , **Table 5.10.** There is a strong, moderate and weak correlation between lichens and moss in biaccumulation of (Pb, Hg, Cr and Zn), (As and Ni) and (Cu and Cd) respectively. Strong correlation between moss and lichen in accumulation of Cr corroborates finding by Begu *et al*. (2012), however Begu *et al*. (2012) also found a strong correlation between Cu and Ni. From this study therefore, lichens and moss can be

used interchangeably as bioaccummulators of Pb, Hg, Cr and Zn. However this contradicts the findings by Bargagli *et al.* (2002b) and Loppi and Bonini (2000) that found lichens to be better bioaccumulators of Hg, Pb and Zn. According to Buck and Brown (1979), lichens are good bioaccumulators of Pb because it binds negatively charged ions (cations) to its cell wall whether they are alive or dead hence leading to high accumulation. But Evans and Hutchinson (1996) argue that lead and mercury are volatile and are continously recycled back to the atmospere from lichens than in moss, this makes their concentrations to be lower in lichens.

Table 5. 10: Correlation Between the Concentration of Heavy Metals in Lichens And Mosses

Heavy Metal	As	Cd	Cr	Cu	Hg	Ni	Pb	Zn
Correlation	0.602	0.180	0.794	0.357	0.821	0.506	0.856	0.751

5.3 Elemental Concentration and Radiation Exposure in Soil

This section presents and discusses the concentration, source apportionment, cluster analysis, Pearson's correlations, pollution indices, spatial variability, and activities of soils at sampled locations

5.3.1 Heavy Metal Concentration in Soil

The highest concentration of mercury (1064.00 mg/kg) was at Lolgorien center. This level is one order above that at other studied locations, **Appendix B, Table B1** and **Figures 5.6**. Other locations with high concentration of mercury were Magoto (364.80 mg/kg) and Kajwang'a (248.78 mg/kg). Even though there were mines at Lolgorien and Kajwang'a, there was no mining at Magoto. High mercury concentration at Magoto is due to high organic matter in the soils at Magoto due to trees cover, mercury is adsorbed by organic matter thereby increasing retention of mercury in such soils (Luo *et al.,* 2008). Mercury concentrations of (34.20 – 103.85 mg/kg) was in soil in the vicinity of Lake Victoria, this an indication Lake Victoria could be polluted by mercury from the gold mines. The populace who rely heavily on fish (Tilapia (*Ngege*), Nile Perch (*Mbuta*), Mud Fish (*Kamomgo*), sardines (*omena)* etc.) as their main source of protein are therefore likely to be exposed to elevated concentrations of mercury (Salazar-Camacho *et al.,* 2017).

High concentration of Cu (471.71 mg/kg), Pb (546.72 mg/kg) and Zn (255.04 mg/kg) in the vicinity of Macalder mines (between Dambre and Osiri) is as a result surface run off and wind erosion of the said heavy metals from heaps of mine wastes that litter Macalder mines where gold mining has been going on since 1920's. These concentrations are in agreement with those in the upper crust as reported by Ichangi *et al.* (1991) implying contributions from local crustal formation. Concentration of As (32.00 mg/kg), Hg (103.85 mg/kg), Zn (209.90 mg/kg), Ni (23.00 mg/kg) and Pb (25.00 mg/kg) at Aneko (Kabuto area) is high compared to other locations around it; for instance, Ongoche [As (4.00 mg/kg), Hg (23.85 mg/kg), Ni (13.40 mg/kg) Zn (39.90 mg/kg) and Pb (10.20 mg/kg)]. This is points to accumulation of these heavy metals due to frequent flooding at Kabuto during rainy seasons.
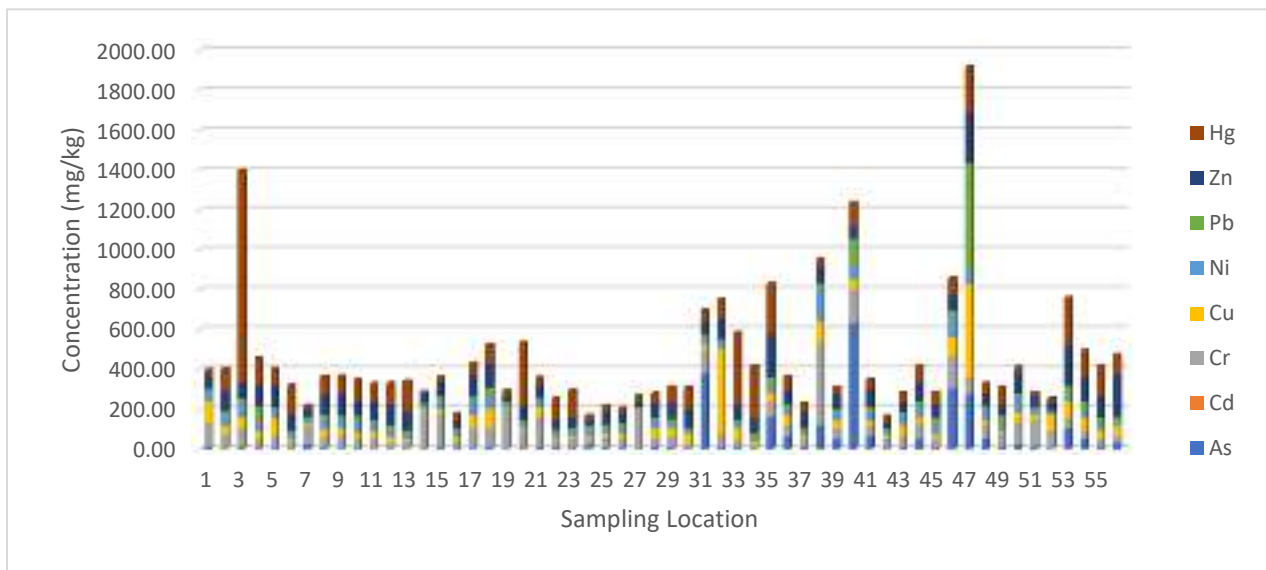
Figure 5. 6: Concentration of heavy metals in soil in the Migori-Transmara gold mining complex

The mean and median concentration (mg/kg) of the heavy metals in soil decrease in the order Hg>Zn>Cr>Cu>As>Ni>Pb>Cd and Hg>Zn>Cr>Cu> Ni>Pb>As > Cd respectively and the median concentrations of Cu As and Hg are 6, 4 and 3 times higher than the background values, **Table 5.11**. Apart from Cr, the BGV are lower than the mean and median concentration of other the heavy metals investigated. This is an indication that all the heavy metals investigated save for Cr have been enriched in the soil these heavy metals in soil. The order of heavy metal

concentration in this study is comparable to the results from goldmines in Nyarugusu gold mines in Tanzania where mercury is also the leading polluter and lead is the least, however the concentration of mercury in this study is over four times higher. As much as these findings are in agreement with the order of the findings by Antwi-Agyei *et al*. (2009) who investigated the concentration of As, Zn, Cu and Pb in Obuasi in Ghana, As is the leading heavy metal in concentration in their study. The mean concentrations of the same heavy metals from Xiangling gold mining region of China (Pb>Zn>Cu>Cr>As>Hg>Cd) shows Zn as one of the highly concentrated heavy metals in soils around gold mines (Wu *et al.,* 2010). Difference in the order and magnitude in concentration of heavy metals is due to difference in geochemical landscape characteristics since the land is basically alluvial. Even though the concentration of mercury in soil in China is low due total ban on artisanal gold mining it had the highest ecological risk. The mean and median concentration mercury is 370 and 272 times higher than the upper limit recommended for agricultural soils by FAO and WHO (Chiroma *et al.,* 2014). The mean of Cr, Cu, Ni, Pb are also below the soil composition in sub–Saharan Africa however, the mean of Zn in this is higher. These concentrations are therefore above levels which serious soil contamination is deemed to exist and therefore remediation is urgently necessary. However, remediation is always site specific and requires risk assessment (Cavanagh and O'Halloran, 2002).

The coefficient of variance of concentration of the heavy metals increases in the order Zn>Ni>Pb>Cr>Cd>Hg>Cu>As where the levels of Hg, Cu and As in soil are the most impacted by mining with CV of 111.11%, 134.39% and 231.75% respectively. The median concentration of all the heavy metals is less than the mean, implying positive skew of all the heavy metals investigated and therefore there are locations where their concentration is very high. High variability in the concentrations of As, Cu, Hg and Pb is also seen from their high standard deviation, this further confirms high anthropogenic influence. Heavy metals are distributed to soils through windblown dust, re-emission, emission and resuspension of dust, leaching by rain water, and seepage to ground (Tutu *et al.*, 2008). They attach themselves to the very fine ore dust particles and can be spread to greater distances with favorable aeolian conditions (Ravi *et al.,* 2011)

Table 5. 11: Summary of Concentration of Heavy Metals in Soil (mg/kg), Maximum Permisible limits in Soil by FAO and WHO and Total elemental composition in sub- Saharan Africa

Description		As	Cd	Cr	Cu	Ni	Pb	Zn	Hg
Mean		46.81	0.09	79.88	54.78	38.49	34.49	85.39	111.01
Std. Deviation		108.48	0.10	64.40	80.06	23.60	72.03	45.32	149.19
Median		7.62	0.05	57.18	36.72	31.60	19.06	77.30	81.15
MAD		4.69	0.05	19.49	16.37	9.74	7.70	22.78	44.39
CV (%)		231.75	111.11	80.73	146.15	61.31	68.43	53.07	134.39
Skewness		3.84	1.66	2.99	4.44	2.77	6.69	1.94	4.96
Minimum		2.00	0.01	16.69	6.30	13.40	6.00	25.80	16.65
Maximum		632.24	0.43	418.40	471.71	155.90	546.92	255.04	1063.99
Background Values		2.00	0.01	196.4	6.30	14.00	16.80	28.00	29.35
Percentiles	25.00	4.10	0.01	40.89	20.72	25.54	13.08	60.30	36.43
	50.00	7.62	0.05	57.18	36.72	31.60	19.06	77.30	81.15
	75.00	28.50	0.13	96.77	53.56	43.88	31.48	100.33	118.06
Soil Composition in Sub Saharan Africa (Towett *et al*., 2015)		-	-	72	17-27	39	18-22	45-47	-
FAO and WHO (Maximum Permissible limits) (Chiroma *et al*., 2014)		20.00	3.00	100.00	100.00	50.00	100.00	300.00	0.30

The average concentrations of Cu and Hg in this study are higher than the average concentrations found in Ghana (Bempah and Ewusi, 2016), South Africa (Kamunda *et al*., 2016) and China (Chen *et al.,* 2017), **Table 5.12**. However, average concentration of Pb (819.17 mg/kg) and Zn (104.00) found in China by Mo *et al.* (2017) and As (79.80 mg/kg), Cr (278.80 mg/kg) and Ni (112.06 mg/kg) found in South Africa by Cespha *et al*. (2016d) are higher than the findings in this study. The difference in the levels of the heavy metals in soils is because of difference in crustal formation as well as agricultural activities and discharge from industries and towns. However, for mercury, the difference in concentration in soil is mainly due to experience of the miners and the method used in its application in gold extraction from the gold bearing ore.

The order in the mean concentration of the heavy metals in soil and mosses agree for all the heavy metals, however their concentration is higher in soil. Difference in concentration is because heavy metals are deposited directly on to soil and are therefore readily adsorbed on the available soil particles compared to adsorption by PM in the air that depends on their resident time in air, size of the PM, heavy metal and weather conditions among other factors.

Table 5. 12: Comparison of Mean Heavy Metal Concentration (Mg/Kg) in Soil with Similar Studies In Gold Mining areas in other Countries

Country	As	Cd	Cr	Cu	Hg	Ni	Pb	Zn	Reference
Kenya	46.81 (2.00 - 632.24)	0.9 (0.01- 0.43)	79.88 (16.69- 418.40)	54.78 (6.30- 471.71)	111.01 (16.65- 1063.99)	38.49 (13.40- 155.90)	34.49 (6.00- 546.92)	85.39 (25.80- 255.04)	Present Study
Tanzania	ND – 126.10	-	ND – 65.00	ND – 130.00	ND – 0.09	4.50 – 65.70	ND – 20.00	15.60 – 252.00	(Almås and Manoko, 2012)
Sudan	-	-	-	19.00		15.33	12.46	20.80	(Ali *et al.,* 2017)
Cameroon	10.73 (5.79 – 14.38)	0.39 (0.21- 0.66)	22.00 (7.45- 35.59)	10.46 (6.17- 14.25)	-	3.69 (1.47- 7.68)	15.02 (11.12- 21.44	11.73 (7.23- 22.49)	(Léopold *et al.,* 2016)
Ghana	6.83	0.19	16.88	16.03	1.06	41.77	19.96	61.87	(Bempah and Ewusi, 2016)
South Africa	79.40	0.05	278.80	42.51	0.09	112.06	4.79	51.30	(Kamunda *et al.,* 2016d)
China	8.57	0.15	88.61	46.92	0.12	28.40	819.17	104.20	(Wu *et al.,* 2010)

5.3.2 Source Apportionment of the Heavy Metals in Soil

This section reports the possible sources of heavy metals in soil around Migori Transamara gold mines using multivariate data analysis

5.3.2.1 Principal component analysis

Four PCs whose eigenvalues were greater than one was extracted, the variables were reduced to four component model accounting for 85.87% of the variance, **Table: (5.13-5.14)**. PC-1

accounting for 28.77% of the total variance was dominated by Zn, Cu and Pb. The second, third and fourth PC was dominated by (Cr and Ni), Cd and As accounting for 23.73%, 17.93%, 15.45% of the total variance respectively.

Table 5. 13: Varimax rotated principal component loadings for four principal components for heavy metals in soil

Element	Component 1	2	3	4
As	0.161	0.247	0.023	0.941
Cd	0.221	-0.057	0.937	0.025
Cr	-0.024	0.865	-0.277	0.146
Cu	0.932	0.162	-0.010	-0.008
Ni	0.138	0.903	0.158	0.146
Pb	0.766	0.030	0.295	0.375
Zn	0.680	-0.069	0.434	0.107

Table 5. 14: Eigen Concentrations and Percentages of Total Variance by Different Principal Components for Heavy Metals in Soil

Component	Initial Eigenvalues Total	% of Variance	Cumulative %	Rotation Sums of Squared Loadings Total	% of Variance	Cumulative %
1	2.754	39.341	39.341	2.014	28.767	28.767
2	1.844	26.343	65.684	1.661	23.725	52.492
3	0.720	10.290	75.973	1.255	17.930	70.422
4	0.693	9.898	85.872	1.081	15.449	85.872
5	0.474	6.778	92.650			
6	0.317	4.532	97.182			
7	0.197	2.818	100.000			

5.3.2.2 Pearson's Correlation of heavy metals in soil

Pearsons correlation between the elements can be a pointer of the association and possible similarity on the sources the investigated heavy metals, **Table 5.15**. There exists a large positive and significant ($p<0.01$) correlation between Ni and Cr (r=0.626), Pb and Cu (r=0.664), Zn and Cu (r=0.500), Zn and Pb (r= 0.563) and moderate significant correlation ($p<0.01$) between Pb and

Cd (r=0.474), As and Pb (r=0.428), As and Ni (r=0.402). Moderate but significant correlation (p<0.05) exists between As and Cr (r=0.315) and Ni and Cu (r=0.275). There also exist a significant (p<0.01) but negative correlation between Cd and Cr (r=-0.268), this shows do not come from the same source.

Table 5. 15: Pearson's Correlation for Heavy Metals in soil

	As	Cd	Cr	Cu	Ni	Pb	Zn
As	1.000						
Cd	0.073	1.000					
Cr	0.315*	-0.268*	1.000				
Cu	0.220	0.246	0.083	1.000			
Ni	0.402**	0.073	0.626**	0.275*	1.000		
Pb	0.428**	0.474**	0.030	0.664**	0.199	1.000	
Zn	0.210	0.449**	-0.161	0.500**	0.139	0.563**	1.000

NB. * and ** denote statistically significant correlation at 0.05 and 0.01 probability level respectively.

5.3.2.3 Hierarchical Cluster Analysis of Heavy Metals in Soil

HCA analysis broadly groups the investigated heavy metals in three broad clusters, (Cd, Ni, Cu, Pb, and Zn), Cr and As, **Figure 5.7**. Cluster one can further be divided into two clusters (Ni and Cd) and (Cu, Zn and Pb). Liu *et al*. (2020) while investigating effects of heavy metal pollution in China's Xiaoqinling gold mining belt also associated Cd, Cu, Pb, and Zn with gold mining. The distance between Cd and Ni is shortest implying highest correlation between them followed by the distance between Cu and Pb.
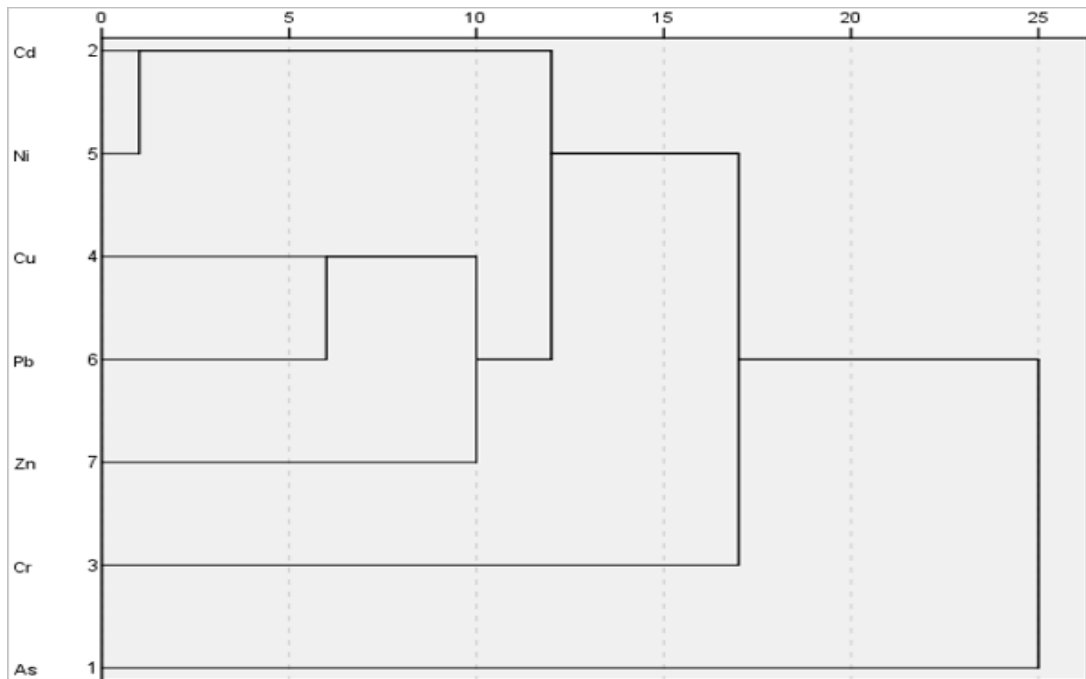
Figure 5. 7: Dendrogram of the Hierarchical cluster analysis of heavy metals in soil

HCA, PCA and Pearson's correlation results agree on the association between Cu, Pb and Zn, suggests Cu, Pb, and Zn are from the impact of gold mining. Zn, Cu and Pb are found rock formation in the Migori and Transmara gold mining areas which consists of Zn – Cu – Pb massive sulphide deposits consisting majorly of aphyric and porphyric tholeiitic massive and pillowed basalts and dolerite sills (Shackleton, 1964). These heavy metals are released into the soil in the process of excavation, transportation and from the tailigs that are left exposed around the mines. In addition Pb and Zn are also coming from exhaust fumes of vehicles (Zou *et al*., 2015).

Association of As with gold bearing ore is seen in HCA and PCA, this shows the Migori Transmara gold bearing ore is made up of arsenopyrites as was also found in Ghana (Akoto *et al*., 2019). Arsenic always associated with gold bearing rocks in the form of arsenopyrite (FeAsS). Association of Cd, Cr and Ni show they are originating from both anthropogenic and natural sources which include burning of fuel oil and incineration of waste, Jianfei *et al*. (2020), also in their study of soils around a mining city in China grouped As, Ni and Cr, association of Ni and Cr was attributed to the crustal soil formation. Large positive and significant correlation between Pd and Cd show could also be coming from agricultural activities like application of phosphate fertilizers and pesticides (Chen *et al*., 2017). This is from the fact that sugarcane and tobacco

farming rely on application of phosphate based fertilizers like diammonium phosphate fertilizer. Fertilizers and pesticides contain trace amounts of Cd and Pb that significantly elevate their concentration in soil (Jones and Javis 1981). According to Alloway (2013), the worldwide concentration of phosphate and nitrogen fertilizers and manure is (0.1 – 170 ppm), (0.05-8.5 ppm) and (0.3 – 0.8 ppm) respectively.

There exists a moderate but significant correlation between Cr and Cd, this confirmed by their grouping and clustering by PCA and HCA respectively, it also shows the heavy metals are originating from more than one source (Ziadat *et a*l., 2015). While Cr is majorly originating for the local soil formation which is a natural phenomenon as have also been also found in the biomonitors, other sources of Cr include burning of coal and municipal wastes (Alloway, 2013 ;Tumolo *et al.,* 2020).

5.3.3 Spatial Variability of heavy metals in Soil

The spatial distribution of the heavy metals confirms mining as their source, this is most evident around Macalder mine where the concentration of all the heavy metals investigated is more than ten times the background concentration values in all the heavy metals apart from chromium, Influence of mining is seen in Hg, Pb, As, Cd and Cu with all the mines having concentrations above ten times the background concentrations **Fig: 5.8 (a-d)** and **Fig: 5.9 (a - d)**. This finding is supported by Dike *et al*. (2020) and Blanchard *et al*. (2018), they found high concentration (Pb, Cd and As) and (Zn, Pb, Cu, Ni and As) in soils around mines in Nigeria and East Cameroon respectively compared to nonpolluted soils. There is a noticeable decrease in the concentration of Cd in soils around all the mines, Pb (Macalder and the mines around it) and Hg (Lolgorien), further confirmation mining has influence on accumulation of these metals in soil since the concentration decreases with increase in distance from the mines. High concentration of Pb could also be explained from the fact that lead is less mobile in soil as was found by Asmoay *et al*. (2019). During the mining process, the heavy metals are left in the vicinity of the mines as mining wastes in the form of gangues, tailings, overburden etc., these wastes find their way to nearby soils through air and surface runoffs. Even though it was expected that the concentration of Hg around Macalder would be the highest, this is not the case instead this is seen around Lolgorien, this can be is because of the high number of miners at Lolgorien. The concentration of Cr in almost all the almost

locations is equal to or below the background concentration suggesting gold mining in this region does not contribute to Cr in soil.
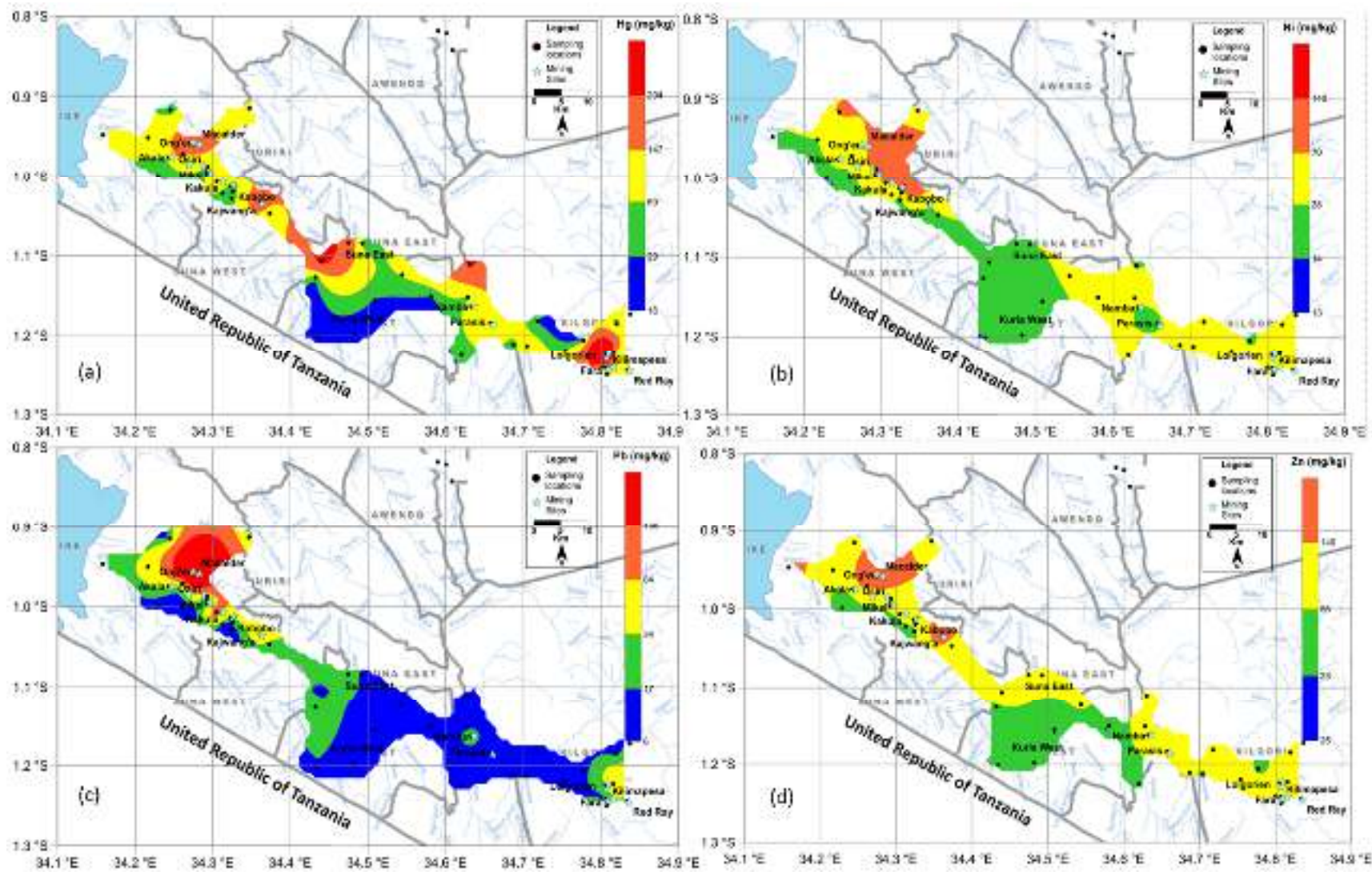
Figure 5. 8: Spatial distribution maps of a) Hg b) Ni c) Ni and d) Zn in soil
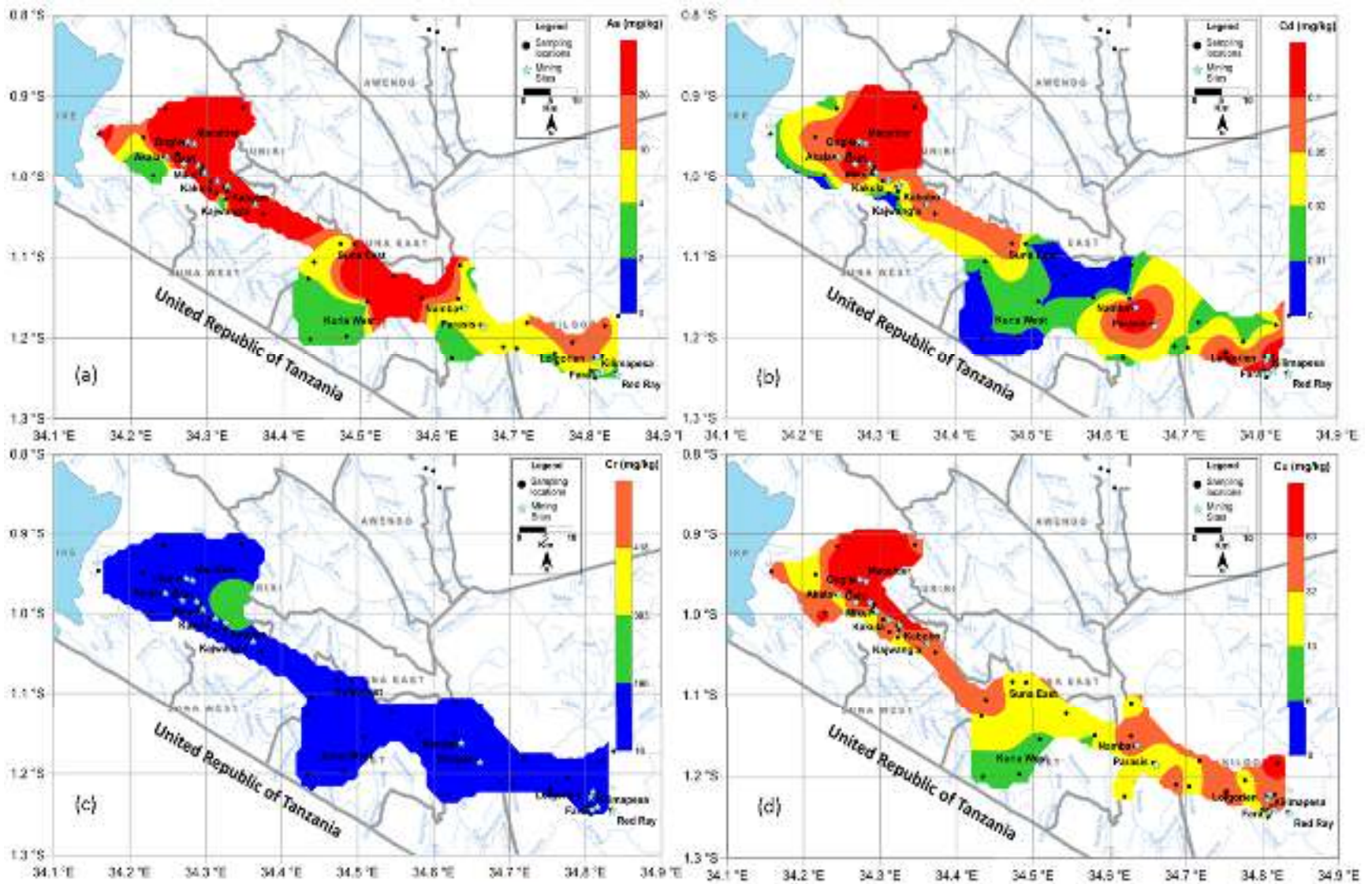
Figure 5. 9: Spatial distribution maps of a) As b) Cd c) Cr and d) Cu in soil

5.3.4 Pollution Indices of Soil around Migori Transmara Gold Mining areas

Pollution indices of soil around Migori Transmara gold mining areas namely contamination and enrichment factor, degree of contamination and geo accumulation index are presented and discussed.

5.3.4.1 Contamination Factor

Calculated Background (B_n) concentrations (mg/kg) of heavy metals in soil were calculated to be As (20), Cd (9), Cr (68), Cu (40), Ni (36), Pb (26), Zn (70) and Hg (79). High contamination factors of As, Pb, Cu, and Hg in soil were at Dambre, Kakula and Lolgorien this is due to repeated damping of tailings and waste rocks compared to Hibwa and Nyambae where there were no mines, **Appendix B; Table B2**. The mean CF of the heavy metals investigated decreases in the order As>Hg>Cu>Pb>Cr>Zn>Ni>Cd, **Table 5.16**.

The soils in Migori Transmara are moderately contaminated by all the heavy metals investigated apart from Cd which has a low CF. Over 10% of the soils are considerably and very highly contaminated with Hg and As respectively. Maximum CF of As, Cr, Cu, Pb and Hg show very high contamination, Ni and Zn show considerable contamination and Cd shows low CF. High CF by As confirms arsenic as a pathfinder for gold, accompany gold as arsenopyrite (FeAsS). Other heavy metals that accompany gold bearing ore in this area are Cu and Pb as shown by their CFs (Ichang'i and MacLean, 1991). The Migori segment is an 80 km by 20 km portion of the Nyanza greenstone belt which forms the northern part of the Archean Tanzanian Craton in western Kenya, northern Tanzania and southeastern Uganda. The Macalder Zn-Cu-Au-Ag volcanogenic massive sulphide deposits is in central facies basalts-greywacke-rhyolite. Gold mineralization occurs in proximal facies tuffs and iron formation, and in oblique and semi-conformable quartz veins. High CF can mainly be attributed to anthropogenic activities with gold mining as the leading cause of contamination as was also reported by Amadi *et al.* (2017) in Nigeria. Other sources of heavy metals include discharge from factories, households, burning of fuels and farming activities.

Table 5. 16: Summary of the Contamination Factors of Soil

Description	As	Cd	Cr	Cu	Ni	Pb	Zn	Hg	Degree of contamination
Mean	2.34	0.01	1.18	1.37	1.07	1.33	1.08	1.41	9.78
Median	0.40	0.01	0.84	0.93	0.87	0.73	0.99	1.03	5.80
MAD	0.22	0.01	0.29	0.41	0.25	0.30	0.28	0.56	2.32
Minimum	0.10	0.00	0.25	0.16	0.37	0.23	0.33	0.21	3.20
Maximum	31.61	0.05	6.15	11.79	4.33	21.04	3.23	13.47	55.48
Std. Deviation	5.42	0.01	0.95	2.00	0.66	2.77	0.57	1.89	9.35
BGV	0.10	0.01	2.89	0.16	0.39	0.65	0.35	0.37	4.91
Percentiles (90%)	6.31	0.03	2.45	2.36	1.76	2.04	1.53	3.10	21.04

5.3.4.2 Degree of Contamination C_{deg}

The average degree of contamination (C_{deg}=9.777) show moderate contamination by the investigated heavy metals, however less than 10% of the samples showed very high degree of contamination, **Table 5. 16**. As and (Cu, Pb and Hg) contributes 24% and 14% respectively to the C_{deg} while each of Cd, Cr, Zn and Ni contribute less than 13%.

4.3.4.3 Enrichment Factor of Soil at Sampled Locations

The EF of mercury was the highest at all the locations investigated with the highest enrichment found Lolgorien center (3069.00), Magoto (1120.80) and Nyathrogo (1030.30) whose concentrations are one order of concentration above the rest of the locations investigated (**Appendix B: Table B3**). Mercury is extremely highly enriched in all the samples analyzed thereby calling for remediation and use of methods like concentration that require minimal mercury besides using gold recovery techniques that do not require mercury. Arsenic is the second highest enriched with the highest EF at Kakula.

The mean EF decreases in the order Hg >As>Pb>Cr>Cu>Ni> Cd, **Table 5.17**. Although the order of EF in the soils around Obuasi goldmines in Ghana (As>Pd>Cu) (Boateng *et al.*, 2012) is as the one in this study, (Cd>Cr>Ni>Pb>Cu) in Sudan is different (Idris *et al.*, , 2018) Mercury is

extremely highly enriched in all the sampled locations which shows there is anthropogenic input of mercury at all the locations. Mean EF of arsenic shows moderate enrichment with less than 25% of the sampling locations showing significant to extremely high enrichment. Maximum EF of Ni and Cd show there are some areas with moderate enrichment and deficient to minimal enrichment respectively. The mean EFs of Cr and Cu show that they originate from crust while that of As, Hg and Pb show they originate from anthropogenic activities. Apart from Cd, maximum EFs of all the investigated heavy metals suggest contribution from human activities like gold mining. The main human activity in this region is gold mining, other sources of heavy metals however include agriculture (fertilizers, pesticides and herbicides), burning of fuel (vehicles and generators) and discharge from households and industries. According to Atafar *et al.* (2010) and Alkhader (2015), most probable sources of the heavy metals (Cd and Pb) and metalloid (As) are parent materials, pesticides and long term application of potassium based fertilizers. Di-ammonium phosphate (DAP) fertilizers, which are usually applied in sugarcane farms, are the alternative sources of As, Cd and Pb in soil in this region. Mercury is extremely highly enriched (EF>81) in all the soil samples which calls for urgent remediation. The main source of mercury in soil are the tailing that are not only rich in mercury but also other metals as well. Tailings rich in heavy metals are left at the mercy of wind and water erosion that leads to the enrichment of soils with the heavy metals present. These heavy metals eventually find their way up the food chain thereby exposing the populace and miners to myriad diseases associated with the heavy metals present. Besides their high concentrations, metals like As, Cd and Pb show extreme toxicity even at trace concentrations (Canfield *et al.*, 2003).

Table 5. 17: Summary of the Enrichment Factor in Soil around Gold Mines in Migori Transmara

Description		As	Cd	Cr	Cu	Ni	Pb	Hg
Mean		4.22	0.30	1.34	1.28	0.72	1.73	317.60
Median		0.82	0.17	0.80	0.94	0.62	1.27	223.55
MAD		0.47	0.12	0.38	0.31	0.17	0.42	71.27
Std. Deviation		11.49	0.29	1.53	1.28	0.46	1.77	423.85
Minimum		0.16	0.02	0.18	0.36	0.15	0.27	81.14
Maximum		72.77	1.35	7.40	8.61	2.68	10.19	3069.00
BGV		0.52	0.11	7.40	0.48	0.70	2.85	248.95
Percentiles	25	0.54	0.05	0.53	0.63	0.46	0.96	140.08
	50	0.82	0.17	0.80	0.94	0.62	1.27	223.55
	75	3.31	0.51	1.46	1.51	0.85	1.81	281.65

5.3.4.4 Geo-Accumulation Index (Igeo)

Geo-accumulation index of mercury is highest in all the sampling locations compared to the rest of the heavy metals studied, **Appendix B, Table B3**. High geo-accumulation index for Pb, Cu, As, and Zn at Macalder is due to accumulation of tailings and gangues that have existed since mining started in 1920's. Fine particles of these wastes are carried by wind and surface run off to areas that are near the heaps of wastes.

The mean geo-accumulation of the investigated heavy metals in soil decreases in the order Hg>Pb>As>Zn>Cu >Cr >Ni>Cd **Table 5.18**. Mercury is very heavily (extremely) contaminated with over 75% of the samples showing very heavy (extreme) contamination, the soils are not contaminated by the other heavy metals in this study. However maximum I_{geo} show there is strong to extreme contamination by Pb and moderate to strong contamination by Cu at Dambre. Dambre is close to Macalder mine which was the first mine in Migori Transmara, therefore due to accumulation over time the levels of the said metals are high.

Table 5. 18: Summary of Geo-Accumulation Index of Soil around Goldmines in Migori Transmara

Description		As	Cd	Cr	Cu	Ni	Pb	Zn	Hg
Mean		-0.65	-3.48	-1.06	-0.91	-1.59	-0.48	-0.90	6.95
Median		-1.22	-3.17	-1.24	-0.89	-1.64	-0.66	-0.88	7.00
MAD		1.06	2.32	0.57	0.76	0.42	0.61	0.38	7.09
Std. Deviation		2.09	1.94	0.89	1.19	0.70	1.12	0.69	1.20
Minimum		-3.29	-5.49	-3.02	-3.42	-2.93	-2.32	-2.47	4.79
Maximum		5.02	-0.07	1.63	2.80	0.61	4.19	0.84	10.79
BGV		-3.29	-5.49	0.54	-3.42	-2.87	-0.84	-2.35	5.61
Percentiles	25	-2.25	-5.49	-1.72	-1.70	-2.00	-1.20	-1.24	5.92
	50	-1.36	-3.17	-1.24	-0.88	-1.69	-0.65	-0.88	7.08
	75	0.54	-1.79	-0.48	-0.33	-1.22	0.07	-0.51	7.62

Pollution indices were generally higher around the mines with soils around Macalder mine leading in all the parameters of the pollution indices implying soil contamination is highest around the mines. This calls for remediation of the mines tails which is the leading source of heavy metals in the mining environment.

5.3.5 Radioactivity in Soils

The mean and range of activity concentrations of ^{238}U, ^{232}Th, ^{40}K, absorbed dose and the annual effective dose were 41.16 Bq/kg, 59.66 ± 35.51 Bq/Kg and 469.37 Bq/Kg, 74.76 ± 59.64 nGy/h and 0.09 ± 0.07 mSv/y respectively, **Fig: 5.10 and 5.11, Appendix B, Table B5**. Highest radioactivity was at Kogego/Agenga: ^{238}U (562.12 Bq/kg) and ^{232}Th (206.24 Bq/kg), D (402.61 nGy/h) and AEDE (0.50 mSv/y). AEDE at Kogego/Agenga (0.494 mSv/y), is 4.5 times above the background. Even though there was no mining around Kogego/Agenga at the time of sampling, there was a mining rush years back when new gold reefs were discovered. However this require further investigation to ascertain its extent and any other source apart from gold mining. Tailings and other wastes rich in radionuclides might have been left behind that eventually found its way to the soil in the vicinity of the mines. AEDE in soil around Lolgorien, Chill, Kuja 1, Macalder, Kuja Bridge, Kabobo Kabuto, Kajwang'a were bewteen 0.098 – 0.153 mSv/y. Apart from Kabuto,

the rest of these locations had active mining at the time of sample collection, the dose at Kabuto is due to accumulation of radionuclides carried by Kuja river and Migori rivers that drain throug the mining areas. Accumulation of radionuclides at Kabuto is due to flooding of the larger river Kuja that leaves silt containing goldmine and other wastes from areas drained by river Kuja and Migori in the nearby farms.

In Hibwa, Kuichami, Chill, Ekiwancah (in East and West Kuria) where also there no mining AEDE was between 0.107-0.153 mSv/y. These results in East and West Kuria are comperable to findings ny Banzi *et al*.,(2002b) who reported 121 nGy/h around Kilimanjaro Christian Medical College (KCMC) in Tanzania suggesting the same composition of the crust. It can be concluded that mining has no serious radiation impact on the soils in these mining areas and therefore there is no significant radiological threat to humans due to mining in Migori Transmara.
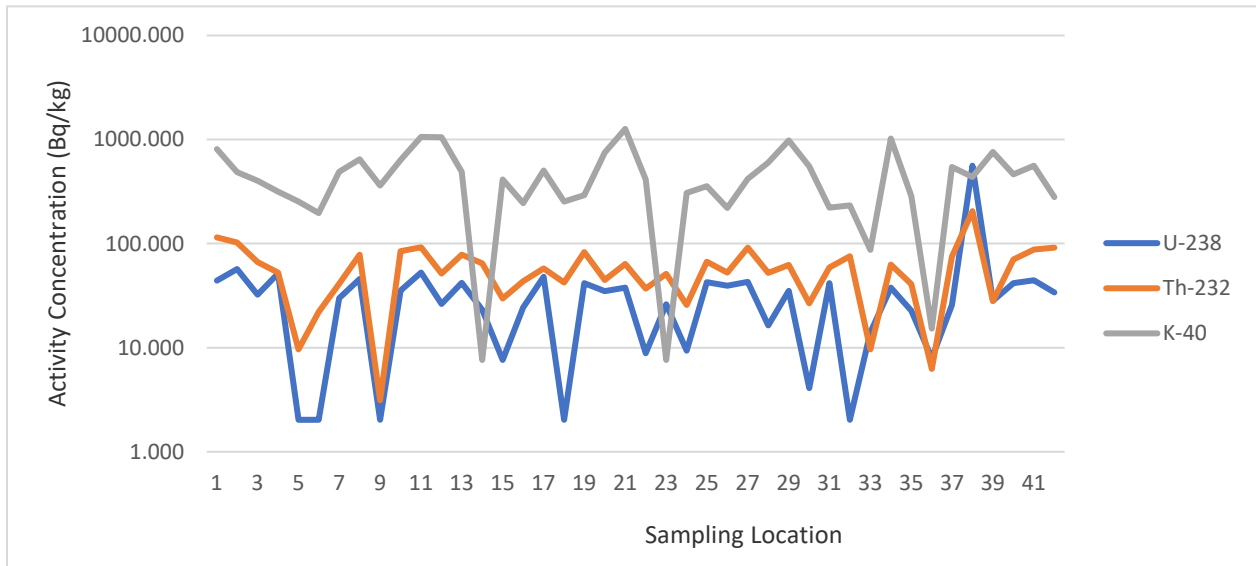
Figure 5. 10: Activity Concentration of ^{238}U, ^{232}Th And ^{40}K in Soil around Migori Transmara Goldmines
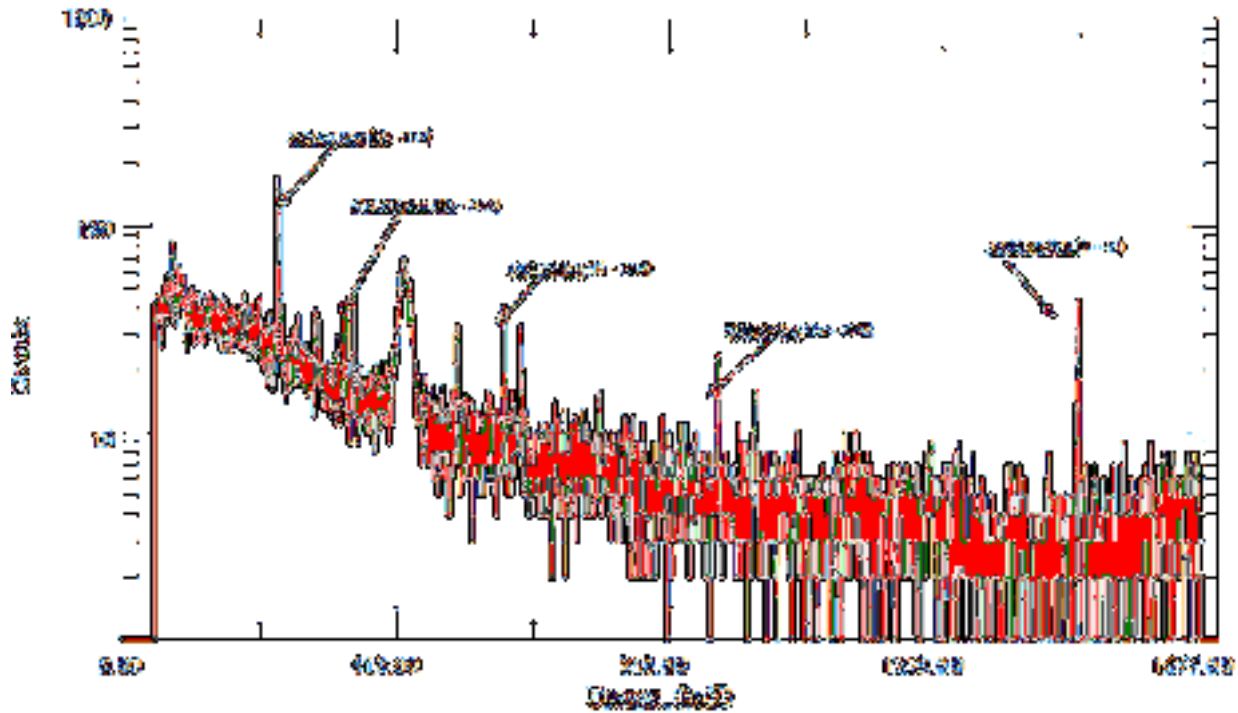
Figure 5. 11: Typical Activity Spectrum of Soil from a HPGe based Gamma Ray Spectrometer

The mean activity concentration of ^{238}U, absorbed dose and annual effective dose are comparable to the findings by Aguko *et al.*(2013) at Wagusu gold mine in Bondo but the activity of ^{238}U and ^{232}Th are lower than the that in tailings at Lurambi (Wanyama *et al*., 2020), **Table 5.19**. Difference in activity counting could be due errors during since Lurambi and Migori are both composed of the Nyanza green stone formation according to Shackleton (1951). Mean radioactivity of all the parameters in this study are below the findings in Uganda and South Africa but lower that the findings in Ghana (Turyahabwa *et al.*, 2016); Kamunda *et al.*, 2016; Adukpo *et al.,* 2014), **Table 5.20** Difference in levels of exposure in different mines is basically due to the geological composition of the crust in the mines. Even though the mean and median activity concentrations are within the worlds average, over half of the activity concentrations all radionuclides studied are above the worlds average which translates to high doses. The AEDE in this is below both the public and mine workers exposure concentrations which are 1 mSv/y and 20 mSv/y respectively, however, care should be taken since effects of any concentration of radiation can be harmful to humans (UNSCEAR, 2000) .

Table 5. 19: Summary of Activity Concentration, Absorbed Dose Rate and Annual Effective Dose of Soil at Sampled Locations

		U-238 (Bq/kg)	Th-232 (Bq/kg)	K-40 (Bq/kg)	Dose Rate (nG/h)	AED (mSv/y)
Mean		41.18	59.65	469.71	74.78	0.09
Std. Deviation		83.92	35.53	297.74	59.63	0.07
Median		33.09	58.37	417.05	70.48	0.09
MAD		10.12	18.62	163.95	23.14	0.03
Skewness		6.10	1.57	0.83	4.14	4.14
Minimum		<5.00	<5.00	<30.00	8.06	0.01
Maximum		562.12	206.24	1268.81	402.61	0.49
BGV		26.28	51.68	1268.81	87.56	0.11
Percentiles	25	12.83	39.93	253.12	43.79	0.05
	50	33.09	58.37	417.05	70.48	0.09
	75	42.05	78.21	610.65	93.02	0.11

Table 5. 20: Mean Radioactivity in soil other places where Artisanal Gold Mining is Practised

Country	^{238}U	^{232}Th	^{40}K	D (nGy/h)	AEDE (mSv/y)	Reference
Kenya	41.16 (2.04-562.12)	59.66(3.13-206.24)	469.37(7.64-1268.81)	74.76(8.06-402.61)	0.09(0.01-0.49)	This Study
Ghana	25.51(7.54-42.34)	28.02(4.18-54.92)	232.98(84.58-478.87)	31.90(11.69-6.51)	0.046(0.014-0.086)	(Adukpo *et al.,* 2014b)
Cameroon	40.1(18.5-85.00)	29.4(11.8-58.00)	217(40.6-582)	-	0.34(0.17 − 0.75)	(Blanchard *et al.,* 2017)
Kenya	84.00 ± 4.23	110.00± 5.15	245.00 +12.39	53.65 ± 6.20	0.30 ± 0.01	(Wanyama, *et al.,* 2020)
Kenya	44.2(7.2-113.8)	40.28(4.6-100.7)	639.55(119.3-1611.8)	73.04	0.085	(Aguko *et al.,* 2013)
Uganda	58.7	193.5	892.9	181.2	0.22	(Turyahabwa *et al.,* 2016)
South Africa	785.53(87.2-2668.9)	43.9(20.5-89.7)	427.0 (226.5-781.0)	407.1	0.5	(Kamunda *et al.,* 2016a)
World average	33	45	420	59	0.48	(UNSCEAR, 2010)

5.3.5.1 Spatial Variability of Activity Concentration, Absorbed Dose and Annual Effective Dose in Soil

Most parts of Kuria East, Kuria West, Suna East and Suna West where there are no or minimal mining have activity concentrations above but below twice the background, 26 – 63 Bq/kg and 52-103 Bq/kg for ^{238}U and ^{232}Th respectively. Spatial distribution of ^{238}U and ^{232}Th in soils around Macalder, Osiri, Mikei, Kakula, Parasis and Namba have activity concentration equal to or below background concentrations, the same is seen in the activity concentration of ^{232}Th in soils around Transmara. However, mines in Transmara show activity concentration between the 52- 103 Bq/kg. The spatial distribution of ^{40}K in all the locations are below the background (<1269Bq/Kg), which is three times higher than the worlds average. This suggest there is a source of ^{40}K that is not gold mining as is also supported by ^{40}K concentrations around Kehancha (1061.840 Bq/kg), Kuichami (1052.392 Bq/kg) and Hibwa (1268.807 Bq/kg).

The spatial variability of the activity concentration of ^{238}U and ^{232}Th in soil appear to be increasing with decrease in distance towards Lake Victoria, **Fig. 5.12 (a-d).** This is due to accumulation of radionuclides over time due to the floods that are prevalent in the lower Kadem (Kabuto) area. Tailings, ores and gangues that litter the mines are washed down to these areas during heavy rains and are left spread out in lower parts of Kadem after flooding is over. and Hibwa (1268.807 Bq/kg).

Spatial distribution of absorbed and annual effective doses in soil in most locations including around the mines are equal to or below the background, 88 nGy/h and 0.11 mSv/y, **Fig: 5.13**. The average absorbed dose in soil around Kehancha, Kuichami and Hibwa is supported by 121 nGy/h reported around KMC by (Banzi et al., 2002a).
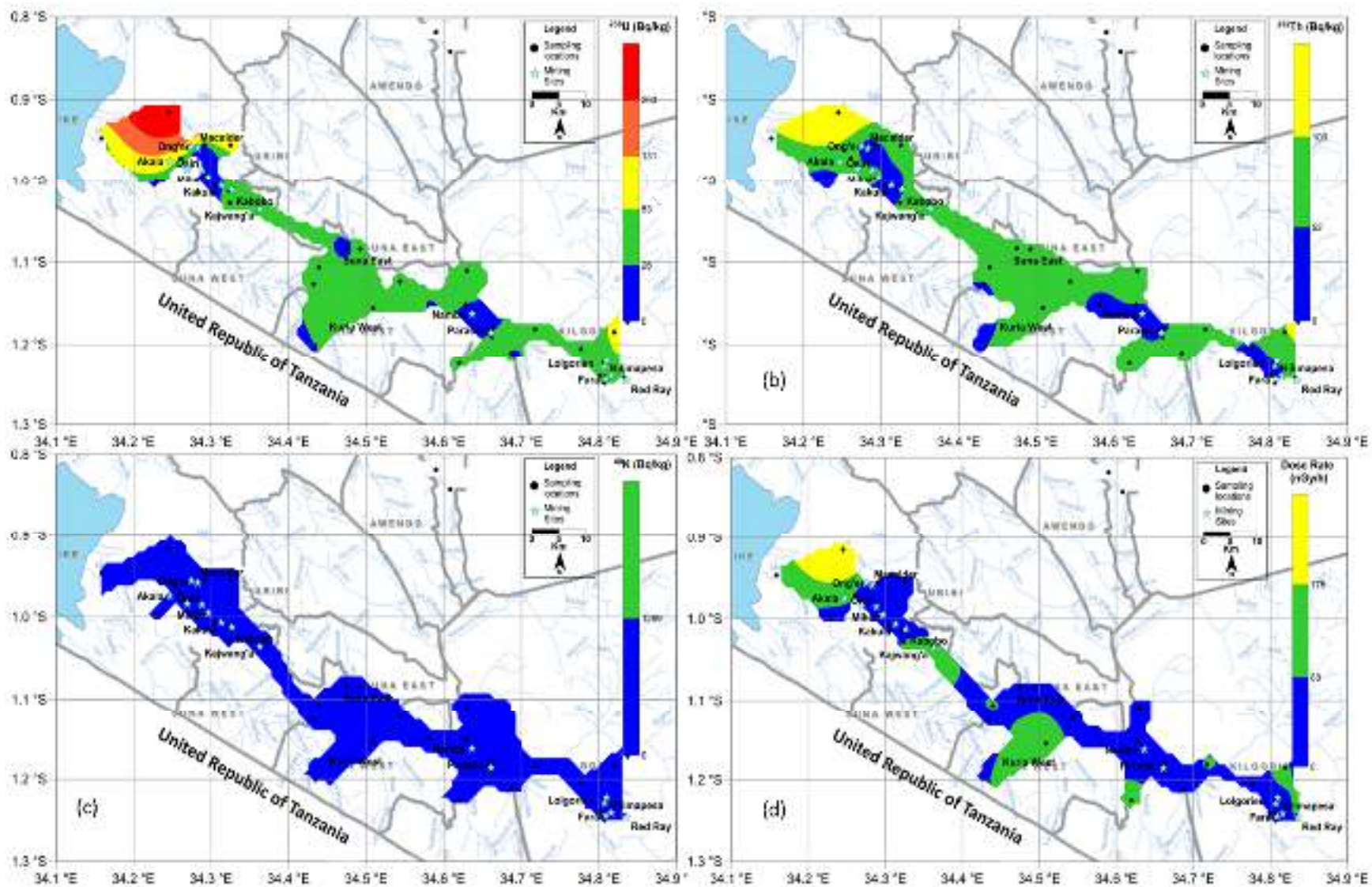
Figure 5. 12: Spatial distribution of a) ^{238}U b) ^{232}Th c) ^{40}K and d) Dose Rate in Soil
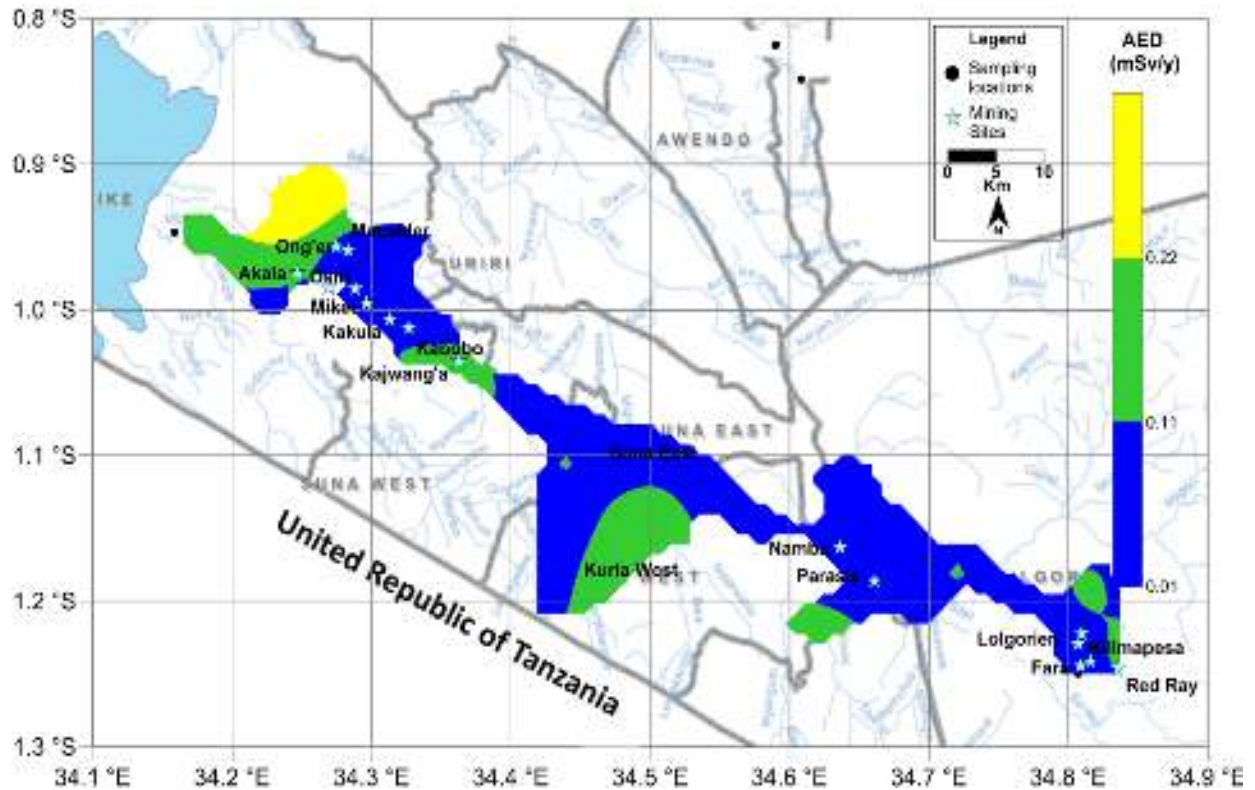
Figure 5. 13: Spatial distribution of AED in soil

Even though there is no evidence from this study that mining contributes significantly to NORM, the miners are exposed to low levels NORM that can still be a danger to their lives. This is because there is no attempt by the miners to either wear dust masks/gloves/gum boots or take precaution against ingestion and inhalation of the dust that may contain radionuclides. To make matters worse, children more often accompany their parents in their endeavors which can affect them since their body tissues and organs are still under development. Pregnant mothers are also not left out in gold mining which endangers fetus life and development especially during the first trimester of pregnancy. Soil and rocks from the mining areas are normally used in the construction of houses, this poses a threat to those living in such houses since the radionuclides continue to decay so long as the nuclei are still active. According to UNSCEAR (2000) the time humans spend in their dwellings is higher therefore duration of exposure will definitely compound the dose.

5.4 Elemental Concentration in Tailings

Concentration of mercury in tailings is highest of the heavy metals investigated in more than 70% out of the 14 sampled locations, **Appendix C, Table C**. Tailings at Macalder had the highest concentration of all the heavy metals studied, this is due to accumulation of tailings since 1920's when mining started at the mine. The highest concentration of mercury (30721.87 mg/kg) was at Lolgorien and Osiri (25005.74 mg/kg), however low concentrations were at Namba (204.85 mg/kg) and Red Ray 1 (484.78 mg/kg). While the concentration of mercury in tailings depends mainly on the efficiency of miners in recovering it after use it also depends on the method application of mercury (like concentration, direct application on the ore etc.), number of miners at the mine, duration of accumulation, weather conditions, topography etc. just as the other heavy metals.

The highest concentration of As (5829.99 mg/kg), Cd (4.14 mg/kg), Cu (2329.99 mg/kg), Ni (766.12 mg/kg), Pb (3238.78 mg/kg) and Zn (1270.83 mg/kg) were found at Macalder with the concentration of Cr at Macalder being within the range of the highest concentration found at Namba. High concentration of the other metals at Macalder is as a result of the upper crust formations since the ore is excavated within the same location in most cases. According to Shackleton (1946), Macalder region is composed of Zn, Cu and Pb massive deposit that dominated by aphyric to porphyritic tholeiitic massive and pillowed basalts and thick doleritic sills. The three minerals accompany ore containing gold in the form of pyrite (FeS_2), bournonite (Pb, Cu, SbS_3), chalcopyrite ($CuFeS_2$), galena (PbS), sphalerite (ZnS), Pyrrhotite (FeS) and tennantite [(Cu, Fe, Zn) As_4S] (Ogola, 2010). A study conducted at the Osprey and Fumani gold tailings dams in South Africa found high concentrations of As (7,824 mg/kg) and Cr (269.3 mg/kg) but lower Zn (96.4 mg/kg) and Cu (64.2 mg/kg) compared to the findings in this study under natural conditions, the concentration of heavy metals is a reflection of their concentrations in the local geology. However, after repeated dumping of the tailings, their concentrations are elevated in and around the dumping sites.

Mean heavy metal concentration in the tailings was decreasing in the order: Hg >As> Pb> Cu> Zn> Ni> Cr> Cd **(Table 5.21).** The mean of Hg (8985.92 mg/kg) is almost fifty times higher than the minimum mercury concentration found in this study and about 500 times higher than the mean

concentration in tailings at Butana in Sudan (Younis, 2018) **(Table 5.22)** This shows that mercury is the main polluter in the tailings in gold processing process in Migori Transmara gold mining areas. After gold recovery, the tailings are normally disposed in the immediate environment in heaps that are left without proper management thereby exposing them to both wind and water erosion. Tailings therefore eventually will find their way to the atmosphere, soil and water bodies near and away from the vicinity of the mines thereby leading to contamination of environment with heavy metals.

Table 5. 21: Summary of Heavy Metals Concentration (mg/Kg) in Mine Tailings in Migori Transmara Goldmines

		As	Cd	Cu	Cr	Ni	Pb	Zn	Hg
Mean		939.03	0.90	406.38	91.59	261.48	437.32	266.56	8985.92
Std. Deviation		1557.67	1.11	644.52	31.09	277.63	878.66	383.96	10252.81
Median		296.14	0.57	132.06	87.17	116.64	136.69	131.35	4415.38
MAD		273.80	0.38	87.60	18.86	89.87	121.16	56.33	4070.56
Skewness		2.71	2.29	2.53	-0.05	0.89	2.95	2.27	1.13
CV		165.88	123.33	158.60	33.94	106.18	200.92	143.67	114.10
Minimum		10.55	0.07	39.22	41.08	17.31	4.48	41.22	204.85
Maximum		5829.27.00	4.14	2329.27	138.56	766.12	3238.78	1270.83	30721.87
Percentiles	25	44.25	0.00	81.50	69.75	45.50	20.00	65.75	786.75
	50	296.00	1.00	132.00	87.00	116.50	136.50	131.00	4415.00
	75	1350.25	1.00	428.00	121.00	547.50	289.00	196.50	15991.50

The mean concentration of arsenic (939.03 mg/kg), with the highest concentration (5829.99 mg/kg) at Macalder mines, shows that the gold ore in this area is mainly associated with Arsenopyrite (FeAsS) (Ogola *et al.,* 2002). Even though the highest concentration found in our study is in the same order as the one found by Kim and Jung in Korea, the mean in this study is one order lower than in their study (Kim and Jung, 2004).

Apart from effect on humans, crop yield is likely to decrease since arsenic finally find its way into the nearby soils. According to Havada (1996), a 100 mg/kg concentration of As in soil can reduce crop yield by 90% and can lead to arsenic poisoning and result to skin and lung cancer. The mean concentration of As in this study is almost the same as the concentration found in Obuasi in Ghana while the mean concentrations of Cu and Zn in our study are six and two times higher respectively

(Bempah *et al.,* 2013). Even though the concentrations of Cr and Zn in our study are within the levels in in Butana in Sudan, the concentrations of Cd and Pb are six and two times respectively lower in this study (Younis, 2018b).

Table 5. 22: Heavy Metal Concentration (mg/Kg) in Tailings in This Study Compared to Other Regions

Element	This Study	Limpopo, South Africa (Matshusa et al., 2012)	Bongwha, Korea (Kim and Jung, 2004)	Butana, Sudan (Younis, 2018b)
As	939.03 (10.55 – 5829.99)	0 – 937	5224 (2927 – 6675)	-
Cd	0.90 (0.07 – 4.14)	-	12.2(5.7 – 25)	5.455 (1.80 – 9.07)
Cr	91.59 (41.08 – 138.56)	-	3.8(0.98 – 21.7)	82.10 (13.8 – 150.4)
Cu	406.38 (39.22 – 2329.27)	11-96	102(35 – 383)	245.91 (16.92 – 474.9)
Hg	8985.92 (204.85 –30721.87)	-	-	20.54 (16.92 – 24.92)
Ni	261.48 (17.31 – 766.12)	0 – 2	-	82.10 (7.59 – 60.71)
Pb	437.32 (4.48 – 3238.78)	28 – 1142	2274(935 – 11135)	1015.9 (35.83 – 1996.0)
Zn	266.56 (41.22 – 1270.83)	15 – 130	-	266.29 (5.92 – 526.66)

A study by Abdul-Wahab and Marikar (2012) while comparing the concentrations of heavy metals in plants growing next to an open gold mine pit and plants in control areas in Wilayet Yangol in Oman found a correlation between the concentration of heavy metals in soil and in plants; therefore, there is a possibility of heavy metals being translocated from soils to parts of the plants which can then be fed on by livestock and eventually end up in humans through food chain.

Infiltration of water through these tailings leads to leaching of heavy metals in large volumes that eventually end up in streams and the river ecosystems, this results in acid mine drainage (AMD) which have serious effects on water bodies (Fashola *et al*., 2016). Apart from leaching, wind dispersion and water erosion end up depositing heavy metals from these tailings to nearby water bodies and soils. In order to manage these tailings, they should be directed into dams and impoundments where they can be treated. Isolating and capping the tailings will control their dispersion by water and wind therefore their mobility in the environment will be controlled.

5.5 Elemental Concentration and Radiation Exposure in River Sediments

This section presents and discusses results on heavy metal and activity concentration of heavy metals and radionuclides respectively as well as radiation exposure in river sediments in rivers draining Migori and Transmara gold mining areas. Pollution indices in river sediments are also discussed.

5.5.1 Heavy metal Concentration in River Sediments

The mean and median concentration (mg/kg) of the heavy metals in the sediments decreases in the order Hg>As>Cr>Zn>Pb>Cu>Ni>Cd and Hg>Zn>Cr>Cu>Ni>As>Pb>Cd respectively, **Table 5.23**. The mean mercury concentration (310.97 mg/kg) in this study is higher than the maximum concentrations in river sediments draining gold mining areas in Tanzania, Ghana, Nigeria and Sudan in studies carried out by Kihampa and Wanaty, (2013), (Arhin *et al*., 2016), (Amadi *et al.,* 2017) and Younis, (2018b) respectively, **Table 5.24**. This is because of good management of tailings in mines that includes covering of the tailing ponds to prevent them from wind and surface run offs as well as banning of processing gold ores along river banks which is rampant in Migori Transmara gold mines. the median concentrations of As and Hg are 6 and 5 times higher than the background values while the mean concentration of Hg and As 1728 and 12 times respectively

above TEC and 293 and 4 times respectively above the PEC, this calls for control measures like avoiding processing gold along river banks and using tailing ponds to store tailings.

The concentration of mercury is higher than the concentration of the other heavy metals studied in most of the sampled locations, **Appendix D and Table D1**. The concentration of arsenic (1132.00 mg/kg) at Masaba, lead (1528.26 mg/kg) at Migori river (between Namba and Parasis) and mercury (2376. 93 and 1902.75 mg/kg) at Kilimapesa and Onuke respectively are one order of magnitude above the concentration of the other metals investigated at those respective locations. Highest concentration of arsenic, lead and mercury in river sediments are 283, 112 and 100 times respectively above their BGV that were 4.00 mg/kg, 13.70 mg/kg and 23.75 respectively. There was active mining in all the sampling locations during sampling, this is an indication that mining impact negatively on heavy metal concentration in the rivers draining Migori Transmara gold mining areas.

The concentration (mg/kg) of the all the heavy metals, apart from Cr, at Kilimapesa [As(171.42),Cd(0.43),Cu(91.44),Ni(62.91),Pb(107.99),Zn(147.66),Hg(2376.93)] and Kuja 3 [As(363.16),Cd(0.0.71),Cu(276.35),Ni(191.95),Pb(191.97),Zn(205.51),Hg(785.34)] where there was intense mining are high compared to their concentrations at Nyambae [As(4.00),Cd(0.0.01),Cu(15.70),Ni(13.10),Pb(20.70),Zn(32.80),Hg(28.75)] and the background where there was no mining. High concentration (186.10 mg/kg) of Cr at Nyambae is as a result of spillage at a tailing pond at North Mara Gold Mining site that may have found its way through atmospheric deposition to nearby soils and rivers (Almås *et al.,* 2009). High concentrations of all the heavy metals apart from Cr were found at Kilimapesa where there are many mines compared to Ekiwancha which is lower in altitude with no mining sites around it. This shows heavy metal pollution concentration in rivers decreases with increase in distance from the mines, this is also confirmed by high heavy metal pollution at Kuja 1 compared to Wath Ong'er. These findings confirm anthropogenic impact of gold mining in the rivers in this gold mining belt and therefore this calls for remediation of tailing ponds and damping sites which is the main source of the heavy metals (Amadi *et al.,* 2017). High concentrations of Hg and Zn at Kabuto suggest their accumulation over time, this is because river Kuja (after the merger between river Kuja and Migori at Wath Ong'er) normally bursts its banks during flooding. Before merging at Wath Ong'er to

form larger river Kuja, river Kuja and Migori drain through the Migori Transmara gold mining areas thereby carrying heavy metal loaded sediments with it.

Table 5. 23: Summary of Heavy Metal Concentration (Mg/Kg) in River Sediments and TEC, PEC, World's and The Continental Crust Average

Description		As	Cd	Cr	Cu	Ni	Pb	Zn	Hg
Mean		119.69	0.11	89.64	60.78	58.09	77.67	82.13	310.97
Std. Deviation		255.40	0.16	58.06	68.04	56.47	232.87	45.86	480.17
Median		22.50	0.02	73.62	44.84	43.75	21.52	79.24	128.90
MAD		14.67	0.01	37.32	11.63	25.00	8.09	36.26	102.16
CV (%)		213.38	145.45	64.77	111.94	97.21	299.82	55.84	154.41
Skewness		3.03	2.05	1.11	3.11	2.03	5.92	1.14	2.93
Minimum		4.00	0.01	20.20	9.77	8.85	9.02	28.30	8.40
Maximum		1132.00	0.71	286.40	373.06	254.69	1528.26	230.27	2376.93
Background Concentrations		4.00	0.01	186.10	22.90	12.60	13.70	35.20	23.75
Worlds Average (Turekian and Wedepohl, 1961)		13.00	0.30	90.00	45.00	68.00	20.00	95.00	0.40
TEC		5.90	0.60	37.30	35.70	18.00	35.00	123.00	0.17
PEC		17.00	3.53	90.00	196.60	35.90	91.30	315.00	0.49
Percentiles	25	9.76	0.01	41.10	17.28	17.98	14.40	38.46	31.59
	50	22.50	0.02	73.62	44.84	43.75	21.52	79.24	128.90
	75	69.66	0.15	138.76	74.85	67.1	36.28	109.21	389.41

TEC- Threshold effect concentration, PEC- Probable effect concentration (MacDonald *et al*., 2000).

Table 5. 24: Mean Heavy Concentration in Sediments in This Study Compared to other Gold Mining Areas

Country	As	Cd	Cr	Cu	Hg	Ni	Pb	Zn	Reference
Kenya	119.69	0.11	89.64	60.78	310.97	58.09	77.67	82.13	This Study
Tanzania	-	0.67	13.98	0.81	16.07		18.78	62.16	Kihampa and Wenaty, (2013)
Ghana	15.8	0.90	354.10	14.70	0.90	17.40	4.70	31.60	(Arhin *et al.,* 2016)
Nigeria	0.25	78.32		42.87	4 4.95	7.40	119.31	42.45	(Amadi *et al.,* 2017)
Sudan	-	14.74	223.51	57.17	11.86	105.00	86.67	58.15	(Younis, 2018b)

From this study, mercury and arsenic are the leading polluters of the local rivers as far as (artisanal) gold mining in this region is concerned. Once metallic mercury finds its way into water bodies, it reacts with organic acids in the environment to organic complexes (soluble mercury) making it available for methylation by biotic and abiotic factors. On transformation into methylmercury, mercury is bioavailable to water plants that are fed on by fish, through fish consumption, humans are exposed to mercury. Piscivorous fish have even higher concentration of mercury through bioaccumulation as was found in Peru thereby exposing humans to even higher concentrations (Martinez *et al.,* 2018). Ngure *et al.* (2017) found high concentrations of T-Hg in the nails and scalp hair of children from Migori gold mining belt.

The mean concentration of all the heavy metals except Cr in river sediments are higher than in soil, for instance the concentration of (Hg and As) and Cd are 3 and 2 Cd times respectively higher. This confirms that sediments are the best matrix to gauge the ecological impact of heavy metals in the surrounding environment (Bessa *et al.,* 2018). According to Thevenon *et al.,* (2011), river sediments act as a sink of pollutants that arise from local human activities and natural geogenic processes, thereby giving useful present and historical information on pollution of the water body and its environs. From these findings, heavy metals concentration in Lake Victoria is likely to be high since these rivers drain into Lake Victoria. According to Machiwa, (2003), there was high concentration of Pb, Cu and Zn in Lake Victoria near Mirongo River Mouth due to mining in Lake Victoria Gold Fields in Tanzania (LVGF)

5.5.2 Source Apportionment of Heavy Metals in River Sediments

5.5.2.1 Principal Component Analysis of heavy metals in sediments

Four PCs contributing 84.01 % of the total variance were reatined, the first PC that is 35.37 % of the total variance comprise of Cd, Cu and Zn. PC-2, PC-3 and PC-4 consist of (Ni and Pb), As and Cr respectively and they contribute 19.21%, 15.21% and 14.29% of the total variance, **Table (5.25 – 26)**.

Table 5. 25: Varimax rotated principal component loadings for four principal components for heavy metals in sediments

Element	Component			
	1	2	3	4
As	0.034	0.02	**0.976**	0.028
Cd	**0.791**	0.136	0.209	-0.087
Cr	-0.118	0.013	0.028	**0.991**
Cu	**0.922**	0.028	-0.074	-0.054
Ni	0.379	**0.703**	0.225	0.056
Pb	-0.06	**0.908**	-0.105	-0.024
Zn	**0.915**	0.078	-0.018	-0.064

Table 5. 26: Eigen Concentrations and Percentages of Total Variance by Different Principal Components for Heavy Metals in Soil

Component	Initial Eigenvalues			Rotation Sums of Squared Loadings		
	Total	% of Variance	Cumulative %	Total	% of Variance	Cumulative %
1	2.680	38.282	38.282	2.476	35.368	35.368
2	1.262	18.031	56.313	1.344	19.206	54.573
3	1.053	15.050	71.363	1.065	15.212	69.785
4	0.890	12.715	84.077	1.000	14.292	84.077
5	0.543	7.754	91.831			
6	0.424	6.054	97.885			
7	0.148	2.115	100.000			

5.5.2.2 Pearson's Correlation Analysis of heavy metals in Sediments

There is a positive, moderate and significant correlation ($p<0.05$) between Ni and Cu ($r=0.351$) and Pb and Ni ($r=0.370$) and positive, strong and significant correlation ($p<0.01$) between Zn and Cu ($r=827$) and Cu and Cd ($r=0.584$), **Table 5.27**. There is also a positive moderate but significant ($p<0.01$) between Ni and Cd ($r=0.386$), Ni and Cu ($r=0.351$) and Pb and Ni ($r=0.370$).

Table 5. 27: Pearson's Correlation for Heavy Metals in River Sediments

	As	Cd	Cr	Cu	Ni	Pb	Zn
As	1.000						
Cd	0.166	1.000					

Cr	0.056	-0.154	1.000				
Cu	0.000	0.584**	-0.171	1.000			
Ni	0.164	0.386**	-0.005	0.351*	1.000		
Pb	-0.019	0.065	0.013	-0.004	0.370*	1.000	
Zn	0.066	0.640**	-0.165	0.827**	0.295	0.096	1.000

NB. * and ** denote statistically significant correlation at 0.05 and 0.01 probability level respectively.

5.5.2.3 Hierarchical Cluster Analysis of heavy metals in River Sediments

HCA clusters the investigated heavy metals in sediments into three groups As, Pb and (Cu, Zn, Ni Cd and Cr), **Fig: 5.14**. As appears to be originating from a point source, this is confirmed by As accounting for 15% of the total variance in PCA and having a high loading of 0.976. This is further affirmed by PCA that show As to be having no significant correlation with any of the other heavy metals investigated as was also found by Donkor *et al.*(2005) in river Pra in Ghana. They further found positive correlation between As and Hg, this was attributed to the fact that mercury is used to extract gold from arsenopyrite bearing ore. Clustering of Cd, Cu, Zn and Ni is also supported by large, positive and significant correlation between Zn and Cu, Cu and Cd, Ni and Cd. Cu, Zn, Ni, Cd and Cr are originating from both anthropogenic and natural like weathering.
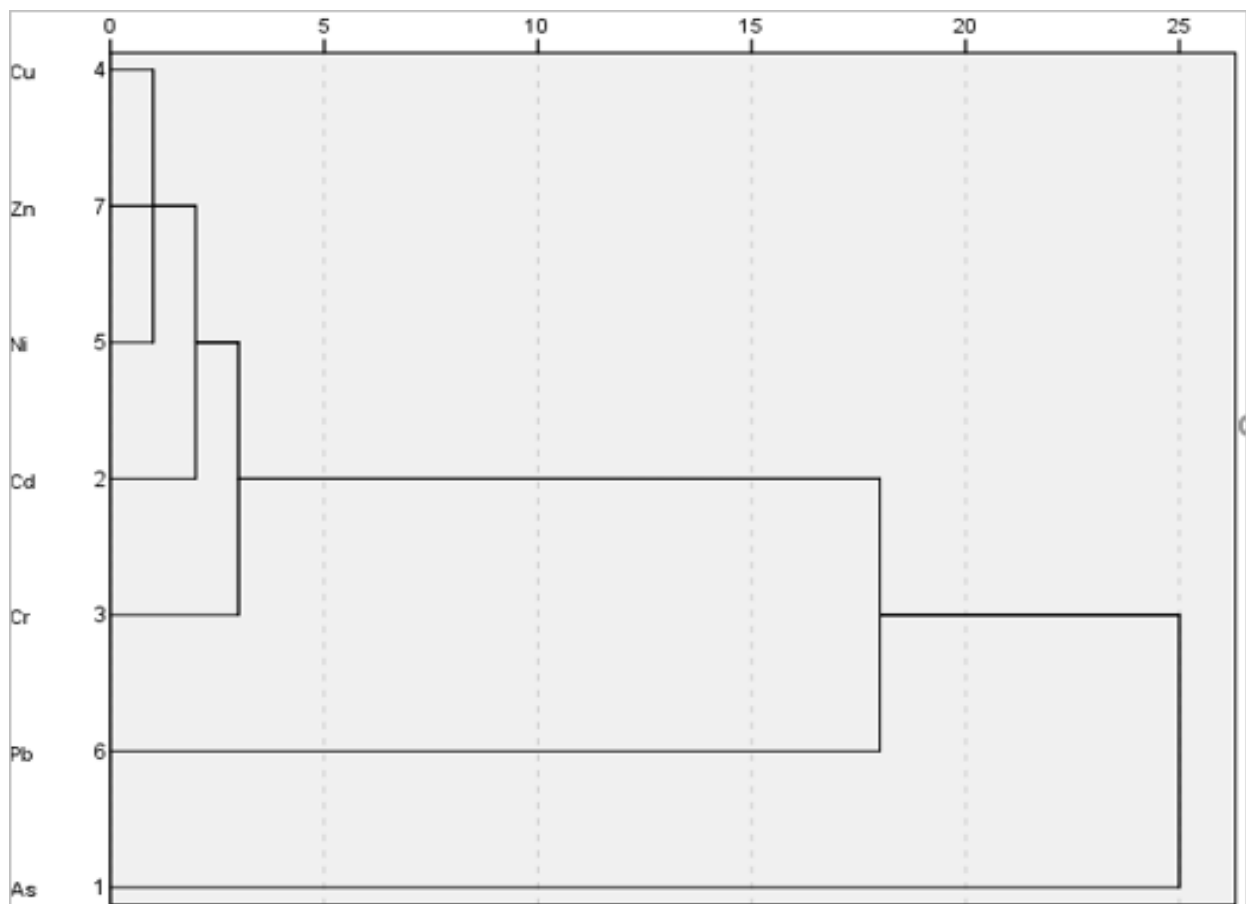
Figure 5. 14: Dendrogram of the Hierarchical cluster analysis of heavy metals in sediments

There is an agreement between PCA in soil and HCA in sediments regarding the sources of the heavy metals in sediments and soil in this study. Since both of them broadly cluster the investigated heavy metals into three i.e. As, Cr and Pb and (Cu, Zn, Ni Cd and Ni) suggesting gold mining, natural soil formation and a mixture gold mining and anthropogenic of the processes as the main source of heavy metals in soil and sediments. Lack of significant correlation between Cr and As with the rest of the heavy metal studied, confirms their origin from different sources as is confirmed PC-3 and PC-4 respectively. Poor correlation between As and Cr is because of their speciation, while salinity of water above the bottom sediments affects variability and speciation of As in river sediments Cr (III) is most adsorbed by sediments compared to Cr(IV) (Jabłońska-Czapla et al., 2015).

5.5.3 Pollution Indices of Heavy Metals in River Sediments

5.5.3.1 Geochemical Background of the Investigated Heavy Metals

In the calculation of geochemical background concentrations, the median concentrations were used since it represents the local data and it is hardly influenced by outliers (Ohta et al., 2005). **Fig: 5.15**. The median concentration (mg/kg) of As, Cd, Cr, Cu, Ni, Pb, Zn and Hg were 22.50, 0.02, 73.62, 44.84, 43.75, 21.52, 79.24 and 128.09 respectively, this is strongly related (r=0.937) to the calculated background concentration of the same heavy metals in soils in the same area. This confirms geochemical background is a representative of the natural concentration range in a given environment medium (Gałuszka and Migaszewski, 2011).
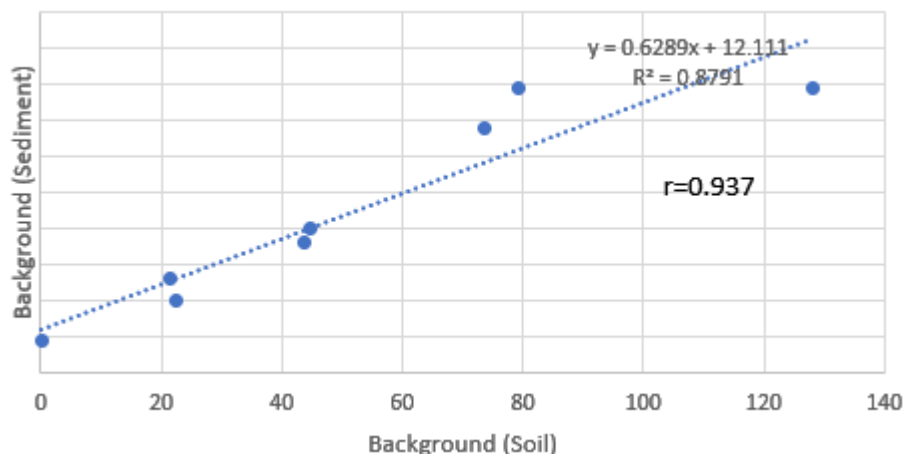
Figure 5. 15: Correlation Between Background Concentrations of Heavy Metals In Sediments And Soil.

5.5.3.2 Contamination Factor

Lead has the highest CF (71.02) in Migori river 6 next to Parasis mines, indicating a point source. (**Appendix D and Table D2**). High CF of As were found at Masaba (50.31), Kakula (43.62) and Mikei (38.26). Mercury has the highest CF (18.44) at Lolgorien (behind Lolgorien center), Migori 2 (5.63) (the highest point of sample collection) and Onuke (14.76) though not as high those of lead and arsenic. There was intense gold mining at all the locations where high concentrations of As, Hg and Pb were found. This supports the high concentration found at these locations and shows the impact of gold mining to the river sediments.

The mean CF in river sediments decreased as follows: As>Pb>Hg>Cu>Ni>Cr>Zn (**Table 5.28**). The mean CFs show there is considerable contamination by As and Pb, moderate contamination by Cr, Cu, Hg, Ni and Zn and low contamination by Cd. Over 25% of the sampling locations are considerably contaminated by As and Hg. Even though the mean contamination factors of Cd, Cr, Cu and Ni show low to moderate contamination, their maximum contamination factors indicate considerable contamination to very high contamination at Migori 9, river Nyathrogo, Migori 4 and river Kwach.

The degree of contamination (C_{deg}=16.4) of the river sediments shows they are considerably contaminated by the studied heavy metals; this is an indication the river waters are also contaminated. However, migration and transformation processes, biological toxicity and bioavailability of heavy metals in the sediments mainly depend on the fractionation of heavy metals while forms of the heavy metals are closely associated with toxic effects and toxicological risk of the sediments.

Table 5. 28: Summary of Contamination Factors of River Sediments in Migori Transmara Gold Mining Areas

Description		As	Cd	Cr	Cu	Ni	Pb	Zn	Hg
Mean		5.32	0.15	1.22	1.36	1.33	3.61	1.04	2.41
Std. Deviation		11.35	0.90	0.79	1.52	1.29	10.82	0.58	3.73
Median		1,00	1.00	1.00	1.00	1.00	1.00	1.00	1.00
MAD		0.66	0.00	0.51	0.62	0.57	0.38	0.46	0.79
Minimum		0.18	0.00	0.27	0.22	0.20	0.43	0.36	0.07
Maximum		50.31	6.00	3.89	8.32	5.82	71.02	2.91	18.44
BGV		0.178	0.001	2.528	0.511	0.288	0.637	0.444	0.184
Percentiles	25	0.43	0.00	0.56	0.39	0.41	0.67	0.49	0.25
	50	1.00	0.00	1.00	1.00	1.00	1.00	1.00	1.00
	75	3.10	0.02	1.88	1.67	1.53	1.69	1.38	3.02

5.5.3.3 Enrichment Factor

Enrichment of the sediments by mercury is the highest at all the sampled locations, with nine locations having of EF of the order of one above the other metals at those locations (**Appendix D; Table D3**). EF of arsenic was second to mercury in a few locations. All sediments investigated for mercury show extremely high enrichment apart from Red Ray that shows very high enrichment. The highest EF of mercury was found at Onuke (3922.77 mg/kg) and Lolgorien (3823.11 mg/kg) which were basically within the same range. High EF of river sediments by mercury and other heavy metals in the Migori Transmara gold mining belt is due to direct discharge of tailings directly and/or indirectly into river during panning by the artisanal miners.

Based on the mean enrichment factor, the following decrease in EF was observed: Hg>As>Pb>Cr>Cu>Ni>Cd, the mean EF of mercury (EF>811.52) shows mercury is extremely highly enriched with over 75% of the sites being extremely highly enriched (**Table 5.29**). There is significant enrichment with arsenic with over 25% of the sites showing significant enrichment.

The mean EF of As and Hg suggests they are enriched at all the locations by human activities (Olando *et al.,* 2020). The means of the rest of the metals show deficient to minimal enrichment. Maximum EF of Cu, (Cr and Ni) and (Pb and As) however show moderate, significant and extremely high enrichment respectively in some areas. Cd is deficient to minimally enriched in all the river sediments investigated. The mean EF of As, Cr, Pb and Hg show they originate from anthropogenic activities while the other natural processes.

Table 5. 29: Summary of Enrichment Factors of River Sediments at Sampled Locations

Description		As	Cd	Cr	Cu	Ni	Pb	Hg
Mean		12.88	0.36	1.64	1.42	1.18	4.57	811.52
Std. Deviation		31.31	0.40	1.69	0.78	1.46	14.24	995.39
Median		2,51	0.11	1.01	1.21	0.76	1.80	391.39
MAD		1.70	0.86	0.42	0.39	0.49	0.94	277.89
Minimum		0.33	0.02	0.14	0.27	0.18	0.34	35.86
Maximum		179.46	1.41	6.87	3.42	9.32	95.62	3922.77
BGV		0.83	0.09	5.581	1.373	0.50	1.849	160.245
Percentiles	25	0.98	0.06	0.66	0.84	0.46	1.03	171.39
	50	2.51	0.11	1.01	1.21	0.76	1.80	391.39
	75	6.12	0.52	1.84	1.94	1.41	3.12	1065.8

5.5.3.4 Geo-Accumulation Index (Igeo)

Geo-accumulation of Hg is the highest at all the sampled locations as is also CF and EF. There is high geo-accumulation index by As and Pb while Cd is the least geo-accumulated is Cd. Geo-accumulation index of lead and mercury at Migori 6 (next to Parasis mines) are the same however, all geo-accumulation indices of mercury were positive (3.807 to 11.952) **(Appendix D; Table D4)**. This shows most of the sediments are extremely polluted with mercury with just a few locations showing strong contamination.

Mean geochemical index decreases in the order Hg>As>Pb>Cu>Cr>Zn>Ni>Cd **(Table 5.30)**. The mean I_{geo} show river sediments in Migori Transmara are very heavily (extremely) polluted by mercury; over 75% of the sampled locations are very heavily (extremely) polluted. Extreme sediment pollution has also been found in river sediments in Nigeria where artisanal gold mining

is practiced (Nwanosike *et al.*,2018). Even though over 50% of the soils are contaminated to moderately contaminated by As, over 25% are moderately to extremely contaminated. River sediments from Kakula and Mikei where there was active mining and ore processing at the river are extremely contaminated. This confirms As is associated with gold bearing ore and the effect of directly washing the ore in rivers. There is no contamination by Cr, Cu, Ni and Pb from their mean, however, their maximum concentrations show there are areas where there is moderate to extreme contamination.

Table 5. 30: Summary Of Geo-Accumulation Index of River Sediments at Sampled Locations.

Description		As	Cd	Cr	Cu	Ni	Pb	Zn	Hg
Mean		0.66	-3.52	-0.89	-0.72	-1.35	-0.04	-1.01	7.71
Std. Deviation		2.20	2.18	0.97	1.25	1.25	1.51	0.82	2.04
Median		0.23	-5.00	-0.88	-0.59	-1.22	-0.48	-0.85	7.74
MAD		1.27	0.500	1.75	0.53	0.76	0.65	1.70	1.71
Minimum		-2.29	-5.49	-2.74	-2.79	-3.53	-1.71	-2.33	3.81
Maximum		5.86	0.66	1.09	2.47	1.32	5.67	0.69	11.95
BGV		-2.29	-5.49	0.46	-1.56	-3.02	-1.13	-2.02	5.31
Percentiles	25	-1.00	-5.49	-1.72	-1.97	-2.50	-1.06	-1.89	5.72
	50	0.20	-4.99	-0.87	-0.59	-1.22	-0.48	-0.85	7.74
	75	1.83	-1.61	0.04	0.15	-0.61	0.27	-0.38	9.34

5.5.4 Radioactivity of River Sediments

Activity concentration of ^{40}K is the highest of the three radionuclides in most of the sampled locations and lowest between Rogambi and Nyangutu where there is no mining (**Appendix D; Table D5 and Figure 5.16 and 5.17**). Location Kuja 1 has the highest activity concentration of ^{232}Th (532.206 Bq/kg), ^{238}U (70.619 Bq/kg), absorbed dose in air (126.674 nGy/h) and annual effective dose (0.153 mSv/yr) which are all about twice the world's average, this is because of accumulation of the radionuclides since this location is just below Macalder mine where mining has been going on for a century. Although the activity of ^{40}K at Kuja 1 is not the highest, it is about as 1.2 times the worlds average (UNSCEAR, 2010). Kabuto also show concentrations in the range of Kuja 1, this is also because of accumulation of radionuclides in this flood prone are thereby exposing the populace to higher concentrations of radiation.
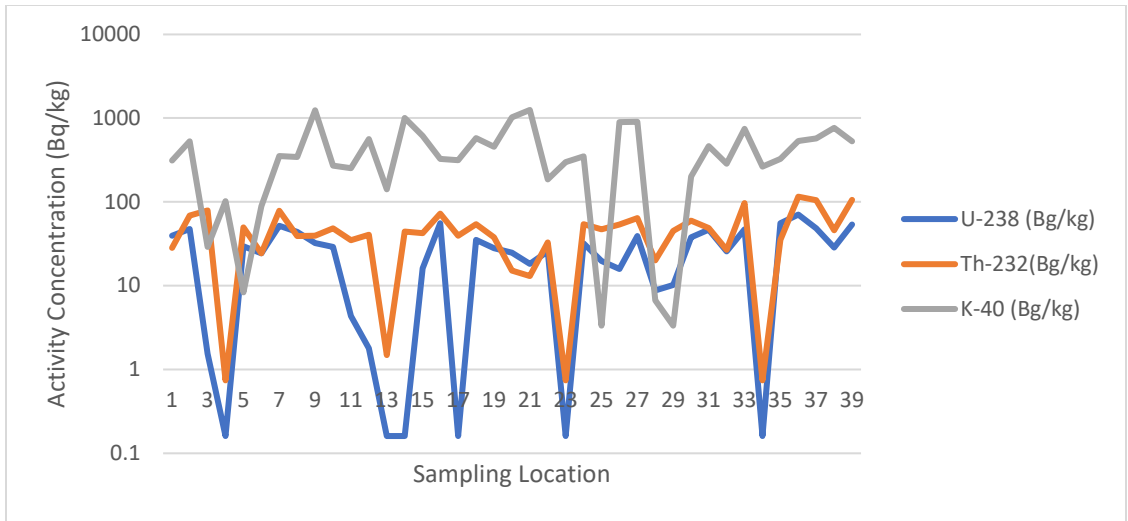
Figure 5. 16: Activity Concentration of ^{40}K, ^{232}Th and ^{238}U in River Sediments

Typical activity counting spectrum of river sediment is as shown below (**Figure 5.17).**
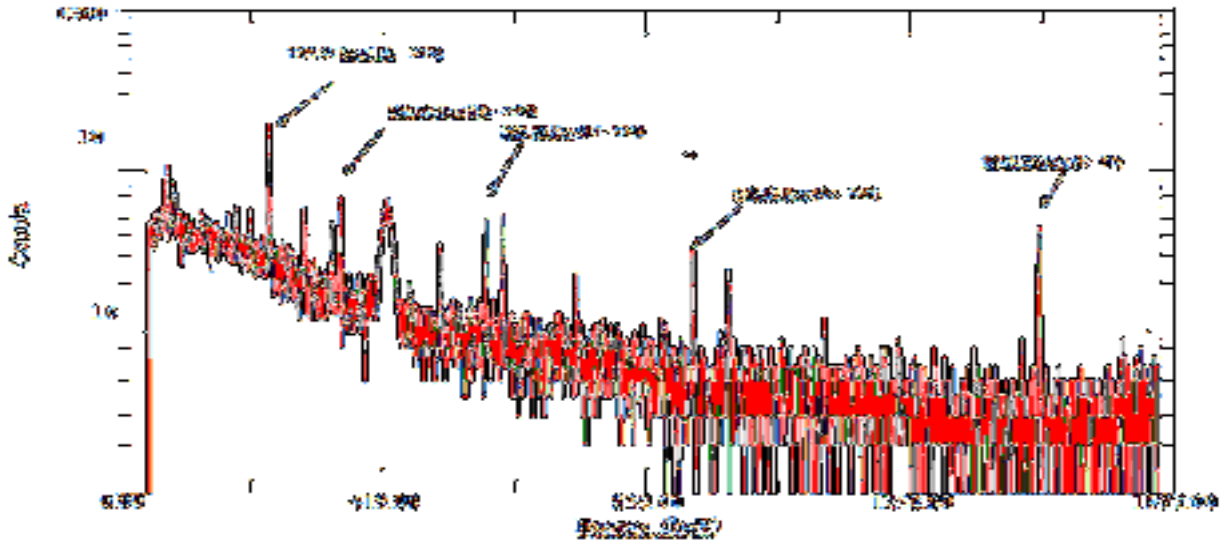
Figure 5. 17: Typical Spectrum of A River Sediment from HPGe Gamma Ray Spectrometer.

High absorbed dose found at Kuja 1,Osiri and Kabuto where the concentrations are 124.674 nGy/h, 111.091 nGy/h and 110.628 nGy/h respectively are about twice the world average. Highest annual effective dose was at Kuja 1(0.153 mSv/y) (next to Macalder mines) followed by Osiri (0.136 mSv/y). The AEDE at Kuja and Osiri are comparable to BGV (0.106 mSv/y) and values at

Tebesi (0.111 mSv/y) where there were no mines, this shows mining contributes minimally to radiation levels in this area.

The average activity concentration in river sediments of ^{238}U, ^{232}Th and ^{40}K were 26.87 ±19.50 (0.16 – 70.62) Bq/kg, 46.31 ±28.59 (0.74 – 115.39) Bq/kg and 438.66 ± 335.36 (3.33 – 1252.45) Bq/kg respectively **(Table 5.31)**. All the radioactivity concentrations in this study are higher than the findings by Adukpo *et al.* (2014b) in Pra basin in Ghana. The mean concentration of ^{238}U is below the worlds average but that of ^{232}Th and ^{40}K are within the world's average, (IAEA, 2011). Over 25% but below 50% of the samples have concentrations of ^{238}Uand ^{40}K above the world's average and about 50% of the samples have ^{232}Th concentrations above the world's average. However, maximum activity concentrations of ^{40}K, ^{232}Th and ^{238}U, are 3.0, 2.5 and 2.2 times above the world's average.

Table 5. 31: Summary of Activity Concentration, Absorbed Dose Rate in Air and Annual Effective Dose in River Sediments

		U-238 (Bq/kg	Th-232 (Bq/kg	K-40 (Bq/kg)	Dose rate (nGy/h)	AED (mSv/yr)
Mean		27.13	45.28	439.26	60.83	0.07
Std. Deviation		19.16	29.22	334.53	30.39	0.04
Median		28.00	42.00	342.00	60.63	0.07
MAD		17.83	15.32	200.03	19.80	0.02
Skewness		0.19	0.56	0.85	0.25	0.25
Kurtosis		-0.87	0.11	0.16	-0.29	-0.29
Minimum		<5.00	<5.00	<30.00	7.02	0.01
Maximum		71.00	115.00	1252.00	128.89	0.16
BGV		51.84	78.41	351.00	86.o5	0.11
Percentiles	25	9.00	27.00	201.00	40.28	0.05
	50	28.00	42.00	342.00	60.63	0.07
	75	44.00	60.00	578.00	79.72	0.10

From the results, as much as mining doesn't seem to be contributing much to exposure to radiation, there are areas like Osiri, Kabuto and Kuja 1 where there is high radiation due to gold mining. This therefore calls for precautions like avoiding directly emptying tailings and other mining wastes directly into rivers.

CHAPTER SIX

6.1 Conclusion and Recommendation

This study was carried out in the Migori-Transamara gold mining areas of Southwestern Kenya where gold mining has been carried out since 1920's. Mining was initially carried out by large scale miners but was later dominated by small-scale artisanal gold miners. The main gold mining areas studied in Migori County include Kanga, Kitere, Mikei, Macalder, Osiri, and Masara while Farah, Lolgorien, Parasis and Red Ray mines are located in Transmara.

The objectives of this study were to determine the concentration of As, Cd, Cr, Cu, Hg, Pb and Zn in lichens, moss, mine tailings, river sediments and soil. It was also to determine the activity concentration of ^{40}K, ^{232}Th and ^{238}U and compute absorbed dose, annual effective dose and pollution indices in soil and river sediments. This study also aimed at finding the relationship between the heavy metals investigated and hence identify their possible sources. Lastly, this study was to use Ordinary Kriging to model the radioecological and heavy metal impact of gold mining.

From this study, it can generally be concluded that gold mining has great impact on heavy metals (As, Cu, Hg, Pb and Zn) in the Migori Transmara gold mining areas but has minimal impact on radiation exposure. The main findings in this study include: -

The concentration of the heavy metals investigated in biomonitors, river sediments and soil show varied concentrations, the concentration of As, Cu, Hg, Pb and Zn were above the background. Heavy metal concentration decreased in the order tailings, river sediments and biomonitors. The concentration of mercury is the highest in all the matrices investigated and above the background in all the sampling locations.

Mean activity concentration of $^{234}U,^{232}Th$ and ^{40}K and radiation doses in soil and sediments are within the worlds average according to UNSCEAR. However, there are some areas like Agenga, Kajwanga, Lolgorien and Farah where radioactivity is high.

The river sediments and soil are moderately contaminated by all the heavy metals investigated apart from Cr and Cd. However, all the soils and over 75% of the river sediments are extremely

highly contaminated by mercury. Over 10% of soils and 25% of river sediments are very highly and considerably contaminated by arsenic respectively.

There is an agreement between PCA in soil and HCA in sediments regarding the sources of the heavy metals in sediments and soil in this region. Since both of them broadly cluster the investigated heavy metals into three i.e. As, Cr and Pb and (Cu, Zn, Ni Cd and Ni) suggesting gold mining, natural soil formation and a mixture gold mining and anthropogenic of the processes as the main source of heavy metals in soil and sediments.

Geostatistical models show higher concentration of the arsenic, copper, lead, zinc and mercury in biomonitors, soil and sediments around the mines. This is evident around Macalder and Lolgorien that are the epicenter of mining in Migori and Transmara respectively. Even though there is no much difference between activity concentration and exposure to radiation in the control area and the around the mines, spatial variability maps generally show slight elevation of activity concentration and radiation exposure around the mines. High heavy metal and activity concentration of ^{238}U and ^{232}Th is also increasing with decrease in distance towards Lake Victoria while activity concentration of ^{40}K is increasing towards Northern Tanzania.

6.2 Recommendations

From the above conclusions, the following are recommenced

Since mercury is the leading polluter in all the matrices, use of gold recovery methods that require minimal/do not require mercury like concentration and borax methods should be encouraged.

Management of tailings that include keeping tailings in dams should be encouraged because it is the main source of the heavy metals in the investigated matrices. Panning of gold ore along river banks should be discouraged since it leads to direct disposal of tailings into rivers thereby increasing the levels of heavy metals and radionuclides in the water bodies

Miners should be educated on the dangers of exposure to heavy metals and radionuclides and also encouraged to wear protective clothing and masks in the course of their mining operations to protect them from health effects of heavy metals and radionuclides.

Further study should carried out along Kenya Tanzania boarder to map out the extent of Chromium in Kenya.

Further study should also be carried in Lake Victoria along the catchment of the gold mines to determine the impact of gold mining on Lake Victoria sediments.

References

Abernathy, C. O., Thomas, D. J. and Calderon, R. L. (2003). Health Effects and Risk Assessment of Arsenic. *The Journal of Nutrition*, *133*(5), 1536S-1538S. https://doi.org/10.1093/jn/133.5.1536S

Ademola, A. K., Bello, A. K. and Adejumobi, A. C. (2014). Determination of natural radioactivity and hazard in soil samples in and around gold mining area in Itagunmodi, south-western, Nigeria. *Journal of Radiation Research and Applied Sciences*, *7*(3), 249–255. https://doi.org/10.1016/j.jrras.2014.06.001

Ademola, J. A. and Okpalaonwuka, N. E. (2010). Occupational exposure to natural radionuclides due to mining activities in Ibadan, Southwestern Nigeria. *Radioprotection*, *45*(1), 43–53. https://doi.org/10.1051/radiopro/2009032

Adler, R. A., Claassen, M., Godfrey, L. and Turton, A. R. (2007). Water, mining, and waste: An historical and economic perspective on conflict management in South Africa. *The Economics of Peace and Security Journal*, *2*(2), Article 2. https://doi.org/10.15355/epsj.2.2.33

Adriano, D. C., Wenzel, W. W., Vangronsveld, J. and Bolan, N. S. (2004). Role of assisted natural remediation in environmental cleanup. *Geoderma*, *122*(2), 121–142. https://doi.org/10.1016/j.geoderma.2004.01.003

Adukpo, O. K., Faanu, A., Lawluvi, H., Tettey-Larbi, L., Emi-Reynolds, G., Darko, E. O., Kansaana, C., Kpeglo, D. O., Awudu, A. R., Glover, E. T., Amoah, P. A., Efa, A. O.,

Agyemang, L. A., Agyeman, B. K., Kpordzro, R. and Doe, A. I. (2014). Distribution and assessment of radionuclides in sediments, soil and water from the lower basin of river Pra in the Central and Western Regions of Ghana. *Journal of Radioanalytical and Nuclear Chemistry*. https://doi.org/10.1007/s10967-014-3637-5

Aguko, W. O., Kinyua, R., and Ongeri, R. (2013) ASSESSMENT OF RADIATION EXPOSURE LEVELS ASSOCIATED WITH GOLD MINING IN SAKWA WAGUSU, BONDO DISTRICT, KENYA. 8.

Akoto, O., Nimako, C., Asante, J., Bailey, D. and Bortey-Sam, N. (2019). Spatial distribution, exposure, and health risk assessment of bioavailable forms of heavy metals in surface soils from abandoned landfill sites in Kumasi, Ghana. *Human and Ecological Risk Assessment: An International Journal*, *25*(7), 1870–1885. https://doi.org/10.1080/10807039.2018.1476125

Ali, M., Elhagwa, A., Elfaki, J. and Sulieman, M. (2017). Influence of the artisanal gold mining on soil contamination with heavy metals: A case study from Dar-Mali locality, North of Atbara, River Nile State, Sudan. *Eurasian Journal of Soil Science*, *6*(1), 28–36. https://doi.org/10.18393/ejss.284261

Alloway, B. J. (2013). Sources of Heavy Metals and Metalloids in Soils. In B. J. Alloway (Ed.), *Heavy Metals in Soils: Trace Metals and Metalloids in Soils and their Bioavailability* (pp. 11–50). Springer Netherlands. https://doi.org/10.1007/978-94-007-4470-7_2

Almås, Å. R., Kweyunga, C., and Manoko, M. L. (2012.). *Investigation of trace metal concentrations in soil, sediments and waters in the vicinity of gold mines in North West Tanzania*. 26.

Almås, Å. R., and Manoko, M. L. K. (2012). Trace Element Concentrations in Soil, Sediments, and Waters in the Vicinity of Geita Gold Mines and North Mara Gold Mines in Northwest Tanzania. *Soil and Sediment Contamination: An International Journal*, *21*(2), 135–159. https://doi.org/10.1080/15320383.2012.649372

Amadi, A. N., Ebieme, E. E., Musa, A., Olashinde, P. I., Ameh, I. M. and Shuaibu, A. M. (2017). Utility of pollution indices in assessment of soil quality around Madaga gold mining site, Niger state, North-central Nigeria. *Ife Journal of Science*, *19*(2), 417. https://doi.org/10.4314/ijs.v19i2.22

Amoakwah, E., Ahsan, S., Rahman, M. A., Asamoah, E., Essumang, D. K., Ali, M. and Islam, K. R. (2020). Assessment of Heavy Metal Pollution of Soil-water-vegetative Ecosystems Associated with Artisanal Gold Mining. *Soil and Sediment Contamination: An International Journal*, *29*(7), 788–803. https://doi.org/10.1080/15320383.2020.1777936

Anazawa, K. and Ohmori, H. (2005). The hydrochemistry of surface waters in andesitic volcanic area, Norikura volcano, central Japan. *Chemosphere*, *59*(5), 605–615. https://doi.org/10.1016/j.chemosphere.2004.10.018

Andrews, K. W., Savitz, D. A. and Hertz-Picciotto, I. (1994). Prenatal lead exposure in relation to gestational age and birth weight: A review of epidemiologic studies. *American Journal of Industrial Medicine*, *26*(1), 13–32. https://doi.org/10.1002/ajim.4700260103

Antwi-Agyei., P., Hogarh., G. N. and Foli., G. (2009). Trace Element Contamination of soils around mine tailing dams at Obuasi, Ghana. African Journal of Environmental Science and Technology 3(11): 353- 359.

Arhin, E., Boansi, A. O. and Zango, M. S. (2016). Trace elements distributions at Datoko-Shega artisanal mining site, northern Ghana. *Environmental Geochemistry and Health*, *38*(1), 203–218. https://doi.org/10.1007/s10653-015-9705-0

Arora, M., Kiran, B., Rani, S., Rani, A., Kaur, B. and Mittal, N. (2008). Heavy metal accumulation in vegetables irrigated with water from different sources. *Food Chemistry*, *111*(4), 811–815. https://doi.org/10.1016/j.foodchem.2008.04.049

Asaduzzaman, K., Mannan, F., Khandaker, M. U., Farook, M. S., Elkezza, A., Amin, Y. B. M., Sharma, S. and Abu Kassim, H. B. (2015). Assessment of Natural Radioactivity Levels and Potential Radiological Risks of Common Building Materials Used in Bangladeshi Dwellings. *PLOS ONE*, *10*(10), e0140667. https://doi.org/10.1371/journal.pone.0140667

Asmoay, A. S. A., Salman, S. A., El-Gohary, A. M. and Sabet, H. S. (2019). Evaluation of heavy metal mobility in contaminated soils between Abu Qurqas and Dyer Mawas Area, El Minya Governorate, Upper Egypt. *Bulletin of the National Research Centre*, *43*(1), 88. https://doi.org/10.1186/s42269-019-0133-7

Aucamp, P. and van Schalkwyk, A. (2003). Trace element pollution of soils by abandoned gold

mine tailings, near Potchefstroom, South Africa. *Bulletin of Engineering Geology and the*

Environment, *62*(2), 123–134. https://doi.org/10.1007/s10064-002-0179-9

Banzi, F. P., Msaki, P. and Makundi, I. N. (2002). A SURVEY OF BACKGROUND

RADIATION DOSE RATES AND RADIOACTIVITY IN TANZANIA: *Health Physics*,

82(1), 80–86. https://doi.org/10.1097/00004032-200201000-00010

Barbieri, M. (2016). The Importance of Enrichment Factor (EF) and Geoaccumulation Index

(Igeo) to Evaluate the Soil Contamination. *Journal of Geology and Geophysics*, *5*(1).

https://doi.org/10.4172/2381-8719.1000237

Bardossy, A. (2019). *Introduction to Geostatistics*. 134.

Bargagli, R. (1995). The elemental composition of vegetation and the possible incidence of soil

contamination of samples. *Science of The Total Environment*, *176*(1), 121–128.

https://doi.org/10.1016/0048-9697(95)04838-3

Bargagli, R., Monaci, F., Borghini, F., Bravi, F. and Agnorelli, C. (2002). Mosses and lichens as

biomonitors of trace metals. A comparison study on Hypnum cupressiforme and Parmelia

caperata in a former mining district in Italy. *Environmental Pollution*, *116*(2), 279–287.

https://doi.org/10.1016/S0269-7491(01)00125-7

Basavarajappa, H. T. and Manjunatha, M. C. (2015). Groundwater Quality Analysis in

Precambrian Rocks of Chitradurga District, Karnataka, India Using Geo-informatics

Technique. *Aquatic Procedia*, *4*, 1354–1365. https://doi.org/10.1016/j.aqpro.2015.02.176

Bempah, C. K. and Ewusi, A. (2016). Heavy metals contamination and human health risk assessment around Obuasi gold mine in Ghana. *Environmental Monitoring and Assessment*, *188*(5), 261. https://doi.org/10.1007/s10661-016-5241-3

Bempah, C. K., Ewusi, A., Obiri-Yeboah, S., Asabere, B., Mensah, F., Boateng, J. and Voigt, H.-J. (2013). Distribution of Arsenic and Heavy Metals from Mine Tailings dams at Obuasi Municipality of Ghana. *American Journal of Engineering Research*, 10.

Bessa, A. Z. E., El-Amier, Y. A., Doumo, E. P. E. and Ngueutchoua, G. (2018). Assessment of Sediments Pollution by Trace Metals in the Moloundou Swamp, Southeast Cameroon. *Annual Research and Review in Biology*, 1–13. https://doi.org/10.9734/ARRB/2018/46070

Betsou, C., Diapouli, E., Tsakiri, E., Papadopoulou, L., Frontasyeva, M., Eleftheriadis, K. and Ioannidou, A. (2021). First-Time Source Apportionment Analysis of Deposited Particulate Matter from a Moss Biomonitoring Study in Northern Greece. *Atmosphere*, *12*(2), 208. https://doi.org/10.3390/atmos12020208

Bhattacharya, P., Sracek, O., Eldvall, B., Asklund, R., Barmen, G., Jacks, G., Koku, J., Gustafsson, J.-E., Singh, N. and Balfors, B. B. (2012). Hydrogeochemical study on the contamination of water resources in a part of Tarkwa mining area, Western Ghana. *Journal of African Earth Sciences*, *66–67*, 72–84. https://doi.org/10.1016/j.jafrearsci.2012.03.005

Blanchard, D. G., Louis, N. E., Abdourahimi, Daniel, B., Saïdou, Emmanuel, N. N. I. J.,

Boniface, K., and Godfroy, K. N. M. (2018). Environmental Pollution by Heavy Metals

in the Gold Mining Region of East Cameroon. *American Journal of Environmental

Sciences, 14(5): 212- 225.* https://doi.org/10.3844/AJESSP.2018.212.225

Blanchard, D. G., Louis, N. E., Flore, T. S. Y., Daniel, B., and Godfroy, K. N. M. (2017).

NORM Measurements and Radiological Hazard Assessment in the Gold Mining Areas of

Eastern Cameroon. Radiation Environment and Medicine **6**:22-28

Boamponsem, L. K., Adam, J. I., Dampare, S. B., Nyarko, B. J. B. and Essumang, D. K. (2010).

Assessment of atmospheric heavy metal deposition in the Tarkwa gold mining area of

Ghana using epiphytic lichens. *Nuclear Instruments and Methods in Physics Research

Section B: Beam Interactions with Materials and Atoms*, *268*(9), 1492–1501.

https://doi.org/10.1016/j.nimb.2010.01.007

Boateng, E., Dowuona, G. N. N., Nude, P. M., Foli, G., Gyekye, P. and Jafaru, H. M. (2012).

Geochemical Assessment of the Impact of Mine Tailings Reclamation on the Quality of

Soils at AngloGold Concession, Obuasi, Ghan*a*. *Research Journal of Environmental

Earth Science* 4(4):466-474.

Boice, J. D. (2012). Radiation epidemiology: A perspective on Fukushima. *Journal of

Radiological Protection: Official Journal of the Society for Radiological Protection*,

32(1), N33-40. https://doi.org/10.1088/0952-4746/32/1/N33

Bowell, R. J., Warren, A., Minjera, H. A. and Kimaro, N. (1995). Environmental impact of

    former gold mining on the Orangi river, Serengeti N.P., Tanzania. *Biogeochemistry*,

    28(3), 131–160. https://doi.org/10.1007/BF02186456

Brown, D. H. and Buck, G. W. (1979). Desiccation Effects and Cation Distribution in

    Bryophytes. *The New Phytologist*, *82*(1), 115–125. JSTOR.

Brunialti, G., Giordani, P., Isocrono, D. and Loppi, S. (2002). Evaluation of data quality in lichen

    biomonitoring studies: The Italian experience. *Environmental Monitoring and*

    Assessment, *75*(3), 271–280. https://doi.org/10.1023/a:1014804318262

Cambardella, C. A., Moorman, T. B., Novak, J. M., Parkin, T. B., Karlen, D. L., Turco, R. F. and

    Konopka, A. E. (1994). Field-Scale Variability of Soil Properties in Central Iowa Soils.

    Soil Science Society of America Journal, *58*(5), 1501–1511.

    https://doi.org/10.2136/sssaj1994.03615995005800050033x

Canfield, R. L., Cory-Slechta, D. A. and Lanphear, B. P. (2003). Intellectual Impairment in

    Children with Blood Lead Concentrations below 10 µg per Deciliter. *The New England*

    Journal of Medicine, 16:1517-26.

Carbonell, G., de Imperial, R. M., Torrijos, M., Delgado, M. and Rodriguez, J. A. (2011). Effects

    of municipal solid waste compost and mineral fertilizer amendments on soil properties

    and heavy metals distribution in maize plants (Zea mays L.). *Chemosphere*, *85*(10),

    1614–1623. https://doi.org/10.1016/j.chemosphere.2011.08.025

Caridi, F., Marguccio, S., Belvedere, A. and Belmusto, G. (2015). *Measurements of Gamma Radioactivity in River Sediment Samples of the Mediterranean Central Basin. 2015*, 61–68. https://doi.org/10.5923/j.ajcmp.20150503.01

Cavanagh, J.-A. E. and O'Halloran, K. (2019). *OVERVIEW OF INTERNATIONAL SOIL CRITERIA AND DERIVATION OF NUMERIC VALUES*. 12.

Chen, M., Lu, W., Hou, Z., Zhang, Y., Jiang, X. and Wu, J. (2017). Heavy metal pollution in soil associated with a large-scale cyanidation gold mining region in southeast of Jilin, China. *Environmental Science and Pollution Research*, *24*(3), 3084–3096. https://doi.org/10.1007/s11356-016-7968-3

Chiroma, T. M., Ebewele, R. O. and Hymore, F. (2014). Comparative assessment of heavy metal levels in soil, vegetables and urban grey water used for irrigation in Yola and Kano. *International Refereed Journal of Engineering and Science (IRJES)*, *3*, 1–9.

Craw, D., Chappell, D., Reay, A. and Walls, D. (2000). Mobilisation and attenuation of arsenic around gold mines, east Otago, New Zealand. *New Zealand Journal of Geology and Geophysics*, *43*(3), 373–383. https://doi.org/10.1080/00288306.2000.9514894

Cressie, N. (1990). The origins of kriging. *Mathematical Geology*, *22*(3), 239–252. https://doi.org/10.1007/BF00889887

Cui, Z.-G., Ahmed, K., Zaidi, S. F. and Muhammad, J. S. (2021). Ins and outs of cadmium-induced carcinogenesis: Mechanism and prevention. *Cancer Treatment and Research Communications*, *27*, 100372. https://doi.org/10.1016/j.ctarc.2021.100372

Ćujić, M., Dragović, S., Sabovljević, M., Slavković-Beškoski, L., Kilibarda, M., Savović, J. and
Onjia, A. (2014). Use of Mosses as Biomonitors of Major, Minor and Trace Element
Deposition Around the Largest Thermal Power Plant in Serbia: Use of Mosses as
Biomonitors of Major, Minor and Trace Element Deposition. *CLEAN - Soil, Air, Water*,
42(1), 5–11. https://doi.org/10.1002/clen.201100656

D'Amore, J. J., Al-Abed, S. R., Scheckel, K. G. and Ryan, J. A. (2005). Methods for Speciation
of Metals in Soils. *Journal of Environmental Quality*, *34*(5), 1707–1745.
https://doi.org/10.2134/jeq2004.0014

Darko, E. O., Tetteh, G. K. and Akaho, E. H. K. (2005). Occupational radiation exposure to
norms in a gold mine. *Radiation Protection Dosimetry*, *114*(4), 538–545.
https://doi.org/10.1093/rpd/nci300

Dike, C. G., Oladele, B. O., Olubi, O. E., Ife-Adediran, O. O. and Aderibigbe, A. (2020).
Ecological and radiological hazards due to natural radioactivity and heavy metals in soils
of some selected mining sites in Nigeria. *Human and Ecological Risk Assessment: An
International Journal*, *26*(5), 1428–1438.
https://doi.org/10.1080/10807039.2019.1585182

Donkor, A. K., Bonzongo, J.-C. J., Nartey, V. K. and Adotey, D. K. (2005). Heavy Metals in
Sediments of the Gold Mining Impacted Pra River Basin, Ghana, West Africa. *Soil and
Sediment Contamination: An International Journal*, *14*(6), 479–503.
https://doi.org/10.1080/15320380500263675

Donkor, A., Nartey, V., Bonzongo, J. and Adotey, D. (2009). Artisanal mining of gold with mercury in Ghana. *West African Journal of Applied Ecology*, *9*(1). https://doi.org/10.4314/wajae.v9i1.45666

Dowdall, M., Vicat, K., Frearson, I., Gerland, S., Lind, B. and Shaw, G. (2004). Assessment of the radiological impacts of historical coal mining operations on the environment of Ny-Alesund, Svalbard. *Journal of Environmental Radioactivity*, *71*(2), 101–114. https://doi.org/10.1016/S0265-931X(03)00144-9

Einax, J. W. and Soldt, U. (1998). Multivariate geostatistical analysis of soil contaminations. *Fresenius' Journal of Analytical Chemistry*, *361*(1), 10–14. https://doi.org/10.1007/s002160050826

Esiole, S. O., Ibeanu, I. G. E., Garba, N. and Onoja, M. A. (2019). Determination of radiological hazard indices from surface soil to individuals in Angwan Kawo Gold Mining Sites, Niger state, Nigeria. *Journal of Applied Sciences and Environmental Management*, *23*, 1541. https://doi.org/10.4314/jasem.v23i8.19

Evans, C. A. and Hutchinson, T. C. (1996). Mercury accumulation in transplanted moss and lichens at high elevation sites in Quebec. *Water, Air, and Soil Pollution*, *90*(3), 475–488. https://doi.org/10.1007/BF00282663

F AlKhader, A. M. (2015). The Impact of Phosphorus Fertilizers on Heavy Metals Content of Soils and Vegetables Grown on Selected Farms in Jordan. *Agrotechnology*, 137. https://doi.org/10.4172/2168-9881.1000137

Faanu, A., Ephraim, J. H. and Darko, E. O. (2011). Assessment of public exposure to naturally

    occurring radioactive materials from mining and mineral processing activities of Tarkwa

    Goldmine in Ghana. *Environmental Monitoring and Assessment*, *180*(1–4), 15–29.

    https://doi.org/10.1007/s10661-010-1769-9

Faanu, A., Lawluvi, H., Kpeglo, D. O., Darko, E. O., Emi-Reynolds, G., Awudu, A. R., Adukpo,

    O. K., Kansaana, C., Ali, I. D., Agyeman, B., Agyeman, L. and Kpodzro, R. (2014).

    Assessment of natural and anthropogenic radioactivity levels in soils, rocks and water in

    the vicinity of Chirano Gold Mine in Ghana. *Radiation Protection Dosimetry*, *158*(1),

    87–99. https://doi.org/10.1093/rpd/nct197

Factor-Litvak, P., Slavkovich, V., Liu, X., Popovac, D., Preteni, E., Capuni-Paracka, S.,

    Hadzialjevic, S., Lekic, V., LoIacono, N., Kline, J. and Graziano, J. (1998).

    Hyperproduction of erythropoietin in nonanemic lead-exposed children. *Environmental*

    Health Perspectives, *106*(6), 361–364. https://doi.org/10.1289/ehp.98106361

Fashola, M., Ngole-Jeme, V. and Babalola, O. (2016). Heavy Metal Pollution from Gold Mines:

    Environmental Effects and Bacterial Strategies for Resistance. *International Journal of*

    Environmental Research and Public Health, *13*(11), 1047.

    https://doi.org/10.3390/ijerph13111047

Gałuszka, A. and Migaszewski, Z. (2011). Geochemical background—An environmental

    perspective. *Mineralogia*, *42*(1), 7–17. https://doi.org/10.2478/v10002-011-0002-y

Gill, J. (1981). *Orogenic Andesites and Plate Tectonics*. Springer-Verlag.

    https://doi.org/10.1007/978-3-642-68012-0

Goovaerts, P. (1999). Geostatistics in soil science: State-of-the-art and perspectives. *Geoderma*,

    89(1–2), 1–45. https://doi.org/10.1016/S0016-7061(98)00078-0

Hakanson, L. (1980). An ecological risk index for aquatic pollution control.a sedimentological

    approach. *Water Research*, *14*(8), 975–1001. https://doi.org/10.1016/0043-

    1354(80)90143-8

Hamelink, J. L. (1994). Bioavailability: Physical, chemical, and biological interactions. *SETAC*

    Special Publications Series (USA).

Hani, A., Pazira, E., Manshouri, M., Babaie Kafaky, S. and Ghahroudi Tali, M. (2010). Spatial

    distribution and mapping of risk elements pollution in agricultural soils of southern

    Tehran, Iran. *Plant, Soil and Environment*, *56*(No. 6), 288–296.

    https://doi.org/10.17221/16/2010-PSE

Harada, M. (1978). Congenital Minamata disease: Intrauterine methylmercury poisoning.

    Teratology, *18*(2), 285–288. https://doi.org/10.1002/tera.1420180216

Herman, A. (2015). Heavy Metals Contamination in Soils and Water in the Vicinity of Small

    Scale Gold Mines at Londoni and Sambaru, Singida Region, Tanzania. *International*

    Journal of Environmental Monitoring and Analysis, *3*(6), 397.

    https://doi.org/10.11648/j.ijema.20150306.13

Herman, A. and Kihampa, C. (2015). Heavy Metals Contamination in Soils and Water in the

      Vicinity of Small Scale Gold Mines at Londoni and Sambaru, Singida Region, Tanzania.

      International Journal of Environmental Monitoring and Analysis, *3*(6), 397.

      https://doi.org/10.11648/j.ijema.20150306.13

Ichang'l, D. W. and MacLean, W. H. (1991). The Archaen volcanic facies in the Migori

      segment, Nyanza greenstone belt, Kenya: Stratigraphy, geochemistry and mineralisation.

      Journal of African Earth Sciences (and the Middle East), *13*(3), 277–290.

      https://doi.org/10.1016/0899-5362(91)90091-C

Idris, I. M., Younis, Y. M. H. and Elbashir, A. A. (2018). *Monitoring the Anthropogenic and*

      Geochemical Environment Surrounding the Butana Drinking Water Sources via the

      Determination of Heavy Metals Composition of the Soil, Streams Sediments and Gold

      Mining Tailings (II). *7*(3), 15.

IJSRD - International Journal for Scientific Research and Development| Vol. 5, Issue 05, 2017 |

      ISSN (online): 2321-0613. *5*(06), 5.

Ikingura, J. R. and Akagi, H. (2002). Lichens as a Good Bioindicator of Air Pollution by

      Mercury in Small-Scale Gold Mining Areas, Tanzania. *Bulletin of Environmental*

      Contamination and Toxicology, *68*(5), 699–704. https://doi.org/10.1007/s001280310

International Atomic Energy Agency. (2011). *Exposure of the public from large deposits of*

      mineral residues. International Atomic Energy Agency.

Jabłońska-Czapla, M., Szopa, S., Zerzucha, P., Łyko, A. and Michalski, R. (2015). Chemometric and environmental assessment of arsenic, antimony, and chromium speciation form occurrence in a water reservoir subjected to thermal anthropopressure. *Environmental Science and Pollution Research*, *22*(20), 15731–15744. https://doi.org/10.1007/s11356-015-4769-z

Jianfei, C., Chunfang, L., Lixia, Z., Quanyuan, W. and Jianshu, L. (2020). Source apportionment of potentially toxic elements in soils using APCS/MLR, PMF and geostatistics in a typical industrial and mining city in Eastern China. *PLOS ONE*, *15*(9), e0238513. https://doi.org/10.1371/journal.pone.0238513

Kamunda, C., Mathuthu, M. and Madhuku, M. (2016). An Assessment of Radiological Hazards from Gold Mine Tailings in the Province of Gauteng in South Africa. *International Journal of Environmental Research and Public Health*, *13*(1), 138. https://doi.org/10.3390/ijerph13010138

Kamunda, C., Mathuthu, M. and Madhuku, M. (2016). Health Risk Assessment of Heavy Metals in Soils from Witwatersrand Gold Mining Basin, South Africa. *International Journal of Environmental Research and Public Health*, *13*(7), 663. https://doi.org/10.3390/ijerph13070663

Kim, M.-J. and Jung, Y. (2004). Vertical Distribution and Mobility of Arsenic and Heavy Metals in and around Mine Tailings of an Abandoned Mine. *Journal of Environmental Science and Health, Part A*, *39*(1), 203–222. https://doi.org/10.1081/ESE-120027379

Kłos, A., Ziembik, Z., Rajfur, M., Dołhańczuk-Śródka, A., Bochenek, Z., Bjerke, J. W.,

    Tømmervik, H., Zagajewski, B., Ziółkowski, D., Jerz, D., Zielińska, M., Krems, P.,

    Godyń, P., Marciniak, M. and Świsłowski, P. (2018). Using moss and lichens in

    biomonitoring of heavy-metal contamination of forest areas in southern and north-eastern

    Poland. *Science of The Total Environment*, *627*, 438–449.

    https://doi.org/10.1016/j.scitotenv.2018.01.211

Komnitsas, K. and Modis, K. (2007). Soil risk assessment of As and Zn contamination in a coal

    mining region using geostatistics. *The Science of the Total Environment*, *371*, 190–196.

    https://doi.org/10.1016/j.scitotenv.2006.08.047

Krige, D.G. (1951) A Statistical Approaches to Some Basic Mine Valuation Problems on the

    Witwatersrand. Journal of the Chemical, Metallurgical and Mining Society of South

    Africa, 52, 119-139.

Laws, E. A. (2000). *Aquatic Pollution: An Introductory Text, 3rd Edition* (3 edition). Wiley.

Léopold, E. N., Sabine, D. D., Philémon, Z. Z. and Jung, M. C. (2016). Physical and Metals

    Impact of Traditional Gold Mining on Soils in Kombo-Laka Area (Meiganga,

    Cameroon). *International Journal of Geosciences*, *07*(09), 1102–1121.

    https://doi.org/10.4236/ijg.2016.79084

Lim, M., Han, G.-C., Ahn, J.-W., You, K.-S. and Kim, H.-S. (2009). Leachability of Arsenic and

    Heavy Metals from Mine Tailings of Abandoned Metal Mines. *International Journal of*

Environmental Research and Public Health, *6*(11), 2865–2879.
https://doi.org/10.3390/ijerph6112865

Loppi, S. and Bonini, I. (2000). Lichens and mosses as biomonitors of trace elements in areas
with thermal springs and fumarole activity (Mt. Amiata, central Italy). *Chemosphere*,
41(9), 1333–1336. https://doi.org/10.1016/S0045-6535(00)00026-6

Loska, K., Wiechuła, D. and Korus, I. (2004). Metal contamination of farming soils affected by
industry. *Environment International*, *30*(2), 159–165. https://doi.org/10.1016/S0160-
4120(03)00157-0

Luo, W., Lu, Y., Zhang, Y., Fu, W., Wang, B., Jiao, W., Wang, G., Tong, X. and Giesy, J. P.
(2010). Watershed-scale assessment of arsenic and metal contamination in the surface
soils surrounding Miyun Reservoir, Beijing, China. *Journal of Environmental
Management*, *91*(12), 2599–2607. https://doi.org/10.1016/j.jenvman.2010.07.023

MacDonald, D. D., Ingersoll, C. G. and Berger, T. A. (2000). Development and Evaluation of
Consensus-Based Sediment Quality Guidelines for Freshwater Ecosystems. *Archives of
Environmental Contamination and Toxicology*, *39*(1), 20–31.
https://doi.org/10.1007/s002440010075

Machiwa, J. F. (2003). Metal concentrations in sediment and fish of Lake Victoria near and away
from catchments with gold mining acctivities. *Tanzania Journal of Science*, *29*, 43–54.
https://doi.org/10.4314/tjs.v29i2.18377

Martinez, V. D., Vucic, E. A., Becker-Santos, D. D., Gil, L. and Lam, W. L. (2011). Arsenic Exposure and the Induction of Human Cancers. *Journal of Toxicology*, *2011*, 431287. https://doi.org/10.1155/2011/431287

McGrath, D., Zhang, C. and Carton, O. T. (2004). Geostatistical analyses and hazard assessment on soil lead in Silvermines area, Ireland. *Environmental Pollution*, *127*(2), 239–248. https://doi.org/10.1016/j.envpol.2003.07.002

Melendez-Perez, J. J., Fostier, A. H., Carvalho, J. A., Windmöller, C. C., Santos, J. C. and Carpi, A. (2014). Soil and biomass mercury emissions during a prescribed fire in the Amazonian rain forest. *Atmospheric Environment*, *96*, 415–422. https://doi.org/10.1016/j.atmosenv.2014.06.032

Mettler, F. A. (2012). Medical effects and risks of exposure to ionising radiation. *Journal of Radiological Protection: Official Journal of the Society for Radiological Protection*, *32*(1), N9–N13. https://doi.org/10.1088/0952-4746/32/1/N9

Mushtakova, V. M., Fomina, V. A. and Rogovin, V. V. (2005). Toxic effect of heavy metals on human blood neutrophils. *Izvestiia Akademii Nauk. Seriia Biologicheskaia*, *3*, 336–338.

Mustapha, A. O., Patel, J. P. and Rathore, I. V. S. (1999). Assessment of Human Exposures to Natural Sources of Radiation in Kenya. *Radiation Protection Dosimetry*, *82*(4), 285–292. https://doi.org/10.1093/oxfordjournals.rpd.a032637

Needleman, H. (2004). Lead Poisoning. *Annual Review of Medicine*, *55*(1), 209–222. https://doi.org/10.1146/annurev.med.55.091902.103653

Nejad, B. (2010). Distribution of Heavy Metals around the Dashkasan Au Mine. *Int. J. Environ. Res.*, 8.

Ng, J. C., Ciminelli, V., Gasparon, M. and Caldeira, C. (2019). Health risk apportionment of arsenic from multiple exposure pathways in Paracatu, a gold mining town in Brazil. *The Science of the Total Environment*, *673*, 36–43. https://doi.org/10.1016/j.scitotenv.2019.04.048

Ngole-Jeme, V. M. and Fantke, P. (2017). Ecological and human health risks associated with abandoned gold mine tailings contaminated soil. *PLOS ONE*, *12*(2), e0172517. https://doi.org/10.1371/journal.pone.0172517

Ngure, V., Lelo, F. and Obwanga, B. (2017). Heavy Metal Pollution from Migori Gold Mining Area, Kenya: Health Implications for Consumers of Fish and Wate*r. Journal of Natural Sciences* 7(6):46-53.

Nieminen, T. M., Ukonmaanaho, L., Rausch, N. and Shotyk, W. (2007). Biogeochemistry of Nickel and Its Release into the Environment. In A. Sigel, H. Sigel. and R. K. O. Sigel (Eds.), *Nickel and Its Surprising Impact in Nature* (pp. 1–29). John Wiley and Sons, Ltd. https://doi.org/10.1002/9780470028131.ch1

Nilin, J., Moreira, L. B., Aguiar, J. E., Marins, R., Moledo de Souza Abessa, D., Monteiro da Cruz Lotufo, T. and Costa-Lotufo, L. V. (2013). Sediment quality assessment in a tropical estuary: The case of Ceará River, Northeastern Brazil. *Marine Environmental Research*, *91*, 89–96. https://doi.org/10.1016/j.marenvres.2013.02.009

Ning, L., Liyuan, Y., Jirui, D. and Xugui, P. (2011). Heavy Metal Pollution in Surface Water of

    Linglong Gold Mining Area, China. *Procedia Environmental Sciences*, *10*, 914–917.

    https://doi.org/10.1016/j.proenv.2011.09.146

Nurcholis, M.-, Yudiantoro, D. F., Haryanto, D. and Mirzam, A.-. (2017). Heavy Metals

    Distribution in the Artisanal Gold Mining Area in Wonogiri. *Indonesian Journal of*

    Geography, *49*(2), 133–144. https://doi.org/10.22146/ijg.15321

Nwanosike, A., E., E., A., M., Olasehinde, P., Unuevho, C. and Ameh, M. (2018). Stream

    Sediments as Pollution Indicators within Shikira Gold Mining Sites, Niger State, North-

    Central Nigeria. *Journal of Mining and Geology*, *54*, 119–131.

Nyangababo, J. T. (1987). Lichens as monitors of aerial heavy metal pollutants in and around

    Kampala. *Bull. Environ. Contam. Toxicol.; (United States)*, 38(1):91-5.

    https://doi.org/10.1007/BF01606564

Nyarko, B. J. B., Adomako, D., Serfor-Armah, Y., Dampare, S. B., Adotey, D. and Akaho, E. H.

    K. (2006). Biomonitoring of atmospheric trace element deposition around an industrial

    town in Ghana. *Radiation Physics and Chemistry*, *75*(9), 954–958.

    https://doi.org/10.1016/j.radphyschem.2005.08.021

Ogola, J. S., Mitullah, W. and Omulo, M. A. (2002). Impact of Gold mining on the Environment

    and Human Health: A Case Study in the Migori Gold Belt, Kenya. *Environmental*

    Geochemistry and Health 24:141-157. https://doi.org/10.1023/A:1014207832471

Ohta, A., Imai, N., Terashima, S. and Tachibana, Y. (2005). Influence of surface geology and mineral deposits on the spatial distributions of elemental concentrations in the stream sediments of Hokkaido, Japan. *Journal of Geochemical Exploration*, *86*(2), 86–103. https://doi.org/10.1016/j.gexplo.2005.04.002

Olando, G., Olaka, L. A., Okinda, P. O. and Abuom, P. (2020). Heavy metals in surface sediments of Lake Naivasha, Kenya: Spatial distribution, source identification and ecological risk assessment. *SN Applied Sciences*, *2*(2):1-14. https://doi.org/10.1007/s42452-020-2022-y

Olobatoke, R. Y. and Mathuthu, M. (2016). Heavy metal concentration in soil in the tailing dam vicinity of an old gold mine in Johannesburg, South Africa. *Canadian Journal of Soil Science*, *96*(3), 299–304. https://doi.org/10.1139/cjss-2015-0081

Pacyna, J. M. and Winchester, J. W. (1990). Contamination of the global environment as observed in the Arctic. *Palaeogeography, Palaeoclimatology, Palaeoecology*, *82*(1), 149–157. https://doi.org/10.1016/S0031-0182(12)80028-9

Patel JP (1991). Environmental radiation survey of the area of high natural radioactivity of Mrima hill of Kenya. Discovery and Innovation, 3(3): 31-35.

Qu, M.-K., Li, W.-D., Zhang, C.-R., Wang, S.-Q., Yang, Y. and He, L.-Y. (2013). Source Apportionment of Heavy Metals in Soils Using Multivariate Statistics and Geostatistics. *Pedosphere*, *23*(4), 437–444. https://doi.org/10.1016/S1002-0160(13)60036-3

Quevauviller, P., Lavigne, R. and Cortez, L. (1989). Impact of industrial and mine drainage wastes on the heavy metal distribution in the drainage basin and estuary of the Sado River (Portugal). *Environmental Pollution (Barking, Essex: 1987)*, *59*(4), 267–286. https://doi.org/10.1016/0269-7491(89)90155-3

Rashed, M. N. (2010). Monitoring of contaminated toxic and heavy metals, from mine tailings through age accumulation, in soil and some wild plants at Southeast Egypt. *Journal of Hazardous Materials*, *178*(1–3), 739–746. https://doi.org/10.1016/j.jhazmat.2010.01.147

Ravi, S., D'Odorico, P., Breshears, D. D., Field, J. P., Goudie, A. S., Huxman, T. E., Li, J., Okin, G. S., Swap, R. J., Thomas, A. D., Pelt, S. V., Whicker, J. J. and Zobeck, T. M. (2011). Aeolian Processes and the Biosphere. *Reviews of Geophysics*, *49*(3). https://doi.org/10.1029/2010RG000328

Reimann, C., Filzmoser, P., Fabian, K., Hron, K., Birke, M., Demetriades, A., Dinelli, E. and Ladenberger, A. (2012). The concept of compositional data analysis in practice—Total major element concentrations in agricultural and grazing land soils of Europe. *Science of The Total Environment*, *426*, 196–210. https://doi.org/10.1016/j.scitotenv.2012.02.032

Salazar-Camacho, C., Salas-Moreno, M., Marrugo-Madrid, S., Marrugo-Negrete, J. and Díez, S. (2017). Dietary human exposure to mercury in two artisanal small-scale gold mining communities of northwestern Colombia. *Environment International*, *107*, 47–54. https://doi.org/10.1016/j.envint.2017.06.011

Schaug, J., Rambæk, J. P., Steinnes, E. and Henry, R. C. (1990). Multivariate analysis of trace element data from moss samples used to monitor atmospheric deposition. *Atmospheric Environment. Part A. General Topics*, *24*(10), 2625–2631. https://doi.org/10.1016/0960-1686(90)90141-9

Schubert, M. and Schulz, H. (2002). Diurnal radon variations in the upper soil layers and at the soil-air interface related to meteorological parameters. *Health Physics*, *83*(1), 91–96. https://doi.org/10.1097/00004032-200207000-00010

Şengül, Ü. (2016). Comparing determination methods of detection and quantification limits for aflatoxin analysis in hazelnut. *Journal of Food and Drug Analysis*, *24*(1), 56–62. https://doi.org/10.1016/j.jfda.2015.04.009

Shackleton, R. M. (1951). A Contribution to the Geology of the Kavirondo Rift Valley. *Quarterly Journal of the Geological Society*, *107*(1–4), 336–337. https://doi.org/10.1144/GSL.JGS.1951.107.01-04.15

Shahbazi-Gahrouei, D., Setayandeh, S. and Gholami, M. (2013). A review on natural background radiation. *Advanced Biomedical Research*, *2*(1), 65. https://doi.org/10.4103/2277-9175.115821

Stamenkovic.S., S., Tatjana, M., V.J., C., N.S., K., Rada, B., Marija, M., N.D., N., V.Lj., M. and M.V., C. (2013). Biological indication of heavy metal pollution in the areas of Donje Vlase and Cerje (southeastern Serbia) using epiphytic lichens. *Archives of Biological Sciences*, *65*(1), 151–159. https://doi.org/10.2298/ABS1301151S

Sun, R., Gao, Y., Xu, J., Yang, Y. and Zhang, Y. (2021). Contamination Features and Source Apportionment of Heavy Metals in the River Sediments around a Lead-Zinc Mine: A Case Study in Danzhai, Guizhou, China. *Journal of Chemistry*, *2021*, e9946026. https://doi.org/10.1155/2021/9946026

Sutherland, R. A. (2000). Bed sediment-associated trace metals in an urban stream, Oahu, Hawaii. *Environmental Geology*, *39*(6), 611–627. https://doi.org/10.1007/s002540050473

Taylor, S. R. and McLennan, S. M. (1995). The geochemical evolution of the continental crust. *Reviews of Geophysics*, *33*(2), 241. https://doi.org/10.1029/95RG00262

Tchounwou, P. B., Yedjou, C. G., Patlolla, A. K. and Sutton, D. J. (2012). Heavy Metals Toxicity and the Environment. *EXS*, *101*, 133–164. https://doi.org/10.1007/978-3-7643-8340-4_6

Thevenon, F., Graham, N. D., Chiaradia, M., Arpagaus, P., Wildi, W. and Poté, J. (2011). Local to regional scale industrial heavy metal pollution recorded in sediments of large freshwater lakes in central Europe (lakes Geneva and Lucerne) over the last centuries. *Science of The Total Environment*, *412–413*, 239–247. https://doi.org/10.1016/j.scitotenv.2011.09.025

Towett, E. K., Shepherd, K. D., Tondoh, J. E., Winowiecki, L. A., Lulseged, T., Nyambura, M., Sila, A., Vågen, T.-G. and Cadisch, G. (2015). Total elemental composition of soils in Sub-Saharan Africa and relationship with soil forming factors. *Geoderma Regional*, *5*, 157–168. https://doi.org/10.1016/j.geodrs.2015.06.002

Trauth, M. (2015). *MATLAB® Recipes for Earth Sciences* (4th ed.). Springer-Verlag. https://doi.org/10.1007/978-3-662-46244-7

Tumolo, M., Ancona, V., De Paola, D., Losacco, D., Campanale, C., Massarelli, C. and Uricchio, V. F. (2020). Chromium Pollution in European Water, Sources, Health Risk, and Remediation Strategies: An Overview. *International Journal of Environmental Research and Public Health*, *17*(15), 5438. https://doi.org/10.3390/ijerph17155438

Tun, A. Z., Wongsasuluk, P. and Siriwong, W. (2020). Heavy Metals in the Soils of Placer Small-Scale Gold Mining Sites in Myanmar. *Journal of Health and Pollution*, *10*(27), 200911. https://doi.org/10.5696/2156-9614-10.27.200911

Turekian, K. K. and Wedepohl, K. H. (1961). Distribution of the Elements in Some Major Units of the Earth's Crust. *Geological Society of America Bulletin*, *72*(2), 175. https://doi.org/10.1130/0016-7606(1961)72[175:DOTEIS]2.0.CO;2

Turyahabwa, E. R. S., Jurua, E., Oriada, R., Mugaiga, A. and Enjiku, D. D. B. (2016). *Determination of Natural Radioactivity Levels due to Mine Tailings from Selected Mines in Southwestern Uganda*. Undefined. /paper/Determination-of-Natural-Radioactivity-Levels-due-Turyahabwa-Jurua/5d072c0cfc193a94f7c516fe68b9815422bce16a

Tutu, H., McCarthy, T. S. and Cukrowska, E. (2008). The chemical characteristics of acid mine drainage with particular reference to sources, distribution and remediation: The Witwatersrand Basin, South Africa as a case study. *Applied Geochemistry*, *23*(12), 3666–3684. https://doi.org/10.1016/j.apgeochem.2008.09.002

United Nations (Ed.). (2000). *Sources and effects of ionizing radiation: United Nations Scientific Committee on the Effects of Atomic Radiation: UNSCEAR 2000 report to the General Assembly, with scientific annexes*. United Nations.

United Nations (Ed.). (2010). *Sources and effects of ionizing radiation: United Nations Scientific Committee on the Effects of Atomic Radiation: UNSCEAR 2008 report to the General Assembly, with scientific annexes*. United Nations.

Veiga, M. M. (2011). *Processing Centers in Artisanal and Small- scale Gold Mining: Evolution or More*.

Wang, X., Liu, W., Li, Z., Teng, Y., Christie, P. and Luo, Y. (2020). Effects of long-term fertilizer applications on peanut yield and quality and plant and soil heavy metal accumulation. *Pedosphere*, *30*(4), 555–562. https://doi.org/10.1016/S1002-0160(17)60457-0

Wanyama, C., Masinde, F. and Makokha, J. (2020). Activity Concentration Levels of Natural Radionuclides in the Sediment Samples from Rosterman Gold Mine, Lurambi Sub - County, Kakamega County, Kenya. 2454–6194.

Webster, R. and Oliver, M. A. (2007). *Geostatistics for environmental scientists* (2. ed). Wiley.

Weissenstein, K. and Sinkala, T. (2011). Soil pollution with heavy metals in mine environments, impact areas of mine dumps particularly of gold- and copper mining industries in Southern Africa. *Arid Ecosystems*, *1*(1), 53. https://doi.org/10.1134/S2079096111010082

Winde, F., Geipel, G., Espina, C. and Schüz, J. (2019). Human exposure to uranium in South
African gold mining areas using barber-based hair sampling. *PLOS ONE*, *14*(6),
e0219059. https://doi.org/10.1371/journal.pone.0219059

Winde, F. and Sandham, L. (2004). Uranium pollution of South African streams–An overview of
the situation in gold mining areas of the Witwatersrand. *GeoJournal*, *61*, 131–149.
https://doi.org/10.1007/s10708-004-2867-4

Wu, Y., Xu, Y., Zhang, J. and Hu, S. (2010). Evaluation of ecological risk and primary empirical
research on heavy metals in polluted soil over Xiaoqinling gold mining region, Shaanxi,
China. *Transactions of Nonferrous Metals Society of China*, *20*(4), 688–694.
https://doi.org/10.1016/S1003-6326(09)60199-0

Yang, P., Mao, R., Shao, H. and Gao, Y. (2009). The spatial variability of heavy metal
distribution in the suburban farmland of Taihang Piedmont Plain, China. *Comptes Rendus
Biologies*, *332*(6), 558–566. https://doi.org/10.1016/j.crvi.2009.01.004

Yard, E. E., Horton, J., Schier, J. G., Caldwell, K., Sanchez, C., Lewis, L. and Gastaňaga, C.
(2012). Mercury exposure among artisanal gold miners in Madre de Dios, Peru: A cross-
sectional study. *Journal of Medical Toxicology: Official Journal of the American College
of Medical Toxicology*, *8*(4), 441–448. https://doi.org/10.1007/s13181-012-0252-0

Younis, Y. M. (2018). Monitoring the Anthropogenic and Geochemical Environment
Surrounding the Butana (Sudan) Drinking Water Sources Via the Determination of
Heavy Metals Composition of the Soil, Streams Sediments and Gold Mining Tailings in

the Wet Season (III). *Biomedical Journal of Scientific and Technical Research*, *9*(4). https://doi.org/10.26717/BJSTR.2018.09.001821

Zeeb, H., Shannoun, F. and Organization, W. H. (2009). *WHO handbook on indoor radon: A public health perspective*. World Health Organization. https://apps.who.int/iris/handle/10665/44149

Zhao, C. Q., Young, M. R., Diwan, B. A., Coogan, T. P. and Waalkes, M. P. (1997). Association of arsenic-induced malignant transformation with DNA hypomethylation and aberrant gene expression. *Proceedings of the National Academy of Sciences of the United States of America*, *94*(20), 10907–10912. https://doi.org/10.1073/pnas.94.20.10907

Zhou, F., Guo, H.-C., Ho, Y.-S. and Wu, C.-Z. (2007). Scientometric analysis of geostatistics using multivariate methods. *Scientometrics*, *73*(3), 265–279. https://doi.org/10.1007/s11192-007-1798-5

Ziadat, A. H., Jiries, A., Berdanier, B. and Batarseh, M. (2015). Bio-monitoring of Heavy Metals in the Vicinity of Copper Mining Site at Erdenet, Mongolia. *Journal of Applied Sciences*, *15*(11), 1297–1304. https://doi.org/10.3923/jas.2015.1297.1304

Zou, J., Dai, W., Gong, S. and Ma, Z. (2015). Analysis of Spatial Variations and Sources of Heavy Metals in Farmland Soils of Beijing Suburbs. *PLOS ONE*, *10*(2), e0118082. https://doi.org/10.1371/journal.pone.0118082

APPENDICES

Appendix A

Heavy metal concentration in lichens and moss

Table A1. Heavy metal concentration in lichens each sampling location (x 10^{-3} mg/kg)

Location No.	As	Cd	Cr	Cu	Ni	Pb	Zn	Hg
1	2.34	1.49	14.78	19.97	15.78	13.52	111.23	155.61
2	0.90	0.23	16.13	17.00	6.24	4.29	40.00	175.84
3	42.78	0.24	30.90	41.68	12.17	32.74	72.44	1646.00
4	3.81	0.47	14.29	13.60	14.84	24.37	72.13	176.05
5	4.47	0.13	14.21	13.83	22.11	11.54	60.24	212.84
6	0.70	0.27	7.34	22.00	19.66	4.36	38.00	159.02
7	1.54	0.18	11.85	12.18	14.44	5.77	43.84	97.68
8	3.51	0.27	17.36	19.12	16.68	7.77	61.18	197.24
9	2.52	0.16	17.75	36.92	18.12	12.01	113.49	744.86
10	8.90	0.14	10.71	15.95	14.03	7.42	76.93	267.25
11	1.88	0.30	12.58	18.95	12.07	12.20	77.09	592.89
12	2.80	0.01	14.84	44.00	49.83	5.38	59.00	191.28
13	370.27	0.12	63.69	22.72	30.51	41.06	164.77	1037.40
14	19.17	0.17	20.18	16.16	18.35	21.48	54.56	212.10
15	797.73	0.43	35.92	23.34	26.02	102.60	87.10	708.23
16	4.28	0.21	9.78	11.19	9.25	3.53	53.38	57.33
17	73.51	0.54	12.78	66.47	10.26	58.96	148.69	275.42
18	23.22	0.14	41.16	46.89	36.31	14.28	146.08	124.53

Table A2: Heavy metal concentration in moss at each sampling location (x 10^{-3} mg/kg)

Sample No.	As	Cd	Cr	Cu	Ni	Pb	Zn	Hg
1	0.54	0.10	5.07	10.26	6.97	4.14	43.77	150.14
2	2.62	0.13	8.61	8.91	6.89	19.48	50.10	1004.36
3	1.50	0.26	55.70	26.00	10.90	5.20	44.00	318.89
4	1.55	0.09	7.70	8.62	6.93	5.47	45.86	233.58
5	3.58	0.18	10.36	11.76	10.46	22.17	65.92	859.63
6	1.90	0.21	11.60	36.00	41.90	4.30	36.00	236.15
7	2.50	0.03	12.70	24.00	25.20	4.20	36.00	286.80
8	0.88	0.21	8.59	7.27	7.11	3.13	31.44	100.56
9	1.60	0.02	85.50	57.00	13.60	3.80	34.00	193.34
10	1.84	0.15	13.51	19.13	9.24	3.79	45.75	177.92
11	1.12	0.09	9.45	18.43	9.01	4.99	62.63	727.20
12	3.00	0.05	17.70	19.00	25.40	6.00	55.00	130.10
13	1.01	0.21	7.96	8.48	6.30	3.84	64.05	98.23
14	3.34	0.47	5.45	13.55	7.80	33.09	113.15	195.49
15	3.10	0.04	14.60	39.00	36.10	5.80	51.00	125.07
16	5.10	0.17	10.81	17.73	7.80	8.74	61.07	302.71
17	2.27	0.41	7.53	13.26	7.16	7.10	54.10	153.85
18	1.00	0.03	102.40	37.00	8.60	3.70	41.00	181.22
19	8.23	0.10	11.02	11.71	7.82	9.67	55.68	202.33
20	1.86	0.12	8.38	11.60	7.52	8.54	41.12	112.77
21	1.40	0.05	94.10	43.00	10.80	3.90	31.00	119.48
22	234.41	0.09	30.81	14.98	18.28	23.41	64.81	2016.91
23	9.78	0.12	14.41	20.90	14.25	12.91	94.32	205.81
24	69.71	0.11	11.47	11.05	13.32	13.57	57.62	469.26
25	7.90	0.01	97.60	42.00	13.40	5.80	33.00	319.81
26	12.35	0.11	16.11	27.69	10.70	26.72	61.35	105.14
27	8.96	0.10	11.81	11.76	10.21	8.56	82.98	244.66
28	8.80	0.17	16.41	12.06	11.95	10.93	51.71	163.39

Appendix B:

Heavy metal concentration in soil, pollution indices and radiation in soil

Table B1. Heavy metal concentration in soil each sampling location (mg/kg)

Sample No	As	Cd	Cr	Cu	Ni	Pb	Zn	Hg
1	15.00	0.01	119.70	106.50	46.40	12.70	66.80	31.40
2	3.74	0.11	64.27	49.64	50.14	22.16	103.43	110.84
3	13.40	0.12	93.42	53.21	60.77	32.44	82.34	1063.99
4	6.15	0.20	45.87	36.72	42.92	83.79	104.72	136.16
5	4.20	0.06	57.18	93.84	38.76	13.54	113.41	81.15
6	3.61	0.14	31.01	14.27	26.27	14.64	79.86	151.27
7	21.00	0.01	97.00	8.90	18.40	13.40	44.60	18.40
8	6.44	0.24	52.05	39.44	43.92	31.39	99.16	94.38
9	4.25	0.28	63.47	36.05	43.48	18.83	115.30	87.68
10	5.16	0.07	49.00	30.29	43.51	39.21	66.64	113.65
11	2.39	0.22	49.70	35.13	35.87	20.62	91.52	95.84
12	2.14	0.43	27.68	29.41	27.68	31.56	100.56	113.47
13	2.37	0.14	31.35	14.93	25.68	19.80	87.91	160.98
14	4.00	0.01	186.40	10.30	17.30	12.50	42.70	16.65
15	10.00	0.01	159.30	31.70	45.70	16.40	71.60	25.80
16	4.00	0.01	38.30	17.40	31.60	11.50	41.70	36.60
17	3.16	0.13	98.92	73.33	73.08	15.88	105.40	61.05
18	11.21	0.11	96.53	96.18	60.48	44.91	119.74	96.80
19	2.00	0.01	196.40	6.30	14.00	16.80	28.00	29.35
20	6.00	0.01	80.60	18.30	26.60	9.00	73.70	319.70
21	7.00	0.01	155.50	51.70	34.80	8.80	62.40	39.45
22	6.08	0.02	38.70	13.79	24.52	14.22	51.16	105.76
23	4.99	0.10	44.54	15.70	26.49	12.43	58.19	134.08
24	19.00	0.01	36.80	12.10	38.50	11.00	25.80	26.45
25	7.00	0.01	52.70	21.30	27.30	14.10	65.70	32.40
26	4.00	0.01	48.20	26.90	25.40	24.70	50.60	29.30
27	2.00	0.01	180.00	10.10	13.50	8.60	26.60	26.95
28	10.00	0.01	40.50	53.90	38.20	16.00	72.80	48.10
29	9.62	0.23	51.16	43.15	26.08	19.70	81.73	82.33
30	4.93	0.17	20.50	51.77	18.99	9.46	94.46	109.18

31	379.00	0.01	118.70	28.10	33.70	13.60	62.80	63.40
32	10.00	0.01	68.30	426.40	41.20	6.00	104.60	94.20
33	7.00	0.01	37.30	65.40	20.40	13.70	77.30	364.80
34	3.02	0.11	16.69	15.88	17.38	27.01	76.02	262.10
35	163.11	0.10	75.31	37.60	28.35	52.98	222.53	248.78
36	66.99	0.06	56.69	43.99	27.20	27.86	73.55	69.23
37	9.11	0.05	38.61	20.97	22.82	16.69	73.41	48.96
38	117.00	0.01	418.40	104.60	155.90	36.40	81.40	38.10
39	50.84	0.01	57.39	34.41	34.56	19.06	78.82	36.25
40	632.24	0.06	169.07	47.42	76.18	127.49	63.49	122.47
41	63.14	0.04	50.99	27.43	40.57	26.13	91.40	51.84
42	5.00	0.01	43.60	23.90	23.60	6.00	32.50	33.60
43	5.92	0.01	59.96	56.88	48.58	12.76	54.68	46.01
44	54.73	0.13	69.67	38.83	43.84	30.14	99.94	80.13
45	7.62	0.11	41.27	25.05	39.83	41.41	69.19	63.66
46	302.10	0.17	166.04	89.85	105.20	28.85	81.76	84.02
47	271.25	0.41	84.83	471.71	60.24	546.92	255.04	228.37
48	52.81	0.05	67.31	20.47	50.86	25.23	64.44	50.22
49	10.83	0.09	62.34	14.02	27.56	53.13	48.66	94.62
50	25.00	0.01	111.80	52.30	73.80	16.70	100.10	34.20
51	16.00	0.01	133.80	21.60	28.40	7.80	53.60	26.20
52	4.00	0.01	87.20	76.80	13.40	10.20	39.90	23.85
53	105.00	0.01	53.20	76.90	26.90	53.50	200.50	243.80
54	54.23	0.36	38.93	61.62	30.77	52.50	124.52	131.00
55	12.03	0.18	36.85	47.08	22.40	40.50	105.62	150.94
56	32.00	0.01	36.10	46.90	23.00	25.00	209.90	103.85

Table B2. Contamination factor of soil each sampling location

Sample No.	As	Cd	Cr	Cu	Ni	Pb	Zn	Hg
1	0.750	0.001	1.760	2.663	1.289	0.488	0.846	0.397
2	0.187	0.012	0.945	1.241	1.393	0.852	1.309	1.403
3	0.670	0.013	1.374	1.330	1.688	1.248	1.042	13.468
4	0.308	0.022	0.675	0.918	1.192	3.223	1.326	1.724
5	0.210	0.007	0.841	2.346	1.077	0.521	1.436	1.027
6	0.181	0.016	0.456	0.357	0.730	0.563	1.011	1.915
7	1.050	0.001	1.426	0.223	0.511	0.515	0.565	0.233
8	0.322	0.027	0.765	0.986	1.220	1.207	1.255	1.195
9	0.213	0.031	0.933	0.901	1.208	0.724	1.459	1.110
10	0.258	0.008	0.721	0.757	1.209	1.508	0.844	1.439
11	0.120	0.024	0.731	0.878	0.996	0.793	1.158	1.213
12	0.107	0.048	0.407	0.735	0.769	1.214	1.273	1.436
13	0.119	0.016	0.461	0.373	0.713	0.762	1.113	2.038
14	0.200	0.001	2.741	0.258	0.481	0.481	0.541	0.211
15	0.500	0.001	2.343	0.793	1.269	0.631	0.906	0.327
16	0.200	0.001	0.563	0.435	0.878	0.442	0.528	0.463
17	0.158	0.014	1.455	1.833	2.030	0.611	1.334	0.773
18	0.561	0.012	1.420	2.405	1.680	1.727	1.516	1.225
19	0.100	0.001	2.888	0.158	0.389	0.646	0.354	0.372
20	0.300	0.001	1.185	0.458	0.739	0.346	0.933	4.047
21	0.350	0.001	2.287	1.293	0.967	0.338	0.790	0.499
22	0.304	0.002	0.569	0.345	0.681	0.547	0.648	1.339
23	0.250	0.011	0.655	0.393	0.736	0.478	0.737	1.697
24	0.950	0.001	0.541	0.303	1.069	0.423	0.327	0.335
25	0.350	0.001	0.775	0.533	0.758	0.542	0.832	0.410
26	0.200	0.001	0.709	0.673	0.706	0.950	0.641	0.371
27	0.100	0.001	2.647	0.253	0.375	0.331	0.337	0.341
28	0.500	0.001	0.596	1.348	1.061	0.615	0.922	0.609
29	0.481	0.026	0.752	1.079	0.724	0.758	1.035	1.042
30	0.247	0.019	0.301	1.294	0.528	0.364	1.196	1.382
31	18.950	0.001	1.746	0.703	0.936	0.523	0.795	0.803
32	0.500	0.001	1.004	10.660	1.144	0.231	1.324	1.192

33	0.350	0.001	0.549	1.635	0.567	0.527	0.978	4.618
34	0.151	0.012	0.245	0.397	0.483	1.039	0.962	3.318
35	8.156	0.011	1.108	0.940	0.788	2.038	2.817	3.149
36	3.350	0.007	0.834	1.100	0.756	1.072	0.931	0.876
37	0.456	0.006	0.568	0.524	0.634	0.642	0.929	0.620
38	5.850	0.001	6.153	2.615	4.331	1.400	1.030	0.482
39	2.542	0.001	0.844	0.860	0.960	0.733	0.998	0.459
40	31.612	0.007	2.486	1.186	2.116	4.903	0.804	1.550
41	3.157	0.004	0.750	0.686	1.127	1.005	1.157	0.656
42	0.250	0.001	0.641	0.598	0.656	0.231	0.411	0.425
43	0.296	0.001	0.882	1.422	1.349	0.491	0.692	0.582
44	2.737	0.014	1.025	0.971	1.218	1.159	1.265	1.014
45	0.180	0.009	0.674	1.096	0.866	1.082	1.174	0.683
46	15.105	0.019	2.442	2.246	2.923	1.110	1.035	1.064
47	13.563	0.046	1.248	11.793	1.673	21.035	3.228	2.891
48	2.641	0.006	0.990	0.512	1.413	0.970	0.816	0.636
49	0.542	0.010	0.917	0.351	0.766	2.043	0.616	1.198
50	1.250	0.001	1.644	1.308	2.050	0.642	1.267	0.433
51	0.800	0.001	1.968	0.540	0.789	0.300	0.678	0.332
52	0.200	0.001	1.282	1.920	0.372	0.392	0.505	0.302
53	5.250	0.001	0.782	1.923	0.747	2.058	2.538	3.086
54	2.712	0.040	0.573	1.541	0.855	2.019	1.576	1.658
55	0.602	0.020	0.542	1.177	0.622	1.558	1.337	1.911
56	1.600	0.001	0.531	1.173	0.639	0.962	2.657	1.315

Table B3. Enrichment factor of soil each sampling location

Sample No.	As	Cd	Cr	Cu	Ni	Pb	Hg
1	1.641	0.047	1.891	3.366	0.970	0.903	111.640
2	0.264	0.337	0.656	1.013	0.677	1.018	254.520
3	1.189	0.462	1.198	1.364	1.031	1.871	3069.000
4	0.429	0.605	0.462	0.740	0.573	3.801	308.800
5	0.271	0.168	0.532	1.747	0.477	0.567	169.940
6	0.330	0.555	0.410	0.377	0.460	0.871	449.870
7	3.441	0.071	2.296	0.421	0.576	1.427	97.982
8	0.475	0.766	0.554	0.840	0.619	1.504	226.050
9	0.269	0.769	0.581	0.660	0.527	0.776	180.610
10	0.566	0.333	0.776	0.960	0.912	2.795	405.040
11	0.191	0.761	0.573	0.810	0.548	1.070	248.710
12	0.156	1.354	0.291	0.617	0.385	1.491	267.990
13	0.197	0.504	0.376	0.359	0.408	1.070	434.910
14	0.685	0.074	4.608	0.509	0.566	1.391	92.608
15	1.021	0.044	2.348	0.935	0.892	1.088	85.580
16	0.701	0.076	0.969	0.881	1.059	1.310	208.450
17	0.219	0.391	0.991	1.469	0.969	0.716	137.570
18	0.684	0.291	0.851	1.696	0.706	1.782	192.000
19	0.522	0.113	7.404	0.475	0.699	2.850	248.950
20	0.595	0.043	1.154	0.524	0.504	0.580	1030.200
21	0.820	0.051	2.630	1.749	0.779	0.670	150.150
22	0.868	0.124	0.798	0.569	0.670	1.320	490.970
23	0.627	0.544	0.808	0.570	0.636	1.015	547.240
24	5.382	0.123	1.506	0.990	2.085	2.025	243.480
25	0.779	0.048	0.847	0.684	0.581	1.019	117.120
26	0.578	0.063	1.005	1.122	0.701	2.319	137.530
27	0.549	0.119	7.143	0.802	0.709	1.536	240.630
28	1.004	0.043	0.587	1.563	0.733	1.044	156.920
29	0.860	0.891	0.661	1.115	0.446	1.145	239.240
30	0.381	0.570	0.229	1.157	0.281	0.476	274.510
31	44.102	0.050	1.995	0.945	0.750	1.029	239.770
32	0.699	0.030	0.689	8.606	0.550	0.272	213.890

33	0.662	0.041	0.509	1.786	0.369	0.842	1120.800
34	0.290	0.458	0.232	0.441	0.319	1.688	818.850
35	5.356	0.142	0.357	0.357	0.178	1.131	265.520
36	6.656	0.258	0.814	1.263	0.517	1.799	223.550
37	0.907	0.216	0.555	0.603	0.434	1.080	158.400
38	10.504	0.039	5.426	2.713	2.676	2.124	111.160
39	4.714	0.040	0.769	0.922	0.613	1.149	109.230
40	72.771	0.299	2.811	1.577	1.676	9.538	458.130
41	5.048	0.139	0.589	0.634	0.620	1.358	134.710
42	1.124	0.097	1.416	1.552	1.014	0.877	245.540
43	0.791	0.058	1.157	2.196	1.241	1.108	199.840
44	4.002	0.412	0.736	0.820	0.613	1.433	190.420
45	0.805	0.503	0.630	0.764	0.804	2.843	218.520
46	27.002	0.658	2.144	2.320	1.798	1.676	244.070
47	7.772	0.509	0.351	3.905	0.330	10.186	212.660
48	5.989	0.246	1.103	0.671	1.103	1.860	185.090
49	1.626	0.586	1.352	0.608	0.791	5.186	461.820
50	1.825	0.032	1.179	1.103	1.030	0.792	81.144
51	2.181	0.059	2.635	0.851	0.740	0.691	116.090
52	0.733	0.079	2.307	4.063	0.469	1.214	141.960
53	3.827	0.016	0.280	0.810	0.187	1.267	288.790
54	3.183	0.916	0.330	1.045	0.345	2.003	249.860
55	0.832	0.540	0.368	0.941	0.296	1.821	339.410
56	1.114	0.015	0.182	0.472	0.153	0.566	117.510

Table B4. Geo-accumulation index of soil at each sampling location

Sample No	As	Cd	Cr	Cu	Ni	Pb	Zn	Hg
1	-0.379	-5.492	-0.174	0.658	-1.136	-1.240	-1.093	5.710
2	-2.382	-2.032	-1.071	-0.443	-1.025	-0.437	-0.462	7.529
3	-0.541	-1.907	-0.531	-0.343	-0.747	0.113	-0.791	10.792
4	-1.665	-1.170	-1.557	-0.878	-1.249	1.482	-0.444	7.826
5	-2.215	-2.907	-1.239	0.475	-1.396	-1.148	-0.329	7.079
6	-2.433	-1.684	-2.122	-2.242	-1.957	-1.035	-0.835	7.978
7	0.107	-5.492	-0.477	-2.923	-2.471	-1.163	-1.676	4.939
8	-1.598	-0.907	-1.375	-0.775	-1.216	0.065	-0.523	7.297
9	-2.198	-0.684	-1.089	-0.905	-1.230	-0.672	-0.306	7.191
10	-1.918	-2.684	-1.462	-1.156	-1.229	0.386	-1.097	7.565
11	-3.028	-1.032	-1.442	-0.942	-1.508	-0.541	-0.639	7.320
12	-3.188	-0.066	-2.286	-1.199	-1.882	0.073	-0.503	7.563
13	-3.041	-1.684	-2.106	-2.177	-1.990	-0.599	-0.697	8.068
14	-2.285	-5.492	0.465	-2.712	-2.560	-1.263	-1.739	4.794
15	-0.963	-5.492	0.239	-1.090	-1.158	-0.871	-0.993	5.426
16	-2.285	-5.492	-1.818	-1.956	-1.691	-1.383	-1.773	5.931
17	-2.625	-1.791	-0.449	0.120	-0.481	-0.918	-0.435	6.669
18	-0.799	-2.032	-0.484	0.511	-0.754	0.582	-0.251	7.334
19	-3.285	-5.492	0.541	-3.421	-2.865	-0.837	-2.347	5.612
20	-1.700	-5.492	-0.744	-1.883	-1.939	-1.737	-0.951	9.058
21	-1.478	-5.492	0.204	-0.385	-1.551	-1.769	-1.191	6.039
22	-1.681	-4.492	-1.803	-2.291	-2.057	-1.077	-1.478	7.462
23	-1.966	-2.170	-1.600	-2.104	-1.945	-1.271	-1.292	7.804
24	-0.037	-5.492	-1.875	-2.480	-1.406	-1.447	-2.466	5.462
25	-1.478	-5.492	-1.357	-1.664	-1.902	-1.089	-1.117	5.755
26	-2.285	-5.492	-1.486	-1.327	-2.006	-0.280	-1.494	5.610
27	-3.285	-5.492	0.415	-2.741	-2.918	-1.803	-2.421	5.489
28	-0.963	-5.492	-1.737	-0.325	-1.417	-0.907	-0.969	6.325
29	-1.019	-0.968	-1.400	-0.646	-1.968	-0.607	-0.802	7.100
30	-1.984	-1.404	-2.719	-0.383	-2.425	-1.665	-0.593	7.508
31	4.281	-5.492	-0.186	-1.264	-1.598	-1.141	-1.182	6.723
32	-0.963	-5.492	-0.983	2.659	-1.308	-2.322	-0.446	7.295
33	-1.478	-5.492	-1.856	-0.046	-2.322	-1.131	-0.882	9.248
34	-2.691	-2.032	-3.016	-2.088	-2.553	-0.151	-0.907	8.771
35	3.064	-2.170	-0.842	-0.844	-1.847	0.820	0.643	8.696

Table B4: Continues……..

36	1.780	-2.907	-1.252	-0.618	-1.907	-0.107	-0.954	6.850
37	-1.098	-3.170	-1.806	-1.687	-2.160	-0.846	-0.957	6.350
38	2.585	-5.492	1.632	0.632	0.612	0.279	-0.808	5.989
39	1.382	-5.492	-1.234	-0.972	-1.561	-0.654	-0.854	5.917
40	5.019	-2.907	0.325	-0.509	-0.421	2.087	-1.166	7.673
41	1.695	-3.492	-1.405	-1.299	-1.330	-0.199	-0.641	6.433
42	-1.963	-5.492	-1.631	-1.498	-2.112	-2.322	-2.132	5.807
43	-1.720	-5.492	-1.171	-0.247	-1.070	-1.233	-1.382	6.261
44	1.489	-1.791	-0.954	-0.798	-1.218	0.007	-0.512	7.061
45	-1.356	-2.032	-1.710	-1.430	-1.357	0.465	-1.042	6.729
46	3.953	-1.404	0.299	0.413	0.045	-0.056	-0.801	7.130
47	3.798	-0.134	-0.670	2.805	-0.760	4.188	0.840	8.572
48	1.437	-3.170	-1.004	-1.721	-1.004	-0.250	-1.145	6.387
49	-0.848	-2.322	-1.115	-2.267	-1.888	0.825	-1.550	7.301
50	0.358	-5.492	-0.272	-0.368	-0.467	-0.845	-0.510	5.833
51	-0.285	-5.492	-0.013	-1.644	-1.845	-1.943	-1.411	5.448
52	-2.285	-5.492	-0.631	0.186	-2.928	-1.556	-1.837	5.313
53	2.429	-5.492	-1.343	0.188	-1.923	0.835	0.493	8.667
54	1.476	-0.322	-1.794	-0.131	-1.729	0.807	-0.195	7.770
55	-0.697	-1.322	-1.873	-0.520	-2.187	0.433	-0.432	7.975
56	0.715	-5.492	-1.903	-0.525	-2.149	-0.263	0.559	7.435

Table B5. Activity concentration, dose rate and annual Effective dose of soil at each sampling location

	U-238 (Bq/kg)	Th-232 (Bq/kg)	K-40 (Bq/kg)	Dose Rate((nG/h)	AED(mSv/y)
1	44.031	114.502	811.276	123.575	0.152
2	56.864	102.490	486.940	108.627	0.133
3	32.277	66.727	401.269	72.068	0.088
4	51.690	52.619	315.121	68.898	0.084
5	<5	9.597	253.073	17.581	0.022
6	<5	21.965	196.532	22.676	0.028
7	29.951	41.145	488.885	59.222	0.073
8	45.593	78.156	646.223	95.412	0.117
9	<5	<5	360.095	17.789	0.022
10	35.456	84.766	636.050	94.293	0.116
11	52.517	92.143	1061.894	124.517	0.153
12	26.278	51.680	1052.392	87.556	0.107
13	41.906	78.365	491.122	87.320	0.107
14	23.206	64.476	<30	50.295	0.062
15	7.636	29.718	413.090	38.827	0.048
16	24.256	43.498	245.427	47.787	0.059
17	48.108	57.775	503.854	78.284	0.096
18	<5	42.386	253.133	37.388	0.046
19	41.554	82.802	292.723	81.505	0.100
20	34.921	44.584	749.577	74.544	0.091
21	37.682	63.759	1268.807	109.209	0.134
22	8.851	36.949	414.684	43.823	0.054
23	26.070	51.334	<30	43.680	0.054
24	9.337	25.792	307.570	32.810	0.040
25	42.476	66.972	356.472	75.047	0.092
26	39.307	52.748	220.456	59.279	0.073
27	42.733	91.443	419.418	92.590	0.114
28	16.354	52.467	602.183	64.537	0.079
29	35.139	62.593	981.516	95.264	0.117
30	<5	26.703	553.194	40.518	0.050
31	41.705	58.962	222.075	64.208	0.079

Table B5: Continues…………..

32	2.500	75.547	232.920	56.568	0.069
33	13.994	9.637	86.859	15.934	0.020
34	37.871	62.633	1024.644	98.362	0.121
35	22.734	40.921	285.477	47.210	0.058
36	7.877	6.255	<30	8.059	0.010
37	25.703	74.785	545.430	79.953	0.098
38	562.116	206.236	436.732	402.607	0.494
39	28.275	28.062	761.902	62.012	0.076
40	41.657	70.425	464.298	81.283	0.100
41	44.433	87.429	559.814	96.847	0.119
42	33.902	91.588	279.828	82.735	0.101

Appendix C.

Table C1. Heavy metal concentration of heavy metals in tailings (mg/kg) each sampling location

Sample No.	As	Cd	Cu	Cr	Ni	Pb	Zn	Hg
1	49.38	0.40	39.22	81.23	659.62	351.58	51.61	2114.38
2	10.55	0.14	42.15	138.56	50.01	25.42	128.26	204.85
3	179.58	2.40	266.07	70.26	509.81	267.74	246.10	2555.49
4	795.97	0.28	92.83	69.18	17.31	81.26	67.48	484.78
5	121.26	0.58	407.73	106.90	184.06	5.42	146.51	30721.90
6	15.18	0.07	127.33	102.65	97.20	4.48	134.44	8909.75
7	358.21	1.27	105.80	41.08	55.14	111.37	96.13	1992.98
8	29.50	0.15	488.27	88.14	84.44	5.14	62.37	22517.70
9	2008.07	0.69	135.34	86.19	361.64	162.01	151.27	840.63
10	1191.96	0.23	46.77	127.06	21.10	76.18	41.22	13816.50
11	234.06	0.72	128.77	74.61	32.45	205.68	180.14	25005.70
12	497.85	0.99	174.22	43.79	136.08	212.69	116.85	9738.79
13	1824.86	0.56	1305.60	118.98	685.71	1374.70	1038.60	624.16
14	5829.99	4.14	2329.30	133.63	766.12	3238.80	1270.83	6275.26

Appendix D

Heavy metal concentration, pollution indeces and radioactivity in river sediment

Table D1: Heavy metal concentration in river sediments at each sampling location (mg/kg)

Sample No.	As	Cd	Cr	Cu	Ni	Pb	Zn	Hg
1	21.00	0.01	144.40	64.90	97.60	11.20	75.50	11.40
2	78.65	0.52	149.99	119.47	136.45	261.03	136.80	515.79
3	9.57	0.34	48.68	64.33	71.43	57.25	97.90	55.48
4	15.80	0.26	99.40	59.48	62.13	21.13	117.34	616.66
5	171.42	0.43	99.70	91.44	62.91	107.99	147.66	2376.93
6	19.12	0.20	83.20	56.17	58.53	22.22	103.64	614.14
7	15.13	0.13	67.37	116.60	56.57	323.10	111.07	68.54
8	24.00	0.01	151.40	18.70	28.10	13.30	33.50	18.10
9	4.68	0.27	56.69	15.07	8.85	22.64	60.47	725.40
10	4.00	0.01	186.10	22.90	12.60	13.70	35.20	23.75
11	17.00	0.20	141.91	52.48	48.34	18.02	79.96	117.47
12	33.00	0.01	84.80	72.30	68.50	21.90	61.00	24.70
13	151.00	0.01	39.70	19.40	46.10	35.00	33.10	154.05
14	26.00	0.01	286.40	27.80	43.80	36.70	46.00	8.40
15	7.66	0.09	41.28	49.52	31.22	18.70	96.26	55.19
16	21.00	0.01	162.40	14.20	17.80	9.50	36.90	114.15
17	10.32	0.30	31.18	373.06	76.49	16.40	230.27	184.82
18	5.62	0.08	27.06	147.45	16.36	24.77	121.82	103.24
19	9.00	0.01	28.30	37.80	37.60	17.60	28.90	39.40
20	19.22	0.02	88.43	9.77	166.43	1528.26	75.92	31.54
21	317.00	0.01	146.90	15.10	27.00	28.00	42.10	31.75
22	61.90	0.12	54.11	77.57	13.85	18.39	81.01	378.44
23	25.00	0.01	52.70	78.70	50.20	25.70	54.30	19.25
24	4.00	0.01	121.40	15.70	13.10	20.70	32.80	28.75
25	30.00	0.01	115.20	75.70	56.90	12.20	115.20	1902.75
26	15.00	0.01	105.30	46.90	43.70	9.20	118.40	85.67
27	1132.00	0.01	166.80	36.90	50.20	68.30	101.30	187.05

Table D1Continues……….

28	6.00	0.01	39.90	22.90	33.20	12.10	32.80	23.65
29	4.00	0.01	22.30	13.10	32.30	17.60	30.00	29.50
30	5.61	0.11	29.57	34.62	14.86	19.70	78.52	117.84
31	41.00	0.01	184.10	12.00	13.10	10.80	28.30	26.05
32	25.34	0.04	73.83	44.81	220.62	17.69	33.08	96.59
33	977.89	0.15	26.47	15.90	33.64	33.07	39.82	205.63
34	322.81	0.13	73.41	92.22	254.69	50.79	98.56	393.06
35	17.34	0.03	70.30	14.97	55.19	13.73	38.01	418.93
36	40.23	0.11	41.04	16.81	10.45	19.65	68.61	230.37
37	860.81	0.28	83.37	49.27	104.21	48.10	88.19	1160.00
38	24.00	0.01	129.30	66.10	87.50	11.80	101.50	168.20
39	198.00	0.01	164.30	110.00	31.00	113.40	115.80	307.55
40	8.00	0.01	20.20	14.90	10.20	12.80	71.50	154.30
41	32.00	0.01	52.50	29.80	17.70	28.60	85.40	139.95
42	72.25	0.14	66.36	44.86	24.29	29.48	83.89	601.79
43	363.16	0.71	53.47	276.35	191.95	191.97	205.51	785.34
44	20.00	0.01	32.90	36.40	18.50	23.10	140.00	331.05

Table D2: Contamination factor of river sediments at each sampling location

Sample No.	As	Cd	Cr	Cu	Ni	Pb	Zn	Hg
1	0.933	0.001	1.961	1.447	2.231	0.520	0.953	0.088
2	3.496	0.065	2.037	2.664	3.119	12.130	1.726	4.001
3	0.425	0.043	0.661	1.435	1.633	2.660	1.235	0.430
4	0.702	0.033	1.350	1.326	1.420	0.982	1.481	4.784
5	7.619	0.054	1.354	2.039	1.438	5.018	1.863	18.440
6	0.850	0.025	1.130	1.253	1.338	1.033	1.308	4.764
7	0.672	0.016	0.915	2.600	1.293	15.014	1.402	0.532
8	1.067	0.001	2.057	0.417	0.642	0.618	0.423	0.140
9	0.208	0.034	0.770	0.336	0.202	1.052	0.763	5.628
10	0.178	0.001	2.528	0.511	0.288	0.637	0.444	0.184
11	0.756	0.025	1.928	1.170	1.105	0.837	1.009	0.911
12	1.467	0.001	1.152	1.612	1.566	1.018	0.770	0.192
13	6.711	0.001	0.539	0.433	1.054	1.626	0.418	1.195
14	1.156	0.001	3.890	0.620	1.001	1.705	0.581	0.065
15	0.340	0.011	0.561	1.104	0.714	0.869	1.215	0.428
16	0.933	0.001	2.206	0.317	0.407	0.441	0.466	0.886
17	0.459	0.038	0.424	8.320	1.748	0.762	2.906	1.434
18	0.250	0.010	0.368	3.288	0.374	1.151	1.537	0.801
19	0.400	0.001	0.384	0.843	0.859	0.818	0.365	0.306
20	0.854	0.003	1.201	0.218	3.804	71.016	0.958	0.245
21	14.089	0.001	1.995	0.337	0.617	1.301	0.531	0.246
22	2.751	6.000	0.735	1.730	0.317	0.855	1.022	2.936
23	1.111	0.001	0.716	1.755	1.147	1.194	0.685	0.149
24	0.178	0.001	1.649	0.350	0.299	0.962	0.414	0.223
25	1.333	0.001	1.565	1.688	1.301	0.567	1.454	14.760
26	0.667	0.001	1.430	1.046	0.999	0.428	1.494	0.665
27	50.311	0.001	2.266	0.823	1.147	3.174	1.278	1.451
28	0.267	0.001	0.542	0.511	0.759	0.562	0.414	0.183
29	0.178	0.001	0.303	0.292	0.738	0.818	0.379	0.229
30	0.249	0.014	0.402	0.772	0.340	0.915	0.991	0.914

Table D2 Continues……….

31	1.822	0.001	2.501	0.268	0.299	0.502	0.357	0.202
32	1.126	0.005	1.003	0.999	5.043	0.822	0.417	0.749
33	43.462	0.019	0.360	0.355	0.769	1.537	0.503	1.595
34	14.347	0.016	0.997	2.057	5.821	2.360	1.244	3.049
35	0.771	0.004	0.955	0.334	1.261	0.638	0.480	3.250
36	1.788	0.014	0.557	0.375	0.239	0.913	0.866	1.787
37	38.258	0.035	1.132	1.099	2.382	2.235	1.113	8.999
38	1.067	0.001	1.756	1.474	2.000	0.548	1.281	1.305
39	8.800	0.001	2.232	2.453	0.709	5.270	1.461	2.386
40	0.356	0.001	0.274	0.332	0.233	0.595	0.902	1.197
41	1.422	0.001	0.713	0.665	0.405	1.329	1.078	1.086
42	3.211	0.018	0.901	1.000	0.555	1.370	1.059	4.669
43	16.140	0.089	0.726	6.163	4.387	8.921	2.594	6.093
44	0.889	0.001	0.447	0.812	0.423	1.073	1.767	2.568

Table D3: Enrichment Factors of river sediments at each sampling location

Sample No.	As	Cd	Cr	Cu	Ni	Pb	Hg
1	2.033	0.042	2.019	1.815	1.806	0.705	35.861
2	4.201	1.204	1.157	1.844	1.393	9.064	895.469
3	0.714	1.100	0.525	1.387	1.019	2.778	134.591
4	0.984	0.702	0.894	1.070	0.740	0.855	1248.140
5	8.484	0.922	0.713	1.307	0.595	3.474	3823.113
6	1.348	0.611	0.847	1.144	0.789	1.018	1407.355
7	0.995	0.371	0.640	2.216	0.712	13.820	146.558
8	5.235	0.095	4.770	1.178	1.172	1.886	128.321
9	0.566	1.414	0.990	0.526	0.204	1.778	2849.057
10	0.830	0.090	5.581	1.373	0.500	1.849	160.245
11	1.554	0.792	1.873	1.386	0.845	1.070	348.914
12	3.953	0.052	1.467	2.502	1.569	1.705	96.168
13	33.340	0.096	1.266	1.237	1.946	5.023	1105.344
14	4.130	0.069	6.572	1.276	1.330	3.790	43.370
15	0.582	0.296	0.453	1.086	0.453	0.923	136.169
16	4.159	0.086	4.646	0.812	0.674	1.223	734.705
17	0.328	0.413	0.143	3.420	0.464	0.338	190.623
18	0.337	0.208	0.234	2.555	0.188	0.966	201.276
19	2.276	0.110	1.034	2.761	1.818	2.893	323.789
20	1.850	0.083	1.229	0.272	3.063	95.620	98.666
21	55.030	0.075	3.683	0.757	0.896	3.159	179.112
22	5.584	0.469	0.705	2.021	0.239	1.078	1109.486
23	3.364	0.058	1.024	3.060	1.292	2.248	84.197
24	0.891	0.097	3.907	1.011	0.558	2.998	208.175
25	1.903	0.027	1.056	1.387	0.690	0.503	3922.770
26	0.926	0.027	0.939	0.836	0.516	0.369	171.836
27	81.660	0.031	1.738	0.769	0.692	3.203	438.543
28	1.337	0.097	1.284	1.474	1.414	1.752	171.246
29	0.974	0.106	0.785	0.922	1.504	2.787	233.542
30	0.522	0.444	0.398	0.931	0.264	1.192	356.431

Table D3 Continues………..

31	10.590	0.112	6.867	0.895	0.647	1.813	218.617
32	5.598	0.383	2.356	2.860	9.317	2.540	693.474
33	179.500	1.193	0.702	0.843	1.180	3.945	1226.447
34	23.940	0.418	0.786	1.975	3.610	2.448	947.157
35	3.334	0.250	1.952	0.831	2.029	1.716	2617.624
36	4.285	0.508	0.631	0.517	0.213	1.360	797.448
37	71.330	1.005	0.998	1.179	1.651	2.591	3123.937
38	1.728	0.031	1.345	1.375	1.204	0.552	393.571
39	12.500	0.027	1.498	2.005	0.374	4.652	630.770
40	0.818	0.044	0.298	0.440	0.199	0.850	512.535
41	2.738	0.037	0.649	0.737	0.290	1.591	389.205
42	6.294	0.528	0.835	1.129	0.405	1.669	1703.721
43	12.910	1.094	0.275	2.839	1.305	4.437	907.587
44	1.044	0.023	0.248	0.549	0.185	0.784	561.603

Table D4: Geo-accumulation index of river sediments at each sampling location

Sample No.	As	Cd	Cr	Cu	Ni	Pb	Zn	Hg
1	0.107	-5.492	0.097	-0.057	-0.064	-1.421	-0.916	4.248
2	2.012	0.209	0.152	0.824	0.420	3.121	-0.059	9.748
3	-1.027	-0.404	-1.472	-0.069	-0.514	0.932	-0.542	6.531
4	-0.304	-0.791	-0.442	-0.182	-0.715	-0.506	-0.280	10.005
5	3.136	-0.066	-0.437	0.438	-0.697	1.848	0.051	11.952
6	-0.028	-1.170	-0.698	-0.265	-0.801	-0.433	-0.459	9.999
7	-0.366	-1.791	-1.003	0.789	-0.850	3.429	-0.359	6.836
8	0.300	-5.492	0.165	-1.852	-1.860	-1.174	-2.089	4.915
9	-2.059	-0.737	-1.252	-2.163	-3.527	-0.406	-1.237	10.240
10	-2.285	-5.492	0.463	-1.560	-3.017	-1.131	-2.017	5.307
11	-0.198	-1.170	0.072	-0.363	-1.077	-0.735	-0.834	7.613
12	0.759	-5.492	-0.671	0.099	-0.574	-0.454	-1.224	5.363
13	2.953	-5.492	-1.766	-1.799	-1.146	0.222	-2.106	8.004
14	0.415	-5.492	1.085	-1.280	-1.220	0.291	-1.631	3.807
15	-1.348	-2.322	-1.709	-0.447	-1.708	-0.682	-0.566	6.523
16	0.107	-5.492	0.267	-2.249	-2.519	-1.659	-1.949	7.572
17	-0.918	-0.585	-2.114	2.466	-0.415	-0.871	0.692	8.267
18	-1.795	-2.492	-2.319	1.127	-2.640	-0.276	-0.226	7.427
19	-1.115	-5.492	-2.254	-0.837	-1.440	-0.769	-2.302	6.037
20	-0.021	-4.492	-0.610	-2.788	0.706	5.671	-0.908	5.716
21	4.023	-5.492	0.122	-2.160	-1.918	-0.100	-1.759	5.726
22	1.666	-1.907	-1.319	0.201	-2.881	-0.706	-0.815	9.301
23	0.358	-5.492	-1.357	0.221	-1.023	-0.223	-1.392	5.004
24	-2.285	-5.492	-0.153	-2.104	-2.961	-0.535	-2.119	5.582
25	0.621	-5.492	-0.229	0.165	-0.842	-1.298	-0.307	11.631
26	-0.379	-5.492	-0.358	-0.525	-1.223	-1.705	-0.267	7.158
27	5.859	-5.492	0.305	-0.871	-1.023	1.187	-0.492	8.284
28	-1.700	-5.492	-1.758	-1.560	-1.619	-1.310	-2.119	5.301
29	-2.285	-5.492	-2.598	-2.365	-1.659	-0.769	-2.248	5.620
30	-1.797	-2.032	-2.191	-0.963	-2.779	-0.607	-0.860	7.618
31	1.072	-5.492	0.448	-2.492	-2.961	-1.474	-2.332	5.440
32	0.378	-3.492	-0.871	-0.591	1.113	-0.762	-2.107	7.331

Table D4 Continues………….

33	5.648	-1.585	-2.351	-2.086	-1.600	0.141	-1.839	8.421
34	4.049	-1.791	-0.879	0.450	1.320	0.760	-0.532	9.356
35	-0.169	-3.907	-0.941	-2.173	-0.886	-1.128	-1.907	9.448
36	1.045	-2.032	-1.718	-2.006	-3.287	-0.610	-1.054	8.585
37	5.464	-0.684	-0.695	-0.454	0.031	0.681	-0.692	10.917
38	0.300	-5.492	-0.062	-0.030	-0.221	-1.346	-0.489	8.131
39	3.344	-5.492	0.283	0.705	-1.718	1.918	-0.299	9.002
40	-1.285	-5.492	-2.741	-2.180	-3.322	-1.229	-0.995	8.007
41	0.715	-5.492	-1.363	-1.180	-2.527	-0.069	-0.739	7.866
42	1.890	-1.684	-1.025	-0.589	-2.070	-0.025	-0.764	9.970
43	4.219	0.658	-1.336	2.034	0.912	2.678	0.528	10.354
44	0.037	-5.492	-2.037	-0.891	-2.463	-0.377	-0.026	9.108

Table D5. Activity concentration (Bq/kg), Dose rate and Annual effective dose rate of river sediments each sampling location

	U-238 (Bq/kg	Th-232 (Bq/kg	K-40 (Bq/kg)	Dose rate (nGy/h)	AED (mSv/yr)
1	39.456	28.283	310.526	48.613	0.060
2	47.213	68.455	527.949	87.651	0.108
3	1.538	79.163	<30	53.693	0.066
4	<5	<5	102.326	7.020	0.009
5	29.456	49.69	<30	46.102	0.057
6	24.27	24.273	88.239	30.138	0.037
7	51.841	78.413	350.995	88.787	0.109
8	43.721	39.153	341.837	58.945	0.072
9	32.288	39.302	1243.55	92.034	0.113
10	28.998	48.332	269.997	55.718	0.068
11	<5	34.958	251.75	34.783	0.043
12	<5	40.508	559.824	51.396	0.063
13	<5	<5	141.361	8.660	0.011
14	<5	44.286	1001.1	72.431	0.089
15	16.053	42.338	615.075	60.716	0.075
16	55.49	72.223	324.385	85.130	0.104
17	<5	39.302	314.094	40.277	0.049
18	35.027	53.967	577.564	74.940	0.092
19	28.012	37.769	454.987	56.074	0.069
20	24.761	15.099	1017.28	63.294	0.078
21	18.221	13.012	1252.45	68.997	0.085
22	25.615	32.771	186.129	40.449	0.050
23	<5	<5	297.409	15.214	0.019
24	31.984	54.287	348.396	64.228	0.079
25	19.649	46.929	<30	40.087	0.049
26	15.754	53.495	894.761	79.721	0.098
27	39.13	64.02	899.222	96.857	0.119
28	8.726	20.052	<30	17.630	0.022
29	10.178	44.884	<30	34.689	0.043
30	37.861	59.606	200.832	64.061	0.079
31	46.62	48.523	462.821	71.467	0.088
32	25.533	26.653	286.5	40.580	0.050

Table D5 Continues……..

33	47.059	96.255	743.141	115.027	0.141
34	<5	<5	264.69	13.839	0.017
35	55.428	35.162	325.724	60.625	0.074
36	70.619	115.389	532.206	128.894	0.158
37	48.235	104.834	573.913	114.101	0.140
38	28.51	45.699	766.006	74.599	0.092
39	53.532	105.34	530.258	114.864	0.141

Table E: Elemental concentration of references (mg/kg) BCR-62 (olive leaves), BCR 141R (loam soil), BCR 320 (river sediments) obtained from European Commission Community Bureau of Reference (BCCBR)

Element	CRM 320 River sediment	BCR 062 Olive leaves (Olea europaea)	BCR 141R Calcareous loam soil
As	76.7 ± 3.4	0.2	8.80 ± 0.40
Cd	0.533 ± 0.026	0.10 ± 0.02	14.6 ± 0.5
Cr	138 ± 7	2	195 ± 7
Cu	44.1 ± 1.0	46.6 ± 1.8	46.4 ± 1.8
Hg	1.03 ± 0.13	0.28 ± 0.02	0.25 ± 0.02
Ni	75.2 ± 1.4	8	103 ± 3
Pb	42.3 ± 1.6	25.0 ± 1.5	57.2 ± 1.2
Zn	142 ± 3	16.0±0.7	283±5

Energy Calibration (KeV)
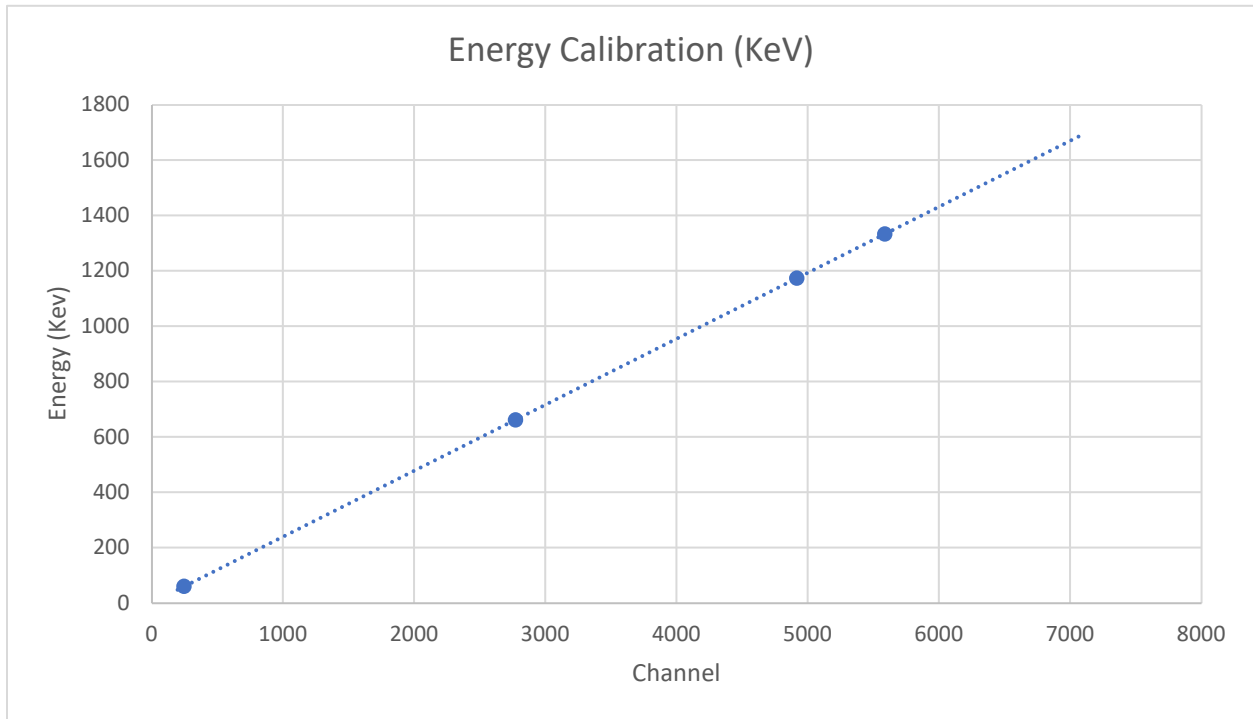
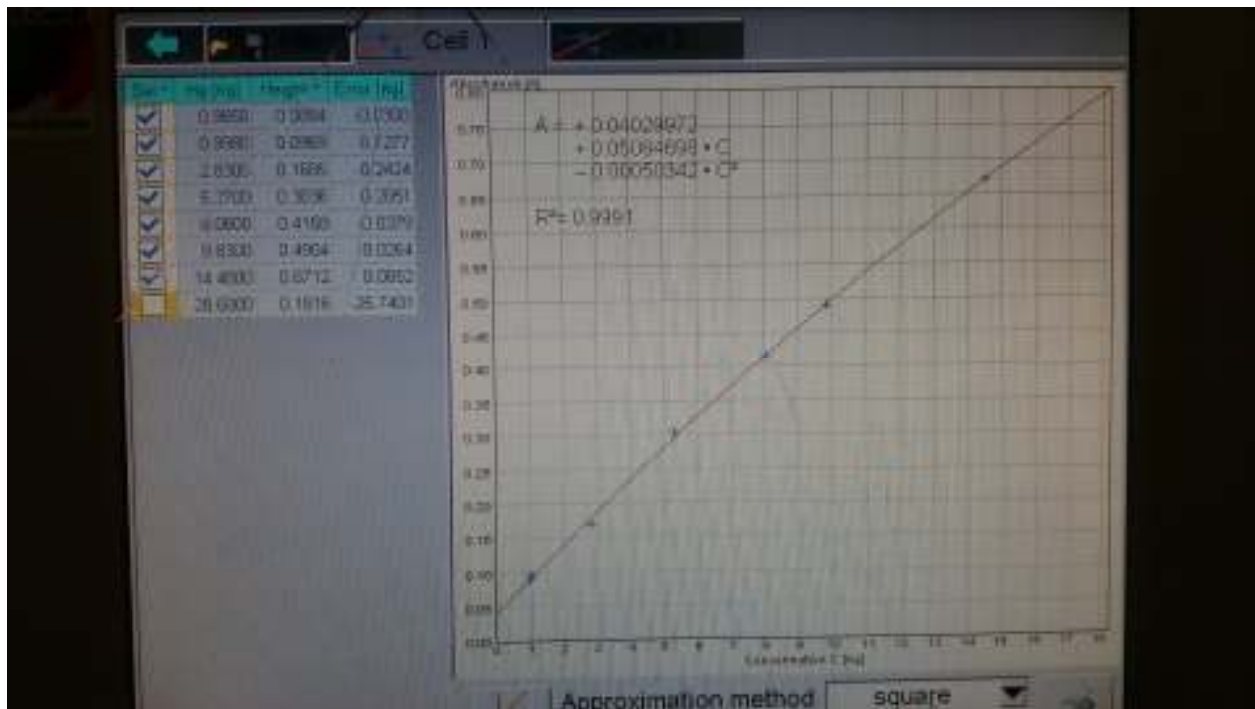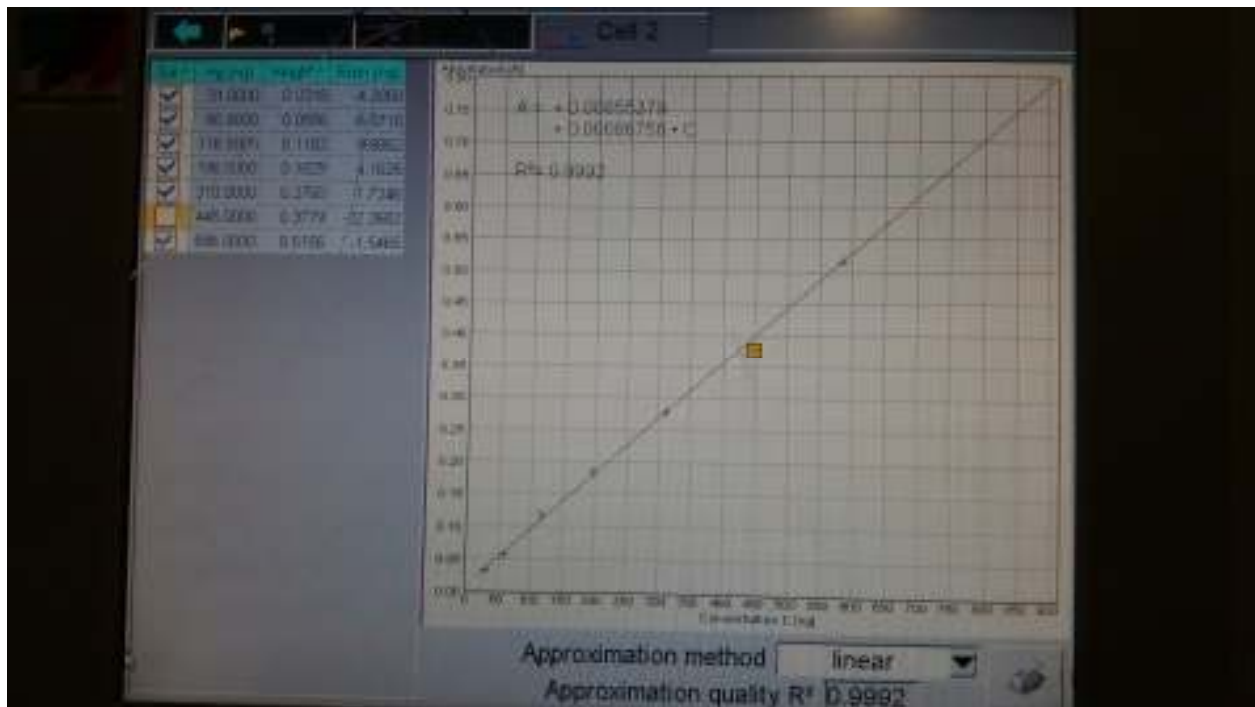Appendix F2: Efficiency Callibration Curve

EFFICIENCY CALIBRATION CURVE
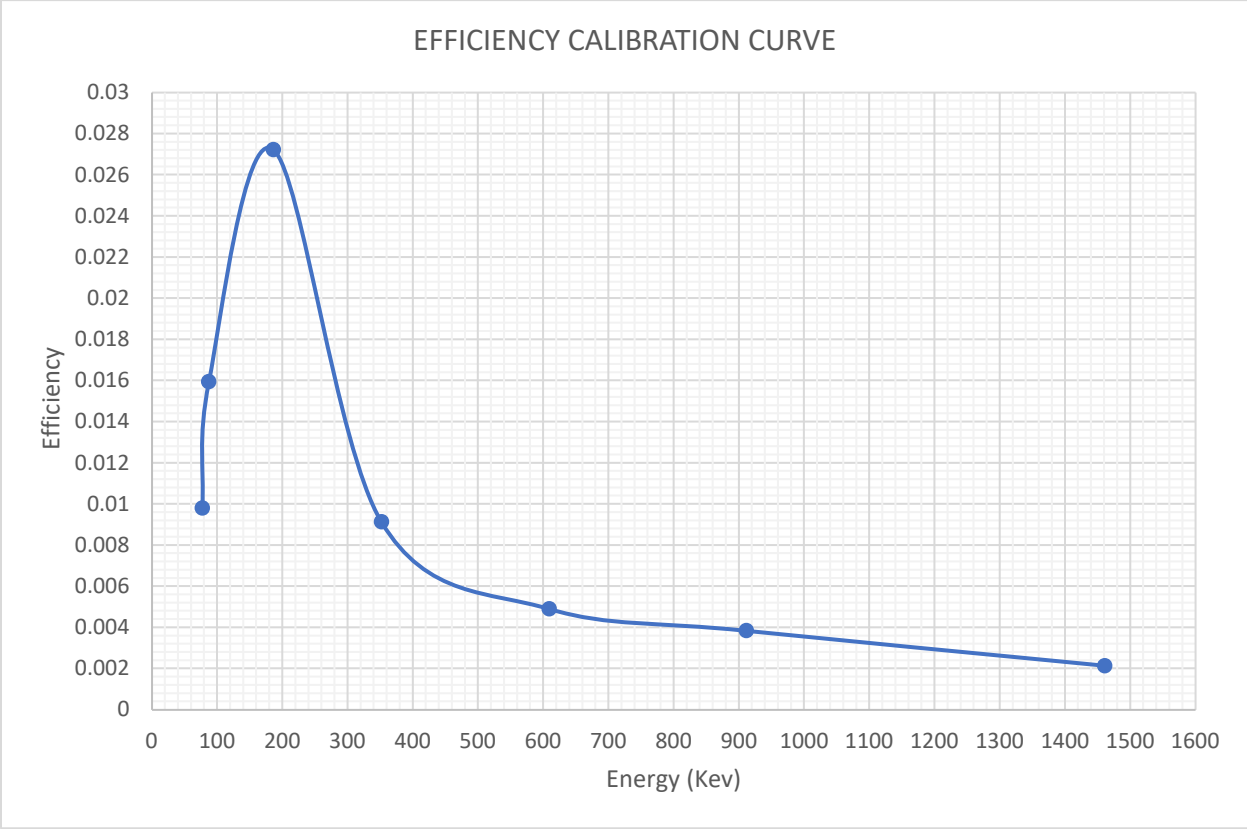
Appendix F3: Callibration curve DMA 480

Appendix E: List of Publications

1. **Odumo, B. O.,** Nanos, N., Carbonell, G., Torrijos, M., Patel, J.P., Rodríguez Martín, J.A. (2018). Artisanal gold-mining in a rural environment: Land degradation in Kenya. *Land Degrad. Development 1-9. D*OI:10.1002/ldr.3078.

2. **Odumo, B.O.,** Carbonell, G., Angeyo, H. K., Patel, J.P., Torrijos, M., Rodríguez Martín, J.A. (2014) Impact of gold mining associated with mercury contamination in soil, biota sediments and tailings in Kenya. *Environmental Science and Pollution Research* 21, 12426-12435. DOI: 10.1007/s11356-014-3190-3

Turnitin Originality Report

Processed on: 10-Sep-2021 17:35 EAT
ID: 1645307254
Word Count: 38168
Submitted: 1

13/09/2021

Certified

CHAIRMAN, DEPARTMENT OF PHYSICS.   21/9/2021

Similarity Index	Similarity by Source
14%	Internet Sources: 11% Publications: 7% Student Papers: 4%

Analysis and MultivariateModeling of Heavy Metals and Associated Radiogenic Impact of Gold Mining in the Migori-Transmara Complex of Southwestern Kenya By I80/83681/2012 Odumo Benjamin Okang'

< 1% match (Internet from 15-Nov-2013)
http://physics.uonbi.ac.ke/departmental_research?order=field_start_year_value&sort=asc&field_research_status_value_many_to_one=Ongoing

---

< 1% match (Internet from 08-Jun-2013)
http://physics.uonbi.ac.ke/departmental_research

< 1% match (Internet from 08-Sep-2021)
https://physics.uonbi.ac.ke/student/benjamin-okang-odumo

< 1% match (student papers from 24-May-2016)
Submitted to University of Nairobi on 2016-05-24

< 1% match (student papers from 02-Sep-2021)
Submitted to University of Nairobi on 2021-09-02

< 1% match (publications)
José Antonio Rodríguez Martín, Nikos Nanos, José Carlos Miranda, Gregoria Carbonell, Luis Gil. "Volcanic mercury in Pinus canariensis", Naturwissenschaften, 2013

< 1% match (student papers from 28-May-2018)
Submitted to Management & Science University on 2018-05-28

< 1% match (publications)
Jan Schaug, Jon P. Rambæk, Eiliv Steinnes, Ronald C. Henry. "Multivariate analysis of trace element data from moss samples used to monitor atmospheric deposition", Atmospheric Environment. Part A. General Topics, 1990

< 1% match (publications)
Osei Akoto, Collins Nimako, Joseph Asante, David Bailey. "Heavy Metals Enrichment in Surface Soil from Abandoned Waste Disposal Sites in a Hot and Wet Tropical Area", Environmental Processes, 2016

< 1% match (Internet from 03-Sep-2013)
http://jtethys.org/wp-content/uploads/2011/10/Ghomi_et_al_2013.pdf

---

< 1% match (publications)
Temitope Ayodeji Laniyan, Adeniyi JohnPaul Adewumi. "Potential ecological and health risks of toxic metals associated with artisanal mining contamination in Ijero, southwest Nigeria", Journal of Environmental Science and Health, Part A, 2020

< 1% match (Internet from 26-Feb-2020)
https://www.science.gov/topicpages/f/facies+del+subfondo

< 1% match (Internet from 08-Mar-2021)
https://www.science.gov/topicpages/m/metallogeny+greenstone+belt.html

---

< 1% match (publications)
QU, Ming-Kai, Wei-Dong LI, Chuan-Rong ZHANG, Shan-Qin WANG, Yong YANG, and Li-Yuan HE. "Source Apportionment of Heavy Metals in Soils Using Multivariate Statistics and Geostatistics", Pedosphere, 2013.

< 1% match (Internet from 09-Dec-2014)
http://pub.iaea.org/MTCD/Publications/PDF/TE-1741_web.pdf

< 1% match (Internet from 04-May-2010)
http://ocw.mit.edu/NR/rdonlyres/Sloan-School-of-Management/15-062Data-MiningSpring2003/E31DD7A9-4B2E-48BF-AB3F-6F4CCAD7F24F/0/lec11.pdf